

LARGE Volume String Compactifications at Finite Temperature

Lilia Anguelova

Dept. of Physics, University of Cincinnati

Cincinnati, OH 45221, USA

E-mail: anguella@ucmail.uc.edu

Vincenzo Calò

Center for Research in String Theory, Queen Mary,

University of London, Mile end Road, London, E1 4NS.

E-mail: v.calò@qmul.ac.uk

Michele Cicoli

DAMTP, Centre for Mathematical Sciences

Wilberforce Road, Cambridge, CB3 0WA, UK.

E-mail: M.Cicoli@damtp.cam.ac.uk

ABSTRACT: We present a detailed study of the finite-temperature behaviour of the LARGE Volume type IIB flux compactifications. We show that certain moduli can thermalise at high temperatures. Despite that, their contribution to the finite-temperature effective potential is always negligible and the latter has a runaway behaviour. We compute the maximal temperature T_{max} , above which the internal space decompactifies, as well as the temperature T_* , that is reached after the decay of the heaviest moduli. The natural constraint $T_* < T_{max}$ implies a lower bound on the allowed values of the internal volume \mathcal{V} . We find that this restriction rules out a significant range of values corresponding to smaller volumes of the order $\mathcal{V} \sim 10^4 l_s^6$, which lead to standard GUT theories. Instead, the bound favours values of the order $\mathcal{V} \sim 10^{15} l_s^6$, which lead to TeV scale SUSY desirable for solving the hierarchy problem. Moreover, our result favours low-energy inflationary scenarios with density perturbations generated by a field, which is not the inflaton. In such a scenario, one could achieve both inflation and TeV-scale SUSY, although gravity waves would not be observable. Finally, we pose a two-fold challenge for the solution of the cosmological moduli problem. First, we show that the heavy moduli decay before they can begin to dominate the energy density of the Universe. Hence they are not able to dilute any unwanted relics. And second, we argue that, in order to obtain thermal inflation in the closed string moduli sector, one needs to go beyond the present EFT description.

KEYWORDS: String compactifications, Finite-temperature effective potential.

Contents

1. Introduction	2
2. Large Volume Scenarios	5
2.1 Type IIB with fluxes	5
2.2 Leading order corrections	7
2.2.1 Non-perturbative corrections	7
2.2.2 α' corrections	8
2.2.3 g_s corrections	8
2.3 Moduli stabilisation in LVS	9
2.3.1 Swiss-cheese Calabi-Yaus	10
2.3.2 Fibred Calabi-Yaus	11
3. Effective potential at finite temperature	13
3.1 General form of temperature corrections	13
3.2 Thermal equilibrium	14
3.2.1 $2 \leftrightarrow 2$ interactions	14
3.2.2 $1 \leftrightarrow 2$ interactions	17
4. Moduli masses and couplings	19
4.1 Single-hole Swiss-cheese	19
4.2 Multiple-hole Swiss-cheese	21
4.3 K3 Fibration	22
4.4 Modulini	26
5. Study of moduli thermalisation	27
5.1 Single-hole Swiss-cheese	28
5.2 Multiple-hole Swiss-cheese	30
5.3 K3 Fibration	32
5.4 Modulini thermalisation	34
6. Finite temperature corrections in LVS	34
6.1 Effective potential	34
6.2 Decompactification temperature	39
6.3 Small moduli cosmology	42
6.4 Lower bound on \mathcal{V}	45
7. Discussion	50
8. Conclusions	54

A. Moduli couplings	55
A.1 Moduli couplings to ordinary particles	56
A.2 Moduli couplings to supersymmetric particles	59
A.3 Moduli self couplings	61

1. Introduction

The low energy effective action of string compactifications on Calabi-Yau (CY) 3-folds typically has a large number of uncharged massless scalar fields with a flat potential, called moduli. This has been a long-standing problem for string phenomenology, as the values of those moduli determine the various parameters (like masses and coupling constants) of the four-dimensional effective description. Hence, the presence of these massless scalars with effective gravitational coupling would lead to unobserved long range fifth forces, as well as a lack of predictability of the theory.

The last decade has seen a lot of progress towards the resolution of this problem. A major ingredient in these developments was the realization of [1, 2, 3] that nonzero background fluxes induce potentials for some of the moduli. In fact, in type IIA all geometric moduli can be stabilized in this way [4]. In type IIB, on the other hand, one also needs to take into account various perturbative and non-perturbative effects [5, 6]. Hence it may seem that IIA compactifications are under better control. The reason this is not so is that the backreaction of the fluxes on the geometry is more severe in type IIA than in type IIB. As a result, generically in type IIA one has to consider as internal spaces manifolds with $SU(3) \times SU(3)$ structure (see [7] for a comprehensive review). The latter are mathematically much more involved than a Calabi-Yau and so are, in principle, much harder to study. In contrast, in type IIB there is a huge class of solutions, such that the backreaction of the fluxes is entirely encoded by a warp factor. Naturally then, it is within this class of IIB CY flux compactifications that moduli stabilization is best understood at present.

An excellent example of IIB compactifications with stabilized moduli, which is very appealing both for particle physics phenomenology and for cosmology, is given by the LARGE Volume Scenarios (LVS) originally proposed in [6]. According to the general analysis of [8], in these compactifications, α' and g_s corrections are combined with non-perturbative effects to generate a potential for the Kähler moduli, whereas the background fluxes induce a potential for the dilaton and the complex structure moduli. Unlike the KKLT set-up [5], the moduli stabilisation is performed without fine tuning of the values of the internal fluxes and the CY volume is fixed at an exponentially large value (in string units). As a consequence, one has a very reliable four-dimensional effective description, as well as a tool for the generation of phenomenologically desirable hierarchies.

The exponentially large volume minimum of LVS is AdS with broken SUSY, even before any uplifting. In contrast, in KKLT constructions the AdS minimum is supersymmetric and the uplifting term is the source of SUSY breaking. In both cases, however, in addition to this minimum there is always the supersymmetric one at infinity. The two minima are separated by a potential barrier V_b , whose order of magnitude is very well approximated

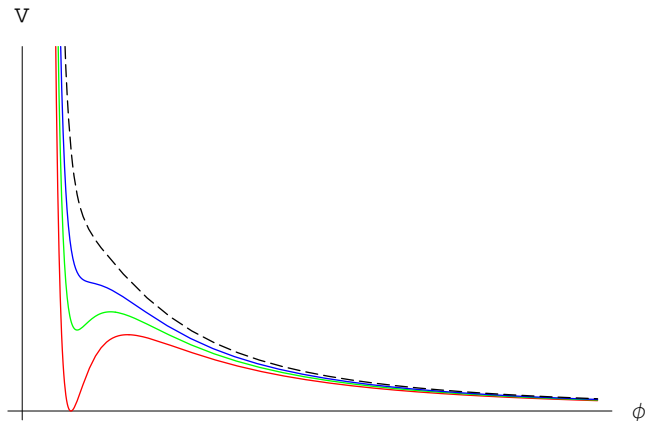


Figure 1: The effective potential V versus the volume modulus ϕ for a typical potential of KKL_T or LARGE Volume compactifications. The different curves show the effect of various sources of energy that, if higher than the barrier of the potential, can lead to a decompactification of the internal space.

by the value of the potential at the AdS vacuum before uplifting. As is well-known, the modulus, related to the overall volume of the Calabi-Yau, couples to any possible source of energy, due to the Weyl rescaling of the metric needed to obtain a 4D supergravity effective action in the Einstein frame. Thus, in the presence of any source of energy, greater than the height of the potential barrier, the system will be driven to a dangerous decompactification limit. For example, during inflation the energy of the inflaton φ could give an additional uplifting term of the form $\Delta V(\varphi, \mathcal{V}) = V(\varphi)/\mathcal{V}^n$ for $n > 0$, that could cause a run-away to infinity [9]. Another source of danger of decompactification is the following. After inflation, the inflaton decays to radiation and, as a result, a high-temperature thermal plasma is formed. This gives rise to temperature-dependent corrections to the moduli potential, which could again destabilise the moduli and drive them to infinity, if the finite-temperature potential has a run-away behaviour. The decompactification temperature, at which the finite-temperature contribution starts dominating over the $T = 0$ potential, is very well approximated by $T_{max} \sim V_b^{1/4}$ since $V_T \sim T^4$. Clearly, T_{max} sets also an upper bound on the reheating temperature after inflation. The discussion of this paragraph is schematically illustrated on Figure 1.

On the other hand, if, instead of having a run-away behaviour, the finite-temperature potential develops new minima, then there could be various phase transitions, which might have played an important role in the early Universe and could have observable signatures today. The presence of minima at high T could also have implications regarding the question how natural it is for the Universe to be in a metastable state at $T = 0$. More precisely, recent studies of various toy models [10, 11, 12, 13, 14] have shown that, despite the presence of a supersymmetric global minimum, it is thermodynamically preferable for a system starting in a high T minimum to end up at low temperatures in a (long-lived) local metastable minimum with broken supersymmetry. Similar arguments, if applicable for more realistic systems, could be of great conceptual value given the present accelerated

expansion of the Universe.

For cosmological reasons then, it is of great importance to understand the full structure of the finite temperature effective potential. We investigate this problem in great detail for the type IIB LVS of [6]. Contrary to the traditional thought that moduli cannot thermalize due to their Planck-suppressed couplings to ordinary matter and radiation, we show that in LVS some of the moduli *can* be in thermal equilibrium with MSSM particles for temperatures well below the Planck scale. The main reason is the presence of an additional large scale in this context, namely the exponentially large CY volume, which enters the various couplings and thus affects the relevant interaction rates. The unexpected result, that some moduli can thermalize, in principle opens up the possibility that the finite temperature potential could develop new minima instead of just having a run-away behaviour as, for example, in [15]. However, we show that this is not the case since, for temperatures below the Kaluza-Klein scale, the T -dependent potential still has a run-away behaviour. Although it is impossible to find exactly the decompactification temperature T_{max} , as it is determined by a transcendental equation, we are able to extract a rather precise analytic estimate for it. As expected, we find that T_{max} is controlled by the SUSY breaking scale: $T_{max}^4 \sim m_{3/2}^3 M_P$. This expression gives also an upper bound on the temperature in the early Universe. We show that this constraint can be translated into a lower bound on the value of the CY volume, by computing the temperature of the Universe T_* , just after the heaviest moduli of LVS decay, and then imposing $T_* < T_{max}$.

Our lower bound implies that, for cosmological reasons, larger values of the volume of the order $\mathcal{V} \sim 10^{15} l_s^6$, which naturally lead to TeV scale supersymmetry, are favoured over smaller values of the order $\mathcal{V} \sim 10^4 l_s^6$, which lead to standard GUT theories. More precisely, what we mean by this is the following. Upon writing the volume as $\mathcal{V} \sim 10^x$ and encoding the fluxes and the Calabi-Yau topology in the definition of a parameter c , we are able to rule out a significant portion of the (x, c) -parameter space that corresponds to small x (for example, for $c = 1$ we obtain $x > 6$). This is rather intriguing, given that other cosmological considerations seem to favour smaller values of the volume. Indeed, the recent inflationary model of [16] requires $\mathcal{V} \sim 10^4 l_s^6$, in order to generate the right amount of density perturbations. Despite that, our lower bound on \mathcal{V} does not represent an unsurmountable obstacle for the realization of inflation. The reason is that the Fibre Inflation model can give rise to inflation even for large values of the volume. Hence, a modification of it, such that the density fluctuations are generated by a curvaton-like field different from the inflaton, would be a perfectly viable model with large \mathcal{V} . The large value of \mathcal{V} would imply a low-energy inflationary scale, and so, in turn, gravity waves would not be observable. However, it is likely that both inflation and TeV scale SUSY could be achieved at the same time, with also the generation of a relevant amount of non-gaussianities in the CMB, which is a typical feature of curvaton models.

On the other hand, we pose a challenge for the solution of the cosmological moduli problem, that the overall breathing mode of LVS with $\mathcal{V} > 10^{10} l_s^6$ is afflicted by [17]. This is so, because we show that unwanted relics cannot be diluted by the entropy released by the decay of the heaviest moduli of LVS, nor by a low-energy period of thermal inflation. More precisely, we show that the heaviest moduli of LVS decay before they can begin to

dominate the energy density of the Universe and, also, that in order to study thermal inflation in the closed string moduli sector, it is necessary to go beyond our low energy EFT description.

The present paper is organized as follows. In Section 2, we review the basic features of the type IIB LVS. In Section 3, we recall the general form of the effective potential at finite temperature and discuss in detail the issue of thermal equilibrium in an expanding Universe. In Section 4, we derive the masses and the couplings to visible sector particles of the moduli and modulini in LVS. Using these results, in Section 5 we investigate moduli thermalization and show that, generically, the moduli corresponding to the small cycles can be in thermal equilibrium with MSSM particles, due to their interaction with the gauge bosons. In Section 6, we study the finite temperature effective potential in LVS. We show that it has a runaway behaviour and find the decompactification temperature T_{max} . Furthermore, we establish a lower bound on the CY volume, which follows from the constraint that the temperature of the Universe just after the small moduli decay should not exceed T_{max} . In Section 7 we discuss some open issues, among which the question why thermal inflation does not occur within our approximations. Finally, after a summary of our results in Section 8, Appendix A contains technical details on the computation of the moduli couplings.

2. Large Volume Scenarios

The distinguishing feature of the type IIB Large Volume Scenarios (LVS) of [6] is that, in addition to the non-perturbative effects considered in [5], they also take into account α' corrections, which lead to moduli stabilisation at an exponentially large volume of the internal manifold. In [6], the Calabi-Yau 3-fold was assumed to have a characteristic topology with one exponentially large cycle and several small del Pezzo 4-cycles. Including string loop corrections, as in [8], extends these scenarios to a larger class of Calabi-Yau manifolds which can also have fibration structure. The exponentially large volume allows to explain many hierarchies observed in nature and guarantees that the low-energy effective field theory is under good control.

In this Section we summarise the basic ingredients of LVS. We begin by recalling necessary material about type IIB flux compactifications. After that we turn to the relevant perturbative and non-perturbative effects and the resulting scalar potential with a LARGE volume minimum.

2.1 Type IIB with fluxes

We will be interested in type IIB CY orientifold compactifications with background fluxes, which preserve $\mathcal{N} = 1$ supersymmetry in 4D [3]. The effective low-energy description is then given by a $d = 4$, $\mathcal{N} = 1$ supergravity characterised by a Kähler potential K , a superpotential W and a gauge kinetic function f_{ab} , where the indices a, b run over the various vector multiplets. In particular, the scalar potential of this theory has the standard

form:

$$V = e^{K/M_P^2} \left(K^{i\bar{j}} D_i W D_{\bar{j}} \bar{W} - 3 \frac{|W|^2}{M_P^2} \right), \quad (2.1)$$

where i, j run over all moduli of the compactification. Generically, the latter consist of the axio-dilaton $S = e^{-\phi} + iC_0$, $h_{1,1}$ Kähler (T -moduli) and $h_{2,1}$ complex structure moduli (U -moduli). The tree level Kähler potential has the following form:

$$\frac{K_{tree}}{M_P^2} = -\ln(S + \bar{S}) - 2 \ln \mathcal{V} - \ln \left(-i \int_{CY} \Omega \wedge \bar{\Omega} \right), \quad (2.2)$$

where \mathcal{V} is the Einstein frame CY volume, in units of the string length $l_s = 2\pi\sqrt{\alpha'}$, and Ω is the CY holomorphic (3,0)-form. Note that the T -moduli enter K_{tree} only through \mathcal{V} and the U -moduli only through Ω . For later purposes, it will be useful to recall a couple of relations regarding the Kähler moduli. Expanding the Kähler form $J = \sum_{i=1}^{h_{1,1}} t^i D_i$ in a basis $\{D_i\}$ of $H^{1,1}(CY, \mathbb{Z})$ and considering orientifold projections such that $h_{1,1}^- = 0 \Rightarrow h_{1,1}^+ = h_{1,1}$, we obtain:

$$\mathcal{V} = \frac{1}{6} \int_{CY} J \wedge J \wedge J = \frac{1}{6} k_{ijk} t^i t^j t^k, \quad (2.3)$$

where k_{ijk} are related to the triple intersection numbers of the CY and the t^i are 2-cycle volumes. The volumes of the Poincaré dual 4-cycles are given by:

$$\tau_i = \frac{\partial \mathcal{V}}{\partial t^i} = \frac{1}{2} \int_{CY} D_i \wedge J \wedge J = \frac{1}{2} k_{ijk} t^j t^k. \quad (2.4)$$

Finally, the scalar components of the chiral superfields, corresponding to the Kähler moduli, that enter the 4D effective action are $T_i = \tau_i + i b_i$, where the axions b_i are the components of the RR 4-form C_4 along the 4-cycle Poincaré dual to D_i . Obviously, from (2.3) and (2.4) one can express \mathcal{V} in (2.2) as a function of $\tau_i = \frac{1}{2}(T_i + \bar{T}_i)$.

Now, turning on background fluxes $G_3 = F_3 + iSH_3$, where F_3 and H_3 are respectively the RR and NSNS 3-form fluxes of type IIB supergravity (for recent reviews on flux compactifications, see [18]), generates an effective superpotential of the form [1]¹:

$$W_{tree} \sim \int_{CY} G_3 \wedge \Omega. \quad (2.5)$$

As a result, one can stabilise the axio-dilaton S and the U -moduli. However, the Kähler moduli T_i do not enter W_{tree} and therefore remain massless at leading semiclassical level. One can obtain an effective description for these fields by integrating out S and U .² Then the superpotential is constant, $W = \langle W_{tree} \rangle \equiv W_0$, and the Kähler potential reads $K = K_{cs} - \ln(2/g_s) + K_0$ with

$$K_0 = -2 \ln \mathcal{V} \quad \text{and} \quad e^{-K_{cs}} = \left\langle -i \int_{CY} \Omega \wedge \bar{\Omega} \right\rangle. \quad (2.6)$$

¹We neglect the effect of warping, generated by non-zero background fluxes, since we will be considering CY compactifications with large internal volume.

²For more details on the consistent supersymmetric implementation of this procedure, see [19].

Before concluding this Subsection, let us make a couple of remarks. First, note that the background flux G_3 may or may not break the remaining 4D $\mathcal{N} = 1$ supersymmetry, depending on whether or not $D_\alpha W = \partial_\alpha W + W \partial_\alpha K$ vanishes at the minimum of the resulting scalar potential. Second, the Kähler potential K_0 satisfies the no-scale property $K_0^{i\bar{j}} \partial_i K_0 \partial_{\bar{j}} K_0 = 3$, which implies that the scalar potential for the Kähler moduli vanishes in accord with the statement above that the fluxes do not stabilise those moduli.

2.2 Leading order corrections

As we recalled in the previous Subsection, at leading semiclassical order the scalar potential for the T -moduli vanishes. So, unlike the situation for the S and U -moduli, in order to stabilise T_i one has to consider the leading order corrections to the tree level action. The first such corrections to be studied were non-perturbative contributions to W . Recall that there is a non-renormalisation theorem forbidding W to be corrected perturbatively. On the other hand, the Kähler potential K does receive perturbative corrections both in α' and in g_s . Therefore, non-perturbative effects are subleading in K and we shall neglect them in the following. Let us now review briefly all these kinds of corrections.

2.2.1 Non-perturbative corrections

Non-perturbative corrections to the superpotential can be due to Euclidean D3 brane (ED3) instantons wrapping 4-cycles in the extra dimensions, or to gaugino condensation in the supersymmetric gauge theories located on D7 branes that also wrap internal 4-cycles. The superpotential that both kinds of effects generate is of the form:³

$$W = \frac{M_P^3}{\sqrt{4\pi}} \left(W_0 + \sum_i A_i e^{-a_i T_i} \right), \quad (2.7)$$

where the coefficients A_i correspond to threshold effects and, in principle, can depend on U and D3 position moduli, but not on T_i . The constants a_i are given by $a_i = 2\pi$ for ED3 branes, and by $a_i = 2\pi/N$ for gaugino condensation in an $SU(N)$ gauge theory. Note that one can neglect multi-instanton effects in (2.7), as long as τ_i are stabilised such that $a_i \tau_i \gg 1$. From (2.1), the above superpotential leads to the following T_i -dependent contribution to the scalar potential (up to a numerical prefactor and powers of g_s and M_P , that we will be more precise about below):

$$\delta V_{(np)} = e^{K_0} K_0^{j\bar{i}} \left[a_j A_j a_i \bar{A}_i e^{-(a_j T_j + a_i \bar{T}_i)} - \left(a_j A_j e^{-a_j T_j} \bar{W} \partial_{\bar{i}} K_0 + a_i \bar{A}_i e^{-a_i \bar{T}_i} W \partial_j K_0 \right) \right]. \quad (2.8)$$

³The prefactor in (2.7) is due to careful dimensional reduction, as can be seen in Appendix A of [29]. However, the authors of [29] define the Einstein metric via $g_{\mu\nu,s} = e^{(\phi - \langle \phi \rangle)/2} g_{\mu\nu,E}$, so that it coincides with the string frame metric in the physical vacuum. On the contrary, we opt for the more traditional definition $g_{\mu\nu,s} = e^{\phi/2} g_{\mu\nu,E}$, which implies no factor of g_s in the prefactor of W .

2.2.2 α' corrections

The Kähler potential receives corrections at each order in the α' expansion. In the effective supergravity description these correspond to higher derivative terms. The leading α' contribution comes from the R^4 term and it leads to the following Kähler potential [30]:

$$\frac{K}{M_P^2} = -2 \ln \left(\mathcal{V} + \frac{\xi}{2g_s^{3/2}} \right) \simeq -2 \ln \mathcal{V} - \frac{\xi}{g_s^{3/2} \mathcal{V}}. \quad (2.9)$$

Here ξ is given by $\xi = -\frac{\chi \zeta(3)}{2(2\pi)^3}$, where $\chi = 2(h_{1,1} - h_{2,1})$ is the CY Euler number, and the Riemann zeta function is $\zeta(3) \simeq 1.2$. Denoting for convenience $\hat{\xi} \equiv \xi/g_s^{3/2}$, eq. (2.9) implies to leading order the following contribution to V (again, up to a prefactor containing powers of g_s and M_P):

$$\delta V_{(\alpha')} = 3e^{K_0} \hat{\xi} \frac{(\hat{\xi}^2 + 7\hat{\xi}\mathcal{V} + \mathcal{V}^2)}{(\mathcal{V} - \hat{\xi})(2\mathcal{V} + \hat{\xi})^2} W_0^2 \simeq \frac{3\xi W_0^2}{4g_s^{3/2} \mathcal{V}^3}, \quad (2.10)$$

where $\mathcal{V} \gg \hat{\xi} \gg 1$ in order for perturbation theory to be valid.

2.2.3 g_s corrections

The Kähler potential receives also string loop corrections. At present, there is no explicit derivation of these corrections from string scattering amplitudes for a generic CY compactification. Nevertheless, it has been possible to conjecture their form indirectly [20]:

$$\delta K_{(g_s)} = \delta K_{(g_s)}^{KK} + \delta K_{(g_s)}^W, \quad (2.11)$$

where

$$\delta K_{(g_s)}^{KK} \sim \sum_{i=1}^{h_{1,1}} \frac{g_s \mathcal{C}_i^{KK}(U, \bar{U}) (a_{il} t^l)}{\mathcal{V}}, \quad (2.12)$$

and

$$\delta K_{(g_s)}^W \sim \sum_i \frac{\mathcal{C}_i^W(U, \bar{U})}{(a_{il} t^l) \mathcal{V}}. \quad (2.13)$$

In (2.11), $\delta K_{(g_s)}^{KK}$ comes from the exchange of closed strings, carrying Kaluza-Klein momentum, between D7- and D3-branes. The expression (2.12) is valid for vanishing open string scalars and is based on the assumption that all the $h_{1,1}$ 4-cycles of the CY are wrapped by D7-branes. The other term $\delta K_{(g_s)}^W$ in (2.12) is due, from the closed string perspective, to the exchange of winding strings between intersecting stacks of D7-branes.

In addition, in (2.12) the linear combination $(a_{il} t^l)$ of the volumes of the basis 2-cycles is transverse to the 4-cycle wrapped by the i -th D7-brane, whereas in (2.13) it gives the 2-cycle where two D7-branes intersect. The functions $\mathcal{C}_i^{KK}(U, \bar{U})$ and $\mathcal{C}_i^W(U, \bar{U})$ are, in principle, unknown. However, for our purposes they can be viewed as $\mathcal{O}(1)$ constants⁴ since

⁴In the $T^6/(\mathbb{Z}_2 \times \mathbb{Z}_2)$ orientifold case, where these constants can be computed explicitly [21], they turn out to be, in our conventions, of $\mathcal{O}(1)$ for natural values of the complex structure moduli: $\text{Re}(U) \sim \text{Im}(U) \sim \mathcal{O}(1)$. Note that [21] uses conventions different from ours.

the complex structure moduli are already stabilised at the classical level by background fluxes.

Comparing (2.12) with (2.9), we notice that $\delta K_{(g_s)}^{KK}$ is generically leading with respect to $\delta K_{(\alpha')}$ due to the presence of the linear combination $(a_{il}t^l)$ in the numerator of (2.12) and the fact that each 4-cycle volume $\tau_i = \frac{1}{2}k_{ijk}t^jt^k$ has to be fixed larger than the string scale in order to trust the effective field theory. However, in ref. [22] it was discovered that for an arbitrary CY background, the leading contribution of (2.12) to the scalar potential is vanishing, so leading to an *extended no-scale structure*. This result renders $\delta V_{(g_s)}$ generically subleading with respect to $\delta V_{(\alpha')}$ and the final formula can be expressed as (neglecting a prefactors with powers of g_s and M_P):

$$\delta V_{(g_s)}^{1-loop} = \left[(g_s \mathcal{C}_i^{KK})^2 a_{ik} a_{ij} K_{k\bar{j}}^0 - 2\delta K_{(g_s)}^W \right] \frac{W_0^2}{\mathcal{V}^2}. \quad (2.14)$$

Notice that for branes wrapped only around the basis 4-cycles the combination appearing in the first term degenerates to $a_{ik} a_{ij} K_{k\bar{j}}^0 = K_{i\bar{i}}^0$. The fact that $\delta V_{(g_s)}$ is generically subleading with respect to $\delta V_{(\alpha')}$ can be easily seen by recalling the generic expression of the tree-level Kähler metric for an arbitrary CY: $K_{i\bar{j}}^0 = t_i t_{\bar{j}} / (2\mathcal{V}^2) - (k_{i\bar{j}k} t^k)^{-1} / \mathcal{V} \sim 1 / (\mathcal{V} t)$. Therefore the ratio between $\delta V_{(\alpha')}$ given by (2.10) (with $\xi \sim \mathcal{O}(1)$ for known CY three-folds) and the expression (2.14) for $\delta V_{(g_s)}$, scales as $\delta V_{(\alpha')} / \delta V_{(g_s)} \sim g_s^{-3/2} t \gg 1$ due to the fact that the size of each two-cycle has to be fixed at a value larger than 1 (in string units) in order to trust the effective field theory and, in addition, the string coupling has to be smaller than unity in order to be in the perturbative regime.

2.3 Moduli stabilisation in LVS

Combining (2.8), (2.10) and (2.14), we obtain the final form of the Kähler moduli effective scalar potential, that contains all the leading order corrections to the vanishing tree-level part (with all prefactors included):

$$\begin{aligned} V &= V_{tree} + \delta V_{(np)} + \delta V_{(\alpha')} + \delta V_{(g_s)}^{1-loop} = \\ &= \frac{g_s e^{K_{cs}} M_P^4}{8\pi \mathcal{V}^2} \left\{ K_0^{j\bar{i}} a_j A_j a_i \bar{A}_i e^{-(a_j T_j + a_i \bar{T}_i)} + 4W_0 \sum_i a_i A_i \tau_i \cos(a_i b_i) e^{-a_i \tau_i} \right. \\ &\quad \left. + \left[\frac{3\xi}{g_s^{3/2}} + \sum_i \left(g_s^2 (\mathcal{C}_i^{KK})^2 \left(\frac{1}{2} \frac{t_i^2}{\mathcal{V}} - A^{ii} \right) - 8 \frac{\mathcal{C}_i^W}{(a_{il} t^l)} \right) \right] \frac{W_0^2}{4\mathcal{V}} \right\}, \end{aligned} \quad (2.15)$$

where $A_{ij} \equiv \frac{\partial \tau_i}{\partial t_j} = k_{ijk} t^k$. Ref. [8] derived the topological conditions that an arbitrary CY has to satisfy in order for the general potential (2.15) to have a non-supersymmetric AdS minimum at *exponentially large* volume. These conditions can be summarised as follows:

1. $h_{2,1} > h_{1,1} > 1 \Leftrightarrow \xi \sim (h_{2,1} - h_{1,1}) > 0$,
2. The CY 3-fold has to have at least one Kähler modulus corresponding to a blow-up mode resolving a point-like singularity (the volume of a del Pezzo 4-cycle).

These conditions give rise to two different LVS. In the first case, the CY has a typical Swiss-cheese topological structure where there is just one LARGE cycle controlling the size of the overall volume and all the other 4-cycles are blow-up modes. The string loop corrections turn out to be negligible. On the other hand, in the case of fibred CY manifolds, with the presence of modes which do not resolve point-like singularities or correspond to the overall volume modulus, g_s corrections play a crucial role to lift the fibration moduli that are left unfixed by $\delta V_{(np)} + \delta V_{(\alpha')}$ (more precisely, the string loop corrections for these modes are always dominant compared to non-perturbative effects). Let us now describe these two cases in more detail.

2.3.1 Swiss-cheese Calabi-Yaus

The original example of LVS of [6], and the one we will study in most detail, is the degree 18 hypersurface in $\mathbb{C}P^4_{[1,1,1,6,9]}$ whose volume is given by

$$\mathcal{V} = \frac{1}{9\sqrt{2}} \left(\tau_b^{3/2} - \tau_s^{3/2} \right), \quad (2.16)$$

where τ_b and τ_s are the two Kähler moduli and the subscripts b and s stand for *big* and *small* respectively. The general expression (2.15) for the scalar potential, in this case takes the form

$$V = \frac{g_s e^{K_{cs}} M_P^4}{8\pi} \left(\lambda \sqrt{\tau_s} \frac{e^{-2a_s \tau_s}}{\mathcal{V}} - \mu \frac{\tau_s e^{-a_s \tau_s}}{\mathcal{V}^2} + \frac{\nu}{\mathcal{V}^3} + \frac{\sigma}{\mathcal{V}^3 \sqrt{\tau_s}} + \frac{\rho}{\mathcal{V}^{10/3}} \right), \quad (2.17)$$

with

$$\lambda = 24\sqrt{2} a_s^2 A_s^2, \quad \mu = 4a_s A_s W_0, \quad \nu = \frac{3\xi W_0^2}{4g_s^{3/2}}, \quad \sigma = (g_s \mathcal{C}_s^{KK} W_0)^2, \quad \rho = \frac{(g_s \mathcal{C}_b^{KK} W_0)^2}{(9\sqrt{2})^{1/3}}. \quad (2.18)$$

Also, in (2.17) the minimisation with respect to the axion b_s has already been performed. For natural values of the tree-level superpotential $W_0 \sim \mathcal{O}(1)$, the scalar potential (2.17) admits a non-supersymmetric AdS minimum at exponentially large volume due to the interplay of α' and non-perturbative effects. This minimum is located at

$$\mathcal{V} \sim W_0 e^{a_s \tau_s} \gg \tau_s \sim \hat{\xi}^{2/3} \gg 1. \quad (2.19)$$

The string loop corrections can be safely neglected since they are subdominant relative to the other corrections due to inverse powers of \mathcal{V} and factors of g_s . There are several ways to up-lift this minimum to Minkowski or dS: adding $\overline{D3}$ branes [5], considering D-terms from magnetised D7 branes [27] or F-terms from a hidden sector [28] etc.

An immediate generalisation of the $\mathbb{C}P^4_{[1,1,1,6,9]}$ model is given by the so called ‘Swiss-cheese’ Calabi-Yaus, whose volume looks like

$$\mathcal{V} = \alpha \left(\tau_b^{3/2} - \sum_{i=1}^{N_{small}} \lambda_i \tau_i^{3/2} \right), \quad \alpha > 0, \quad \lambda_i > 0 \quad \forall i = 1, \dots, N_{small}. \quad (2.20)$$

Examples having this form with $h_{1,1} = 3$ are the the degree 15 hypersurface embedded in $\mathbb{C}P^4_{[1,3,3,3,5]}$ and the degree 30 hypersurface in $\mathbb{C}P^4_{[1,1,3,10,15]}$ [23]. More generally, in ref. [25] it was proved that examples of Swiss-cheese CY 3-folds with $h_{1,1} = n + 2$, $0 \leq n \leq 8$, can be obtained by starting from elliptically fibred CY manifolds over a del Pezzo dP_n base⁵, and then performing particular flop transitions that flop away all n $\mathbb{C}P^1$ -cycles in the base. In this case, assuming that all the small cycles get non-perturbative effects, the 4-cycle τ_b , controlling the overall size of the CY, is stabilised exponentially large, $\mathcal{V} \simeq \alpha \tau_b^{3/2} \sim W_0 e^{a_i \tau_i}$, while the various 4-cycles, τ_i , controlling the size of the ‘holes’ of the Swiss-cheese, get fixed at small values $\tau_i \sim \mathcal{O}(10)$, $\forall i = 1, \dots, N_{small}$. However, in ref. [24] it was discovered that the Swiss-cheese structure of the volume is not enough to guarantee that all the rigid ‘small’ cycles τ_i can indeed be stabilised small. In fact, a further condition is that each rigid ‘small’ cycle τ_i must be del Pezzo. In [24], there are 3 examples of Swiss-cheese CY 3-folds with $h_{1,1} = 4$ where just one 4-cycle has the topology $\mathbb{C}P^2$ (and so it is dP_0).

2.3.2 Fibred Calabi-Yaus

The first examples of LVS with a topological structure more complicated than the Swiss-cheese one, were discovered in [8]. The authors focused on a K3 fibred CY with $h_{2,1} > h_{1,1} = 3$, obtained by adding a blow-up mode to the geometry $\mathbb{C}P^4_{[1,1,2,2,6]}$. The volume reads:

$$\mathcal{V} = \alpha \left(\sqrt{\tau_1} \tau_2 - \gamma \tau_s^{3/2} \right) = t_1 \tau_1 - \alpha \gamma \tau_s^{3/2}, \quad (2.21)$$

where the constants α and γ are positive, and t_1 is the volume of the $\mathbb{C}P^1$ base of the K3 fibration. Working in the parameter regime $\tau_2 > \tau_1 \gg \tau_s$, where the volume of the CY is large, while the blow-up cycle τ_s remains comparatively small⁶, the general expression (2.15) for V becomes (having already minimised V with respect to the axion $b_s = \text{Im} T_s$):

$$V = \frac{g_s e^{K_{cs}} M_P^4}{8\pi} \left[\beta \sqrt{\tau_s} \frac{e^{-2a_s \tau_s}}{\mathcal{V}} - \mu \frac{\tau_s e^{-a_s \tau_s}}{\mathcal{V}^2} + \frac{\nu}{\mathcal{V}^3} + \left(\frac{A}{\tau_1^2} - \frac{B}{\mathcal{V} \sqrt{\tau_1}} + \frac{C \tau_1}{\mathcal{V}^2} \right) \frac{W_0^2}{\mathcal{V}^2} \right], \quad (2.22)$$

with λ , μ and ν as given in (2.18) and

$$\beta = \frac{\lambda}{9\sqrt{2}\alpha\gamma}, \quad A = (g_s C_1^{KK})^2, \quad B = 4\alpha C_{12}^W, \quad C = 2(\alpha g_s C_2^{KK})^2. \quad (2.23)$$

It is evident that the leading $\delta V_{(\alpha')} + \delta V_{(np)}$ part of the potential depends only on two Kähler moduli, \mathcal{V} and τ_s , instead of all three. And, in fact, it turns out to be of exactly the same form as (2.17) above. Hence, viewing \mathcal{V} , τ_s and τ_1 as the three independent moduli (instead of τ_1 , τ_2 and τ_s), it is clear that, without taking into account the subleading g_s corrections, τ_1 is a flat direction of the scalar potential. Also, it is evident that at this order, \mathcal{V} and τ_s are stabilised as in the $\mathbb{C}P^4_{[1,1,1,6,9]}$ model of Subsection 2.3.1:

$$\langle \tau_s \rangle = \left(\frac{\hat{\xi}}{2\alpha\gamma} \right)^{2/3} \quad \text{and} \quad \langle \mathcal{V} \rangle = \left(\frac{3\alpha\gamma}{4a_s A_s} \right) W_0 \sqrt{\langle \tau_s \rangle} e^{a_s \langle \tau_s \rangle}. \quad (2.24)$$

⁵A del Pezzo dP_n surface is obtained by blowing-up $\mathbb{C}P^2$ (or $\mathbb{C}P^1 \times \mathbb{C}P^1$) on $0 \leq n \leq 8$ points.

⁶in this limit $t_1 \sim \tau_2 / \sqrt{\tau_1} > \sqrt{\tau_1}$, corresponding to interesting geometries having the two dimensions of the base, spanned by the cycle t_1 , larger than the other four of the K3 fibre, spanned by τ_1 .

	g_s	ξ	W_0	a_3	A_3	α	γ	C_1^{KK}	C_2^{KK}	C_{12}^W	$\langle \tau_s \rangle$	$\langle \tau_1 \rangle$	$\langle \mathcal{V} \rangle$
LV	0.1	0.4	1	π	1	0.5	0.39	0.1	0.1	5	10.5	10^6	$3 \cdot 10^{13}$
SV	0.3	0.9	100	$\pi/5$	1	0.13	3.65	0.15	0.08	1	4.3	9	1710

Table 1: Some model parameters.

Obviously, loop corrections shift insignificantly the VEVs of these two moduli. However, g_s corrections are crucial to generate a potential for τ_1 that admits a minimum at

$$\frac{1}{\tau_1^{3/2}} = \left(\frac{B}{8A\mathcal{V}} \right) \left[1 + (\text{sign } B) \sqrt{1 + \frac{32AC}{B^2}} \right]. \quad (2.25)$$

Some concrete numerical choices for the various underlying parameters, without any fine-tuning, are listed in Table 1. The ‘LV’ case gives very large volumes, $\mathcal{V} \simeq 10^{13}$ and the modulus τ_1 is stabilised at hierarchically large values, $\tau_2 > \tau_1 \gg \tau_s$. The string scale and the gravitino mass turn out to be

$$M_s = \frac{M_P}{\sqrt{4\pi\mathcal{V}}} \sim 10^{11} \text{GeV}, \quad m_{3/2} = e^{K/2M_P^2} \frac{W}{M_P^2} = \frac{g_s^{1/2} e^{K_{cs}/2} W_0 M_P}{\sqrt{8\pi\mathcal{V}}} \sim 10 \text{TeV}. \quad (2.26)$$

This gives a solution of the hierarchy problem but the huge value of the volume destroys the standard picture of gauge coupling unification. The ‘SV’ case instead has $\mathcal{V} \sim 10^3$ much smaller (and so with $M_s \sim M_{GUT}$ and a very high gravitino mass). This set of parameter values is not chosen just in relation to GUT theories but also in order to provide observable density fluctuations for the inflationary model of [16]. In that model, the inflaton is the modulus τ_1 , whose potential is loop-generated, and the main feature of the model is that it produces detectable gravity waves.

More general examples of this kind of LVS have been discovered in [25]. These authors noticed that starting from an elliptically fibred CY over a dP_n base, and then flopping away only $r < n$ (instead of all n) of the CP^1 -cycles in the base, one obtains another elliptically fibred CY (instead of a Swiss-cheese one), whose volume looks like:

$$\mathcal{V} = \text{Vol}(X_{n-r}) - \sum_{i=1}^r \lambda_i \tau_i^{3/2}, \quad \lambda_i > 0 \quad \forall i = 1, \dots, r, \quad (2.27)$$

where X_{n-r} is the resulting elliptical fibration over a dP_{n-r} base. It is natural to expect that the scalar potential for these examples has an AdS minimum at exponentially large volume, together with $(h_{1,1} - N_{\text{small}} - 1) = n - r$ flat directions that will be lifted by g_s corrections.

We should note that string loop corrections can play an important role for compactifications on Swiss-cheese CY manifolds as well. Namely, they can be crucial, even in this case, to achieve full moduli stabilisation when the topological condition, that all rigid 4-cycles be del Pezzo, is not satisfied or when one imposes the phenomenological condition that the 4-cycles supporting chiral matter do not get non-perturbative effects [23].⁷

⁷Also D-terms could play a significant role as pointed out still in [23].

3. Effective potential at finite temperature

At nonzero temperature, the effective potential receives a temperature-dependent contribution. The latter is determined by the particle species that are in thermal equilibrium and, more precisely, by their masses and couplings. In this Section, we review the general form of the finite temperature effective potential and discuss in detail the establishment of thermal equilibrium in an expanding Universe. In particular, we elaborate on the relevant interactions at the microscopic level. This lays the foundation for the explicit computation, in Section 6.1, of the finite temperature effective potential in LVS.

3.1 General form of temperature corrections

The general structure of the effective scalar potential is the following one:

$$V_{TOT} = V_0 + V_T, \quad (3.1)$$

where V_0 is the $T = 0$ potential and V_T the thermal correction. As discussed in Section 2, V_0 has the general form:

$$V_0 = \delta V_{(np)} + \delta V_{(\alpha')} + \delta V_{(g_s)}, \quad (3.2)$$

where the tree level part is null due to the no-scale structure (recall that we are studying the scalar potential for the Kähler moduli), $\delta V_{(np)}$ arises due to non-perturbative effects, $\delta V_{(\alpha')}$ are α' corrections and the contribution $\delta V_{(g_s)}$ comes from string loops and, as noticed in [22], matches the Coleman-Weinberg potential of the effective field theory. In addition, $\delta V_{(g_s)}$ has an extended no-scale structure, which is crucial for the robustness of LVS since it renders $\delta V_{(g_s)}$ subleading with respect to $\delta V_{(np)}$ and $\delta V_{(\alpha')}$.

On the other hand, the finite temperature corrections V_T have the generic loop expansion:

$$V_T = V_T^{1-loop} + V_T^{2-loops} + \dots \quad (3.3)$$

The first term V_T^{1-loop} is a 1-loop thermal correction describing an ideal gas of non-interacting particles. It has been derived for a renormalisable field theory in flat space in [33], using the zero-temperature functional integral method of [34], and reads:

$$V_T^{1-loop} = \pm \frac{T^4}{2\pi^2} \int_0^\infty dx x^2 \ln \left(1 \mp e^{-\sqrt{x^2 + m(\varphi)^2/T^2}} \right), \quad (3.4)$$

where the upper (lower) signs are for bosons (fermions) and m is the background field dependent mass parameter. At temperatures much higher than the mass of the particles in the thermal bath, $T \gg m(\varphi)$, the 1-loop finite temperature correction (3.4) has the following expansion:

$$V_T^{1-loop} = -\frac{\pi^2 T^4}{90} \alpha + \frac{T^2 m(\varphi)^2}{24} + \mathcal{O}(T m(\varphi)^3), \quad (3.5)$$

where for bosons $\alpha = 1$ and for fermions $\alpha = 7/8$. The generalisation of (3.5) to supergravity, coupled to an arbitrary number of chiral superfields, takes the form [31]:

$$V_T^{1-loop} = -\frac{\pi^2 T^4}{90} \left(g_B + \frac{7}{8} g_F \right) + \frac{T^2}{24} (Tr M_b^2 + Tr M_f^2) + \mathcal{O}(T M_b^3), \quad (3.6)$$

where g_B and g_F are, respectively, the numbers of bosonic and fermionic degrees of freedom and M_b and M_f are the moduli-dependent bosonic and fermionic mass matrices of all the particles forming the thermal plasma.

If the particles in the thermal bath interact among themselves, we need to go beyond the ideal gas approximation. The effect of the interactions is taken into account by evaluating higher thermal loops. The high temperature expansion of the 2-loop contribution looks like:

$$V_T^{2-loops} = \alpha_2 T^4 \left(\sum_i f_i(g_i) \right) + \beta_2 T^2 (Tr M_b^2 + Tr M_f^2) \left(\sum_i f_i(g_i) \right) + \dots, \quad (3.7)$$

where α_2 and β_2 are known constants, i runs over all the interactions through which different species reach thermal equilibrium, and the functions f_i are determined by the couplings g_i and the number of bosonic and fermionic degrees of freedom. For example, for gauge interactions $f(g) = const \times g^2$, whereas for the scalar $\lambda\phi^4$ theory one has that $f(\lambda) = const \times \lambda$.

Now, since we are interested in the moduli-dependence of the finite temperature corrections to the scalar potential, we can drop the first term on the RHS of (3.6) and focus only on the T^2 term, which indeed inherits moduli-dependence from the bosonic and fermionic mass matrices. However, notice that in string theory the various couplings are generically functions of the moduli. Thus, also the first term on the RHS of (3.7) depends on the moduli and, even though it is a 2-loop effect, it could compete with the second term on the RHS of (3.6), because it scales as T^4 whereas the latter one scales only as T^2 . This issue has to be addressed on a case by case basis, by studying carefully what particles form the thermal bath.

3.2 Thermal equilibrium

In an expanding Universe, a particle species is in equilibrium with the thermal bath if its interaction rate, Γ , with the particles in that bath is larger than the expansion rate of the Universe. The latter is given by $H \sim g_*^{1/2} T^2 / M_P$, during the radiation dominated epoch, with g_* being the total number of degrees of freedom. Thermal equilibrium can be established and maintained by $2 \leftrightarrow 2$ interactions, like scattering or annihilation and the inverse pair production processes, and also by $1 \leftrightarrow 2$ processes, like decays and inverse decays (single particle productions). Let us now consider each of these two cases in detail.

3.2.1 $2 \leftrightarrow 2$ interactions

In this case the thermally averaged interaction rate can be inferred on dimensional grounds by noticing that:

$$\langle \Gamma \rangle \sim \frac{1}{\langle t_c \rangle}, \quad (3.8)$$

where $\langle t_c \rangle$ is the mean time between two collisions (interactions). Moreover

$$t_c \sim \frac{1}{n\sigma v}, \quad (3.9)$$

where n is the number density of the species, σ is the effective cross section and v is the relative velocity between the particles. Thus $\langle \Gamma \rangle \sim n \langle \sigma v \rangle$. For relativistic particles, one has that $\langle v \rangle \sim c$ ($\equiv 1$ in our units) and also $n \sim T^3$. Therefore

$$\langle \Gamma \rangle \sim \langle \sigma \rangle T^3. \quad (3.10)$$

The cross-section σ has dimension of $(length)^2$ and for $2 \leftrightarrow 2$ processes its thermal average scales with the temperature as:

1. For renormalisable interactions:

$$\langle \sigma \rangle \sim \alpha^2 \frac{T^2}{(T^2 + M^2)^2}, \quad (3.11)$$

where $\alpha = g^2/(4\pi)$ (g is the gauge coupling) and M is the mass of the particle mediating the interactions under consideration.

- a) For long-range interactions $M = 0$ and (3.11) reduces to:

$$\langle \sigma \rangle \sim \alpha^2 T^{-2} \Rightarrow \langle \Gamma \rangle \sim \alpha^2 T. \quad (3.12)$$

This is also the form that (3.11) takes for short-range interactions at energies $E \gg M$.

- b) For short-range interactions at scales lower than the mass of the mediator, the coupling constant becomes dimensionful and (3.11) looks like:

$$\langle \sigma \rangle \sim \alpha^2 \frac{T^2}{M^4} \Rightarrow \langle \Gamma \rangle \sim \alpha^2 \frac{T^5}{M^4}. \quad (3.13)$$

2. For processes including gravity:

- a) Processes with two gravitational vertices:

$$\langle \sigma \rangle \sim d \frac{T^2}{M_P^4} \Rightarrow \langle \Gamma \rangle \sim d \frac{T^5}{M_P^4}, \quad (3.14)$$

where d is a dimensionless moduli-dependent constant.

- b) Processes with one renormalisable and one gravitational vertex:

$$\langle \sigma \rangle \sim \sqrt{d} \frac{g^2}{M_P^2} \Rightarrow \langle \Gamma \rangle \sim \sqrt{d} \frac{g^2 T^3}{M_P^2}, \quad (3.15)$$

where d is the same moduli-dependent constant as before.

Let us now compare these interaction rates with the expansion rate of the Universe, $H \sim g_*^{1/2} T^2 / M_P$, in order to determine at what temperatures various particle species reach or drop out of thermal equilibrium, depending on the degree of efficiency of the relevant interactions.

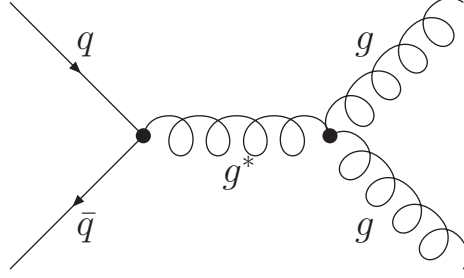


Figure 2: QCD scattering process $q\bar{q} \rightarrow gg$ through which quarks and gluons reach thermal equilibrium.

1.a) Renormalisable interactions with massless mediators:

$$\langle \Gamma \rangle > H \Leftrightarrow \alpha^2 T > g_*^{1/2} T^2 M_P^{-1} \Rightarrow T < \alpha^2 g_*^{-1/2} M_P. \quad (3.16)$$

QCD processes, like the ones shown in Figure 2, are the main examples of this kind of interactions. The same behaviour of σ is expected also for the other MSSM gauge groups for energies above the EW symmetry breaking scale. Therefore, MSSM particles form a thermal bath via strong interactions for temperatures $T < \alpha_s^2 g_*^{-1/2} M_P \sim 10^{15}$ GeV [36].

1.b) Renormalisable interactions with massive mediators:

$$\langle \Gamma \rangle > H \Leftrightarrow \alpha^2 \frac{T^5}{M^4} > g_*^{1/2} \frac{T^2}{M_P} \Rightarrow \left(\frac{g_*^{1/2} M^4}{\alpha^2 M_P} \right)^{1/3} < T < M. \quad (3.17)$$

Examples of interactions with effective dimensionful couplings are weak interactions below M_{EW} . In this case, the theory is well described by the Fermi Lagrangian. An interaction between electrons and neutrinos, like the one shown in Figure 3, gives rise to a cross-section of the form of (3.13):

$$\langle \sigma_w \rangle \sim \frac{\alpha_w^2}{M_Z^4} \langle p^2 \rangle \sim \frac{\alpha_w^2}{M_Z^4} T^2, \quad (3.18)$$

where α_w is the weak fine structure constant and $p \sim T$. Thus, neutrinos are coupled to the thermal bath if and only if

$$T > \left(\frac{g_*^{1/2} M_Z^4}{\alpha_w^2 M_P} \right)^{1/3} \sim 1 \text{ MeV}. \quad (3.19)$$

2. Gravitational interactions:

$$\text{a) } \langle \Gamma \rangle > H \Leftrightarrow d \frac{T^5}{M_P^4} > g_*^{1/2} \frac{T^2}{M_P} \Rightarrow T > g_*^{1/6} \frac{M_P}{d^{1/3}}. \quad (3.20)$$

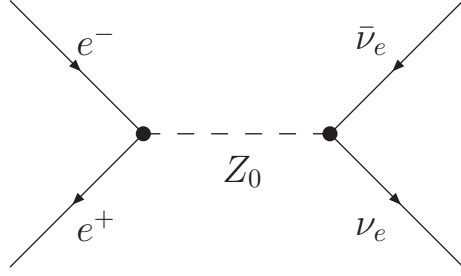


Figure 3: Weak interaction between electrons and neutrinos through which they reach thermal equilibrium.

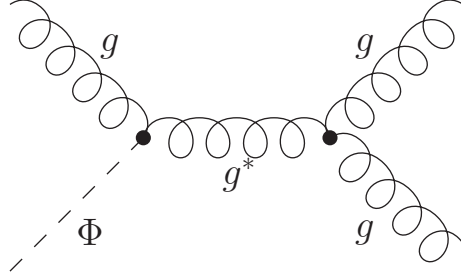


Figure 4: Scattering process $\Phi g \rightarrow gg$ through which the modulus Φ and gluons can reach thermal equilibrium.

$$\text{b) } \quad \langle \Gamma \rangle > H \Leftrightarrow \sqrt{d} \frac{g^2 T^3}{M_P^2} > g_*^{1/2} \frac{T^2}{M_P} \Rightarrow T > \frac{g_*^{1/2} M_P}{g^2 \sqrt{d}}. \quad (3.21)$$

As before, case (a) refers to $2 \leftrightarrow 2$ processes with two gravitational vertices, whereas in case (b) one vertex is gravitational and the other one is a renormalisable interaction. A typical Kähler modulus of string compactifications generically couples to the gauge bosons of the field theory, that lives on the stack of branes wrapping the cycle whose volume is given by that modulus. Scattering processes, annihilation and pair production reactions, that arise due to that coupling, all have cross-sections of the form (3.14) and (3.15). For all the Kähler moduli in KKLT constructions $d \sim \mathcal{O}(1)$ and so $\langle \Gamma \rangle$ is never greater than H for temperatures below the Planck scale, for both cases (a) and (b). Therefore, those moduli will never thermalise through $2 \leftrightarrow 2$ processes. However, we shall see in Section 5 that the situation is different for the small modulus in LVS, since in that case $d \sim \nu^2 \gg 1$. A typical $2 \leftrightarrow 2$ process of type (b), with a modulus Φ and a non-abelian gauge boson g going to two g 's, is shown in Figure 4. Here Φ denotes the canonically normalized field, which at leading order in the large-volume expansion corresponds to the small modulus. We will give the precise definition of Φ in Section 4.

3.2.2 $1 \leftrightarrow 2$ interactions

In order to work out the temperature dependence of the interaction rate for decay and inverse decay processes, recall that the rest frame decay rate $\Gamma_D^{(R)}$ does not depend on the temperature. For renormalisable interactions with massless mediators or mediated by

particles with mass M at temperatures $T > M$, it takes the form:

$$\Gamma_D^{(R)} \sim \alpha m, \quad (3.22)$$

where m is the mass of the decaying particle and $\alpha \sim g^2$, with g being either a gauge or a Yukawa coupling. On the other hand, for gravitational interactions or for renormalisable interactions mediated by particles with mass M at temperatures $T < M$, we have ($M \equiv M_P$ in the case of gravity):

$$\Gamma_D^{(R)} \sim D \frac{m^3}{M^2}, \quad (3.23)$$

with D a dimensionless constant (note that in the case of gravity $D = \sqrt{d}$, where d is the same moduli-dependent constant as in Subsection 3.2.1).

Now, the decay rate that has to be compared with H is not $\Gamma_D^{(R)}$, but its thermal average $\langle \Gamma_D \rangle$. In order to evaluate this quantity, we need to switch to the ‘laboratory frame’ where:

$$\Gamma_D = \Gamma_D^{(R)} \sqrt{1 - v^2} = \Gamma_D^{(R)} \frac{m}{E}, \quad (3.24)$$

and then take the thermal average:

$$\langle \Gamma_D \rangle = \Gamma_D^{(R)} \frac{m}{\langle E \rangle}. \quad (3.25)$$

In the relativistic regime, $T \gtrsim m$, the Lorentz factor $\gamma = \langle E \rangle / m \sim T/m$, whereas in the non-relativistic regime, $T \lesssim m$, $\gamma = \langle E \rangle / m \sim 1$.

Notice that, by definition, in a thermal bath the decay rate of the direct process is equal to the decay rate of the inverse process. However, for $T < m$ the energy of the final states of the decay process is of order T , which means that the final states do not have enough energy to re-create the decaying particle. So the rate for the inverse decay, Γ_{ID} , is Boltzmann-suppressed: $\Gamma_{ID} \sim e^{-m/T}$. Hence, the conclusion is that, for $T < m$, one can never have $\Gamma_D = \Gamma_{ID}$ and thermal equilibrium will not be attained. Let us now summarize the various decay and inverse decay rates:

1. Renormalisable interactions with massless mediators or mediated by particles with mass M at $T > M$:

$$\langle \Gamma_D \rangle \simeq \begin{cases} g^2 \frac{m^2}{T}, & \text{for } T \gtrsim m \\ g^2 m, & \text{for } T \lesssim m, \end{cases} \quad (3.26)$$

$$\langle \Gamma_{ID} \rangle \simeq \begin{cases} g^2 \frac{m^2}{T}, & \text{for } T \gtrsim m \\ g^2 m \left(\frac{m}{T}\right)^{3/2} e^{-m/T}, & \text{for } T \lesssim m. \end{cases} \quad (3.27)$$

Therefore, particles will reach thermal equilibrium via decay and inverse decay processes if and only if

$$\langle \Gamma \rangle > H \Leftrightarrow g^2 \frac{m^2}{T} > g_*^{1/2} \frac{T^2}{M_P} \Rightarrow m < T < \left(\frac{g^2 m^2 M_P}{g_*^{1/2}} \right)^{1/3}. \quad (3.28)$$

2. Gravity or renormalisable interactions mediated by particles with mass M at $T < M$:

$$\langle \Gamma_D \rangle \simeq \begin{cases} D \frac{m^4}{M^2 T}, & \text{for } T \gtrsim m \\ D \frac{m^3}{M^2}, & \text{for } T \lesssim m, \end{cases} \quad (3.29)$$

$$\langle \Gamma_{ID} \rangle \simeq \begin{cases} D \frac{m^4}{M^2 T}, & \text{for } T \gtrsim m \\ D \frac{m^3}{M^2} \left(\frac{m}{T}\right)^{3/2} e^{-m/T}, & \text{for } T \lesssim m \end{cases} \quad (3.30)$$

with $M \equiv M_P$ in the case of gravity. Therefore, particles will reach thermal equilibrium via decay and inverse decay processes if and only if

$$\langle \Gamma \rangle > H \Leftrightarrow D \frac{m^4}{M^2 T} > g_*^{1/2} \frac{T^2}{M_P} \Rightarrow 1 < \frac{T}{m} < \left(D \frac{m M_P}{g_*^{1/2} M^2} \right)^{1/3}. \quad (3.31)$$

In the case of gravitational interactions, (3.31) becomes

$$1 < \frac{T}{m} < \left(D \frac{m}{g_*^{1/2} M_P} \right)^{1/3}. \quad (3.32)$$

In KKLT constructions, $D \sim \mathcal{O}(1)$ and $m \sim m_{3/2}$. So (3.32) can never be satisfied and hence moduli cannot reach thermal equilibrium via decay and inverse decay processes. However, we shall see in Section 5 that in LVS one has $D \sim \mathcal{V} \gg 1$ and so $1 \leftrightarrow 2$ processes could, in principle, play a role in maintaining thermal equilibrium between moduli and ordinary MSSM particles.

4. Moduli masses and couplings

As we have seen in the previous section, the temperature, at which a thermal bath is established or some particles drop out of thermal equilibrium, depends on the masses and couplings of the particles. To determine the latter, one needs to use canonically normalised fields. In this Section, we study the canonical normalisation of the Kähler moduli kinetic terms and use the results to compute the masses of those moduli and their couplings to visible sector particles.

4.1 Single-hole Swiss-cheese

We start by focusing on the simplest Calabi-Yau realisation of LVS, the ‘single-hole Swiss-cheese’ case described in Subsection 2.3.1 (i.e., the degree 18 hypersurface embedded in $\mathbb{C}P^4_{[1,1,1,6,9]}$). First of all, we shall review the canonical normalisation derived in [17]. In order to obtain the Lagrangian in the vicinity of the zero temperature vacuum, one expands the moduli fields around the $T = 0$ minimum:

$$\tau_b = \langle \tau_b \rangle + \delta \tau_b, \quad (4.1)$$

$$\tau_s = \langle \tau_s \rangle + \delta \tau_s. \quad (4.2)$$

where $\langle \tau_b \rangle$ and $\langle \tau_s \rangle$ denote the VEV of τ_b and τ_s . One then finds:

$$\mathcal{L} = K_{i\bar{j}} \partial_\mu (\delta\tau_i) \partial^\mu (\delta\tau_j) - \langle V_0 \rangle - \frac{1}{2} V_{i\bar{j}} \delta\tau_i \delta\tau_j + \mathcal{O}(\delta\tau^3), \quad (4.3)$$

where $i = b, s$ and $\langle V_0 \rangle$ denotes the value of the zero temperature potential at the minimum. To find the canonically normalized fields Φ and χ , let us write $\delta\tau_b$ and $\delta\tau_s$ as:

$$\delta\tau_i = \frac{1}{\sqrt{2}} [(\vec{v}_\Phi)_i \Phi + (\vec{v}_\chi)_i \chi]. \quad (4.4)$$

Then the conditions for the Lagrangian (4.3) to take the canonical form:

$$\mathcal{L} = \frac{1}{2} \partial_\mu \Phi \partial^\mu \Phi + \frac{1}{2} \partial_\mu \chi \partial^\mu \chi - \langle V_0 \rangle - \frac{1}{2} m_\Phi^2 \Phi^2 - \frac{1}{2} m_\chi^2 \chi^2 \quad (4.5)$$

are the following:

$$K_{i\bar{j}} (\vec{v}_\alpha)_i (\vec{v}_\beta)_j = \delta_{\alpha\beta} \quad \text{and} \quad \frac{1}{2} V_{i\bar{j}} (\vec{v}_\alpha)_i (\vec{v}_\beta)_j = m_\alpha^2 \delta_{\alpha\beta}. \quad (4.6)$$

These relations are satisfied when \vec{v}_Φ , \vec{v}_χ (properly normalised according to the first of (4.6)) and m_Φ^2 , m_χ^2 are, respectively, the eigenvectors and the eigenvalues of the mass-squared matrix $(M^2)_{i\bar{j}} \equiv \frac{1}{2} (K^{-1})_{i\bar{k}} V_{\bar{k}j}$.

Substituting the results of [17] for \vec{v}_Φ and \vec{v}_χ in (4.4), we can write the original Kähler moduli $\delta\tau_i$ as (for $a_s \tau_s \gg 1$):

$$\delta\tau_b = \left(\sqrt{6} \langle \tau_b \rangle^{1/4} \langle \tau_s \rangle^{3/4} \right) \frac{\Phi}{\sqrt{2}} + \left(\sqrt{\frac{4}{3}} \langle \tau_b \rangle \right) \frac{\chi}{\sqrt{2}} \sim \mathcal{O}(\mathcal{V}^{1/6}) \Phi + \mathcal{O}(\mathcal{V}^{2/3}) \chi, \quad (4.7)$$

$$\delta\tau_s = \left(\frac{2\sqrt{6}}{3} \langle \tau_b \rangle^{3/4} \langle \tau_s \rangle^{1/4} \right) \frac{\Phi}{\sqrt{2}} + \left(\frac{\sqrt{3}}{a_s} \right) \frac{\chi}{\sqrt{2}} \sim \mathcal{O}(\mathcal{V}^{1/2}) \Phi + \mathcal{O}(1) \chi. \quad (4.8)$$

As expected, these relations show that there is a mixing of the original fields. Nevertheless, $\delta\tau_b$ is mostly χ and $\delta\tau_s$ is mostly Φ . On the other hand, the mass-squareds are [17]:

$$m_\Phi^2 \simeq \text{Tr}(M^2) \simeq \left(\frac{g_s e^{K_{cs}}}{8\pi} \right) \frac{24\sqrt{2}\nu a_s^2 \langle \tau_s \rangle^{1/2}}{\mathcal{V}^2} M_P^2 \sim \left(\frac{\ln \mathcal{V}}{\mathcal{V}} \right)^2 M_P^2 \quad (4.9)$$

$$m_\chi^2 \simeq \frac{\text{Det}(M^2)}{\text{Tr}(M^2)} \simeq \left(\frac{g_s e^{K_{cs}}}{8\pi} \right) \frac{27\nu}{4a_s \langle \tau_s \rangle \mathcal{V}^3} M_P^2 \sim \frac{M_P^2}{\mathcal{V}^3 \ln \mathcal{V}}. \quad (4.10)$$

We can see that there is a large hierarchy of masses among the two particles, with Φ being heavier than the gravitino mass (recall that $m_{3/2} \sim M_P/\mathcal{V}$) and χ lighter by a factor of $\sqrt{\mathcal{V}}$.

Using the above results and assuming that the MSSM is built via magnetised D7 branes wrapped around the small cycle, we can compute the couplings of the Kähler moduli fields of the $\mathbb{C}P^4_{[1,1,1,6,9]}$ model to visible gauge and matter fields. This is achieved by expanding the kinetic and mass terms of the MSSM particles around the moduli VEVs. The details are provided in Appendix A, where we focus on $T > M_{EW}$ since we are interested in thermal corrections at high temperatures. This, in particular, means that all fermions and gauge bosons are massless and the mixing of the Higgsinos with the EW gauginos, that gives neutralinos and charginos, is not present. We summarise the results for the moduli couplings in Tables 2 and 3.

	Gauge bosons ($F_{\mu\nu}F^{\mu\nu}$)	Gauginos ($\bar{\lambda}\lambda$)	Matter fermions ($\bar{\psi}\psi$)	Higgsinos ($\bar{H}\tilde{H}$)
χ	$\frac{1}{M_P \ln \mathcal{V}}$	$\frac{1}{\mathcal{V} \ln \mathcal{V}}$	No coupling	$\frac{1}{\mathcal{V} \ln \mathcal{V}}$
Φ	$\frac{\sqrt{\mathcal{V}}}{M_P}$	$\frac{1}{\mathcal{V}^{3/2} \ln \mathcal{V}}$	No coupling	$\frac{1}{\sqrt{\mathcal{V}} \ln \mathcal{V}}$

Table 2: $\mathbb{C}P^4_{[1,1,1,6,9]}$ case: moduli couplings to spin 1 and 1/2 MSSM particles for $T > M_{EW}$.

	Higgs ($\bar{H}H$)	Higgs-Fermions ($H\bar{\psi}\psi$)	SUSY scalars ($\bar{\varphi}\varphi$)	χ^2	Φ^2
χ	$\frac{M_P}{\mathcal{V}^2 (\ln \mathcal{V})^2}$	$\frac{1}{M_P \mathcal{V}^{1/3}}$	$\frac{M_P}{\mathcal{V}^2 (\ln \mathcal{V})^2}$	$\frac{M_P}{\mathcal{V}^3}$	$\frac{M_P}{\mathcal{V}^2}$
Φ	$\frac{M_P}{\mathcal{V}^{5/2} (\ln \mathcal{V})^2}$	$\frac{1}{M_P \mathcal{V}^{5/6}}$	$\frac{M_P}{\mathcal{V}^{5/2} (\ln \mathcal{V})^2}$	$\frac{M_P}{\mathcal{V}^{5/2}}$	$\frac{M_P}{\mathcal{V}^{3/2}}$

Table 3: $\mathbb{C}P^4_{[1,1,1,6,9]}$ case: moduli couplings to spin 0 and 1/2 MSSM particles and cubic self-couplings for $T > M_{EW}$.

4.2 Multiple-hole Swiss-cheese

Let us now consider the more general Swiss-cheese CY three-folds with more than one small modulus and with volume given by (2.20). In this case we find:

$$\begin{aligned}
\mathcal{L}_{kin} &= \frac{3}{4 \langle \tau_b \rangle^2} \partial_\mu (\delta \tau_b) \partial^\mu (\delta \tau_b) + \frac{3}{8} \sum_i \frac{\lambda_i \epsilon_i}{\langle \tau_b \rangle \langle \tau_i \rangle} \partial_\mu (\delta \tau_i) \partial^\mu (\delta \tau_i) \\
&\quad - \frac{9}{4} \sum_i \frac{\lambda_i \epsilon_i}{\langle \tau_b \rangle^2} \partial_\mu (\delta \tau_b) \partial^\mu (\delta \tau_i) + \frac{9}{4} \sum_{i < j} \frac{\lambda_i \lambda_j \epsilon_i \epsilon_j}{\langle \tau_b \rangle^2} \partial_\mu (\delta \tau_i) \partial^\mu (\delta \tau_j), \quad (4.11)
\end{aligned}$$

where $\epsilon_i \equiv \sqrt{\frac{\tau_i}{\tau_b}} \ll 1$ and also we have kept only the leading (in the limit $\tau_b \gg \tau_i \forall i$) contribution in each term. Notice that the mixed terms are subleading compared to the diagonal ones. So, to start with, one can keep only the first line in (4.11). Then at leading order the canonically normalized fields χ and Φ_i , $i = 1, \dots, N_{small}$, are defined via:

$$\delta \tau_b = \sqrt{\frac{2}{3}} \langle \tau_b \rangle \chi \sim \mathcal{O}(\mathcal{V}^{2/3}) \chi, \quad \delta \tau_i = \frac{2}{\sqrt{3} \lambda_i} \langle \tau_b \rangle^{3/4} \langle \tau_i \rangle^{1/4} \Phi_i \sim \mathcal{O}(\mathcal{V}^{1/2}) \Phi_i. \quad (4.12)$$

As was to be expected, this scaling with the volume agrees with the behaviour of $\delta \tau_b$ and $\delta \tau_s$ in (4.7), (4.8). Now, let us work out the volume scaling of the subdominant mixing terms since it is important for the computation of the various moduli couplings. Proceeding order by order in a large- \mathcal{V} expansion, we end up with:

$$\delta \tau_b \sim \mathcal{O}(\mathcal{V}^{2/3}) \chi + \sum_i \mathcal{O}(\mathcal{V}^{1/6}) \Phi_i, \quad (4.13)$$

$$\delta \tau_i \sim \mathcal{O}(\mathcal{V}^{1/2}) \Phi_i + \mathcal{O}(1) \chi + \sum_{j \neq i} \mathcal{O}(\mathcal{V}^{-1/2}) \Phi_j. \quad (4.14)$$

This shows that the mixing between the small moduli is strongly suppressed by inverse powers of the overall volume, in accord with the subleading behaviour of the last term in (4.11). Furthermore, the fact that the leading order volume-scaling of (4.13)-(4.14)

is the same as (4.7)-(4.8), implies that all small moduli behave in the same way as the only small modulus of the $\mathbb{C}P^4_{[1,1,1,6,9]}$ model. Hence, if all the small moduli are stabilised by non-perturbative effects, the moduli mass spectrum in the general case will look like (4.9)-(4.10), with (4.9) valid for all the small moduli. In addition, if we assume that all the 4-cycles corresponding to small moduli are wrapped by MSSM D7 branes, the moduli couplings to matter fields are again given by Tables 2 and 3, where now Φ stands for any small modulus Φ_i .

However, in general the situation may be more complicated. In fact, the authors of [23] pointed out that 4-cycles supporting MSSM chiral matter cannot always get non-perturbative effects.⁸ A possible way to stabilise these 4-cycles is to use g_s corrections as proposed in [8]. In this case, the leading-order behaviour of (4.9) should not change: $m_{\Phi_i}^2 \sim \frac{M_P^2}{\mathcal{V}^2}$.⁹ However, the moduli couplings to MSSM particles depend on the underlying brane set-up. So let us consider the following main cases:

1. All the small 4-cycles are wrapped by MSSM D7 branes except τ_{np} which is responsible for non-perturbative effects, being wrapped by an ED3 brane. It follows that the MSSM couplings of Φ_{np} are significantly suppressed compared to the MSSM couplings of the other small cycles (still given by Tables 2 and 3). This is due to the mixing term in (4.14) being highly suppressed by inverse powers of \mathcal{V} .
2. All the small 4-cycles are wrapped by MSSM D7 branes except τ_{np} which is supporting a pure $SU(N)$ hidden sector that gives rise to gaugino condensation. This implies that the coupling of Φ_{np} to hidden sector gauge bosons will have the same volume-scaling as the coupling of the other small moduli with visible sector gauge bosons. However, the coupling of the MSSM 4-cycles with hidden sector gauge bosons will be highly suppressed.
3. All the small 4-cycles τ_i support MSSM D7 branes which are also wrapped around the 4-cycle responsible for non-perturbative effects τ_{np} , but they have chiral intersections only on the other small cycles. In this case, the coupling of Φ_{np} to MSSM particles would be the same as the other Φ_i . However, if τ_{np} supports an hidden sector that undergoes gaugino condensation, the coupling of the MSSM 4-cycles with the gauge bosons of this hidden sector would still be highly suppressed.

4.3 K3 Fibration

We turn now to the K3 fibration case described in Section 2.3.2. We shall consider first the ‘LV’ case, in which the modulus related to the K3 divisor is fixed at a very large value,

⁸This is because an ED3 wrapped on the same cycle will have, in general, chiral intersections with the MSSM branes. Thus the instanton prefactor would be dependent on the VEVs of MSSM fields which are set to zero for phenomenological reasons. In the case of gaugino condensation, this non-perturbative effect would be killed by the arising of chiral matter.

⁹It may be likely that $m_{\Phi_i}^2$ depends on subleading powers of $(\ln \mathcal{V})$ due to the fact that the loop corrections are subdominant with respect to the non-perturbative ones (see [8]), but the main \mathcal{V}^{-2} dependence should persist.

and then the ‘SV’ case, in which the overall volume is of the order $\mathcal{V} \sim 10^3$ and the K3 fiber is small.

In order to compute the moduli mass spectroscopy and couplings, it suffices to canonically normalise the fields just in the vicinity of the vacuum. The non-canonical kinetic terms look like (with $\varepsilon \equiv \sqrt{\langle \tau_s \rangle / \langle \tau_1 \rangle}$):

$$\begin{aligned} \mathcal{L}_{kin} = & \frac{1}{4\langle \tau_1 \rangle^2} \partial_\mu(\delta\tau_1) \partial^\mu(\delta\tau_1) + \frac{1}{2\langle \tau_2 \rangle^2} \partial_\mu(\delta\tau_2) \partial^\mu(\delta\tau_2) - \frac{3\gamma\varepsilon}{4\langle \tau_2 \rangle \langle \tau_1 \rangle} \partial_\mu(\delta\tau_1) \partial^\mu(\delta\tau_s) \\ & - \frac{3\gamma\varepsilon}{2\langle \tau_2 \rangle^2} \partial_\mu(\delta\tau_2) \partial^\mu(\delta\tau_s) + \frac{\gamma\varepsilon^3}{2\langle \tau_2 \rangle^2} \partial_\mu(\delta\tau_1) \partial^\mu(\delta\tau_2) + \frac{3\gamma\varepsilon}{8\langle \tau_2 \rangle \langle \tau_s \rangle} \partial_\mu(\delta\tau_s) \partial^\mu(\delta\tau_s). \end{aligned} \quad (4.15)$$

Large K3 fiber

In the ‘LV’ case where the K3 fiber is stabilised at large value, $\varepsilon \ll 1$. Therefore at leading order in a large volume expansion, where $\langle \tau_2 \rangle > \langle \tau_1 \rangle \gg \langle \tau_s \rangle$, all the cross-terms in (4.15) are subdominant to the diagonal ones, and so can be neglected:

$$\mathcal{L}_{kin} \simeq \frac{1}{4\langle \tau_1 \rangle^2} \partial_\mu(\delta\tau_1) \partial^\mu(\delta\tau_1) + \frac{1}{2\langle \tau_2 \rangle^2} \partial_\mu(\delta\tau_2) \partial^\mu(\delta\tau_2) + \frac{3\gamma\varepsilon}{8\langle \tau_2 \rangle \langle \tau_s \rangle} \partial_\mu(\delta\tau_s) \partial^\mu(\delta\tau_s). \quad (4.16)$$

Therefore, at leading order the canonical normalisation close to the minimum becomes rather easy and reads:

$$\delta\tau_1 = \sqrt{2\langle \tau_1 \rangle} \chi_1 \sim \mathcal{O}\left(\mathcal{V}^{2/3}\right) \chi_1, \quad (4.17)$$

$$\delta\tau_2 = \langle \tau_2 \rangle \chi_2 \sim \mathcal{O}\left(\mathcal{V}^{2/3}\right) \chi_2, \quad (4.18)$$

$$\delta\tau_s = \sqrt{\frac{4\langle \tau_1 \rangle^{1/2} \langle \tau_2 \rangle \langle \tau_s \rangle^{1/2}}{3\gamma}} \Phi \sim \mathcal{O}\left(\mathcal{V}^{1/2}\right) \Phi. \quad (4.19)$$

However, in order to derive all the moduli couplings, we need also to work out the leading order volume-scaling of the subdominant mixing terms in (4.18) and (4.19). This can be done order by order in a large- \mathcal{V} expansion and, after some algebra, we obtain:

$$\delta\tau_1 = \alpha_1 \langle \tau_1 \rangle \chi_1 + \alpha_2 \frac{\sqrt{\langle \tau_1 \rangle}}{\langle \tau_2 \rangle} \langle \tau_s \rangle^{3/2} \chi_2 + \alpha_3 \frac{\langle \tau_1 \rangle^{3/4}}{\sqrt{\langle \tau_2 \rangle}} \langle \tau_s \rangle^{3/4} \Phi, \quad (4.20)$$

$$\delta\tau_2 = \alpha_4 \frac{\sqrt{\langle \tau_1 \rangle}}{\langle \tau_2 \rangle} \langle \tau_s \rangle^{3/2} \chi_1 + \alpha_5 \langle \tau_2 \rangle \chi_2 + \alpha_6 \frac{\sqrt{\langle \tau_2 \rangle}}{\langle \tau_1 \rangle^{1/4}} \langle \tau_s \rangle^{3/4} \Phi, \quad (4.21)$$

$$\delta\tau_s = \alpha_7 \frac{\langle \tau_1 \rangle}{\langle \tau_2 \rangle} \langle \tau_s \rangle \chi_1 + \alpha_8 \langle \tau_s \rangle \chi_2 + \alpha_9 \langle \tau_1 \rangle^{1/4} \sqrt{\langle \tau_2 \rangle} \langle \tau_s \rangle^{1/4} \Phi, \quad (4.22)$$

where the α_i , $i = 1, \dots, 9$ are $\mathcal{O}(1)$ coefficients. The volume-scalings of (4.20), (4.21) and (4.22) are the following:

$$\delta\tau_1 \sim \mathcal{O}\left(\mathcal{V}^{2/3}\right) \chi_1 + \mathcal{O}\left(\mathcal{V}^{-1/3}\right) \chi_2 + \mathcal{O}\left(\mathcal{V}^{1/6}\right) \Phi, \quad (4.23)$$

$$\delta\tau_2 \sim \mathcal{O}\left(\mathcal{V}^{-1/3}\right) \chi_1 + \mathcal{O}\left(\mathcal{V}^{2/3}\right) \chi_2 + \mathcal{O}\left(\mathcal{V}^{1/6}\right) \Phi, \quad (4.24)$$

$$\delta\tau_s \sim \mathcal{O}(1) \chi_1 + \mathcal{O}(1) \chi_2 + \mathcal{O}\left(\mathcal{V}^{1/2}\right) \Phi. \quad (4.25)$$

This shows that, if we identify each of τ_1 and τ_2 with the large modulus τ_b in the Swiss-cheese case, (4.23) and (4.24) have the same volume scaling as (4.7), as one might have expected. Moreover, the similarity of (4.25) and (4.8) shows that also the small moduli in the two cases behave in the same way. Therefore, we can conclude that (4.9) is valid also for the K3 Fibration case under consideration:

$$m_\Phi \sim \left(\frac{\ln \mathcal{V}}{\mathcal{V}} \right) M_P. \quad (4.26)$$

On the other hand, we need to be more careful in the study of the mass spectrum of the large moduli τ_1 and τ_2 . We can work out this ‘fine structure’, at leading order in a large- \mathcal{V} expansion, first integrating out τ_s and then computing the eigenvalues of the matrix. The latter are obtained by multiplying the inverse Kähler metric by the Hessian of the potential both evaluated at the minimum. The leading order behaviour of the determinant of this matrix is:

$$\text{Det} (K^{-1}d^2V) \sim \frac{\tau_2^4 \sqrt{\ln \mathcal{V}}}{\mathcal{V}^9}, \quad \text{with } \mathcal{V} \sim \sqrt{\tau_1 \tau_2}. \quad (4.27)$$

Because $m_{\chi_2}^2 \gg m_{\chi_1}^2$, we have at leading order at large volume:

$$m_{\chi_2}^2 \simeq \text{Tr} (K^{-1}d^2V) \sim \frac{\sqrt{\ln \mathcal{V}}}{\mathcal{V}^3} M_P^2 \quad (4.28)$$

$$m_{\chi_1}^2 \simeq \frac{\text{Det} (K^{-1}d^2V)}{\text{Tr} (K^{-1}d^2V)} \sim \frac{\tau_2^4}{\mathcal{V}^6} M_P^2 \sim \frac{M_P^2}{\tau_1^3 \tau_2}. \quad (4.29)$$

Identifying τ_1 with τ_2 , (4.29) simplifies to $m_{\chi_1}^2 \sim \mathcal{V}^{-10/3}$, confirming the qualitative expectation that the τ_1 direction is systematically lighter than \mathcal{V} in the large- \mathcal{V} limit.

Using the results of this Section and assuming that the MSSM branes are wrapped around the small cycle¹⁰, it is easy to repeat the computations of Appendix A for the K3 fibration. Due to the fact that the leading order \mathcal{V} -scaling of (4.23)-(4.25) matches that of the single-hole Swiss-cheese model, we again find the same couplings as those given in Tables 2 and 3, where now χ stands for any of χ_1 and χ_2 .

Small K3 fiber

In the ‘SV’ case where the K3 fiber is stabilised at small value, $\varepsilon \simeq 1$. Therefore at leading order in a large volume expansion, where $\langle \tau_2 \rangle \gg \langle \tau_1 \rangle > \langle \tau_s \rangle$, the first term in (4.15) is dominating the whole kinetic Lagrangian. Hence we conclude that, at leading order, the canonical normalisation of $\delta\tau_1$ close to the $T = 0$ minimum is again given by (4.17). However, now its volume scaling reads:

$$\delta\tau_1 \sim \mathcal{O}(1) \chi_1 + (\text{subleading mixing terms}). \quad (4.30)$$

To proceed order by order in a large volume expansion, note that the third and the sixth term in (4.15) are suppressed by just one power of $\langle \tau_2 \rangle$, whereas the second, fourth and fifth

¹⁰We also ignore the incompatibility between localising non-perturbative effects and the MSSM on the same 4-cycle.

term are suppressed by two powers of the large modulus. Thus, we obtain the following leading order behaviour for the canonical normalisation of the two remaining moduli:

$$\delta\tau_2 \sim \mathcal{O}(\mathcal{V}) \chi_1 + \mathcal{O}(\mathcal{V}) \chi_2 + \mathcal{O}(\mathcal{V}) \Phi, \quad (4.31)$$

$$\delta\tau_s \sim \mathcal{O}(\mathcal{V}^{1/2}) \chi_1 + \mathcal{O}(\mathcal{V}^{1/2}) \Phi + \text{subleading mixing terms}. \quad (4.32)$$

Notice that the canonically normalised field χ_1 corresponds to the K3 divisor τ_1 , whereas Φ is a mixing of τ_1 and the blow-up mode τ_s . Finally χ_2 is a combination of all the three states, and so plays the role of the ‘large’ field. The moduli mass spectrum will still be given by (4.26), (4.28) and (4.29). However now the volume scaling of (4.29) simplifies to $m_{\chi_1}^2 \sim \mathcal{V}^{-2}$, confirming the qualitative expectation that χ_1 is also a small field with a mass of the same order of magnitude of m_Φ .

The computation of the moduli couplings depends on the localisation of the MSSM within the compact CY. As we have seen in Subsection 2.3.2, the scalar potential receives non-perturbative corrections in the blow-up mode τ_s . Therefore, in order for the non-perturbative contributions to be non-vanishing, the MSSM branes have to wrap either the small K3 fiber τ_1 or the 4-cycle given by the formal sum $\tau_s + \tau_1$ with chiral intersections on τ_1 . In both cases, we cannot immediately read off the moduli couplings from the results of Appendix A. This is due to the difference of the leading order volume scaling of the canonical normalisation between the ‘SV’ case for the K3 fibration and the Swiss-cheese scenario.¹¹

However, as we shall see in the next Section, in the Swiss-cheese case, the relevant interactions through which the small moduli can thermalise, are with the gauge bosons. As we shall see in Section 5.3, these interactions will also be the ones that are crucial for moduli thermalisation in the K3 fibration case. Therefore, here we shall focus on them only. Following the calculations in Subsection A.1 of Appendix A, we infer that if only τ_1 is wrapped by MSSM branes, then the coupling of χ_1 with MSSM gauge bosons is of the order $g \sim 1/M_P$ without any factor of the overall volume, while the coupling of Φ with gauge bosons will be more suppressed by inverse powers of \mathcal{V} . On the other hand, if both τ_1 and τ_s are wrapped by MSSM branes, then the couplings of both small moduli with the gauge bosons are similar to the ones in the Swiss-cheese case: $g \sim \sqrt{\mathcal{V}}/M_P$. Moreover, if gaugino condensation is taking place in the pure $SU(N)$ theory supported on τ_s , then both χ_1 and Φ couple to the hidden sector gauge bosons with strength $g \sim \sqrt{\mathcal{V}}/M_P$.

We end this Subsection by commenting on K3 fibrations with more than one blow-up mode. In such a case, it is possible to localise the MSSM on one of the small blow-up modes and the situation is very similar to the one outlined for the multiple-hole Swiss-cheese. The only difference is the presence of the extra modulus related to the K3 fiber, which will couple to the MSSM gauge bosons with the same strength as the small modulus supporting the MSSM. This is because of the particular form of the canonical normalisation, which, for example in the case of two blow-up modes τ_{s1} and τ_{s2} , looks like (4.30) and (4.31) together

¹¹We stress also that presently there is no knowledge of the Kähler metric for chiral matter localised on deformable cycles.

with:

$$\delta\tau_{s1} \sim \mathcal{O}(\mathcal{V}^{1/2}) \chi_1 + \mathcal{O}(\mathcal{V}^{1/2}) \Phi_1 + \text{subleading mixing terms}, \quad (4.33)$$

$$\delta\tau_{s2} \sim \mathcal{O}(\mathcal{V}^{1/2}) \chi_1 + \mathcal{O}(\mathcal{V}^{1/2}) \Phi_2 + \text{subleading mixing terms}. \quad (4.34)$$

4.4 Modulini

In this Subsection we shall concentrate on the supersymmetric partners of the moduli, the modulini. More precisely, we will consider the fermionic components of the chiral superfields, whose scalar components are the Kähler moduli. The kinetic Lagrangian for these modulini reads:

$$\mathcal{L}_{kin} = \frac{i}{4} \frac{\partial^2 K}{\partial \tau_i \partial \tau_j} \delta \bar{\tau}_j \gamma^\mu \partial_\mu (\delta \tilde{\tau}_i), \quad (4.35)$$

where the Kähler metric is the same as the one that appears in the kinetic terms of the Kähler moduli. Therefore, the canonical normalisation of the modulini takes exactly the same form as the canonical normalisation of the corresponding moduli. For example, in the single-hole Swiss-cheese case, we have:

$$\delta \tilde{\tau}_b = \left(\sqrt{6} \langle \tau_b \rangle^{1/4} \langle \tau_s \rangle^{3/4} \right) \frac{\tilde{\Phi}}{\sqrt{2}} + \left(\sqrt{\frac{4}{3}} \langle \tau_b \rangle \right) \frac{\tilde{\chi}}{\sqrt{2}} \sim \mathcal{O}(\mathcal{V}^{1/6}) \tilde{\Phi} + \mathcal{O}(\mathcal{V}^{2/3}) \tilde{\chi}, \quad (4.36)$$

$$\delta \tilde{\tau}_s = \left(\frac{2\sqrt{6}}{3} \langle \tau_b \rangle^{3/4} \langle \tau_s \rangle^{1/4} \right) \frac{\tilde{\Phi}}{\sqrt{2}} + \left(\frac{\sqrt{3}}{a_s} \right) \frac{\tilde{\chi}}{\sqrt{2}} \sim \mathcal{O}(\mathcal{V}^{1/2}) \tilde{\Phi} + \mathcal{O}(1) \tilde{\chi}. \quad (4.37)$$

We focus now on the modulini mass spectrum. We recall that in LVS the minimum is non-supersymmetric, and so the Goldstino is eaten by the gravitino via the super-Higgs effect. The Goldstino is the supersymmetric partner of the scalar field, which is responsible for SUSY breaking. In our case this is the modulus related to the overall volume of the Calabi-Yau, as can be checked by studying the order of magnitude of the various F-terms. Therefore, the volume modulino is the Goldstino. More precisely, in the $\mathbb{C}P^4_{[1,1,1,6,9]}$ case, $\tilde{\chi}$ is eaten by the gravitino, whereas the mass of $\tilde{\Phi}$ can be derived as follows:

$$m_{\tilde{\Phi}}^2 = \text{Tr} M_f^2 = \langle e^G K^{i\bar{j}} K^{l\bar{m}} (\nabla_i G_l + \frac{G_i G_l}{3}) (\nabla_{\bar{j}} G_{\bar{m}} + \frac{G_{\bar{j}} G_{\bar{m}}}{3}) \rangle, \quad (4.38)$$

where the function $G = K + \ln |W|^2$ is the supergravity Kähler invariant potential, and $\nabla_i G_j = G_{ij} - \Gamma_{ij}^l G_l$, with the connection $\Gamma_{ij}^l = K^{l\bar{m}} \partial_i K_{j\bar{m}}$. Equation (4.38) at leading order in a large volume expansion, can be approximated as

$$m_{\tilde{\Phi}}^2 \simeq \langle e^G | (K^{s\bar{s}} (\nabla_s G_s + \frac{G_s G_s}{3}))|^2 \rangle \quad (4.39)$$

where $\nabla_s G_s \simeq G_{ss} - \Gamma_{ss}^s G_s$ and $\Gamma_{ss}^s \simeq K^{s\bar{s}} \partial_s K_{s\bar{s}}$. In the single-hole Swiss-cheese case, for $a_s \tau_s \gg 1$, we obtain:

$$m_{\tilde{\Phi}}^2 \simeq \left\langle \frac{g_s e^{K_{cs}} M_P^2}{\pi} \left(36 a_s^4 A_s^2 \tau_s e^{-2a_s \tau_s} - \frac{6\sqrt{2} a_s^2 A_s W_0}{\mathcal{V}} \sqrt{\tau_s} e^{-a_s \tau_s} + \frac{W_0^2}{2\mathcal{V}^2} \right) \right\rangle. \quad (4.40)$$

Evaluating (4.40) at the minimum, we find that the mass of the modulino $\tilde{\Phi}$ is of the same order of magnitude as the mass of its supersymmetric partner Φ :

$$m_{\tilde{\Phi}}^2 \simeq \frac{a_s^2 \langle \tau_s \rangle^2 W_0^2}{\mathcal{V}^2} M_P^2 \sim \left(\frac{\ln \mathcal{V}}{\mathcal{V}} \right)^2 M_P^2 \sim m_{\Phi}^2. \quad (4.41)$$

Similarly, it can be checked that, in the general case of multiple-hole Swiss-cheese Calabi-Yaus and K3 fibrations, the masses of the moduli also keep being of the same order of magnitude as the masses of the corresponding supersymmetric partners.

We now turn to the computation of the moduli couplings. In fact, we are interested only in the modulino-gaugino-gauge boson coupling since, as we shall see in Section 5, this is the relevant interaction through which the moduli reach thermal equilibrium with the MSSM thermal bath. This coupling can be worked out by recalling that the small modulus τ_s couples to gauge bosons X as (see appendix A.1):

$$\mathcal{L}_{gauge} \sim \frac{\tau_s}{M_P} F_{\mu\nu} F^{\mu\nu}. \quad (4.42)$$

The supersymmetric completion of this interaction term contains the following modulino-gaugino-gauge boson coupling:

$$\mathcal{L} \sim \frac{\tilde{\tau}_s}{M_P} \sigma^{\mu\nu} \lambda' F_{\mu\nu}. \quad (4.43)$$

Now, expanding $\tilde{\tau}_s$ around its minimum and going to the canonically normalised fields $G_{\mu\nu}$ and λ defined as (see appendices A.1 and A.2):

$$G_{\mu\nu} = \sqrt{\langle \tau_s \rangle} F_{\mu\nu}, \quad \lambda = \sqrt{\langle \tau_s \rangle} \lambda', \quad (4.44)$$

we obtain:

$$\mathcal{L} \sim \frac{\delta \tilde{\tau}_s}{M_P \langle \tau_s \rangle} \sigma^{\mu\nu} \lambda G_{\mu\nu}. \quad (4.45)$$

Hence, by means of (4.37), we end up with the following *dimensionful* couplings:

$$\mathcal{L}_{\tilde{\chi}\tilde{X}X} \sim \left(\frac{1}{M_P \ln \mathcal{V}} \right) \tilde{\chi} \sigma^{\mu\nu} \lambda G_{\mu\nu}, \quad (4.46)$$

$$\mathcal{L}_{\tilde{\Phi}\tilde{X}X} \sim \left(\frac{\sqrt{\mathcal{V}}}{M_P} \right) \tilde{\Phi} \sigma^{\mu\nu} \lambda G_{\mu\nu}. \quad (4.47)$$

5. Study of moduli thermalisation

Using the general discussion of Section 3.2 and the explicit expressions for the moduli masses and couplings of Section 4, we can now study in detail which particles form the thermal bath. Consequently, we will be able to write down the general form that the finite temperature corrections of Section 3.1 take in the LVS.

We shall start by focusing on the simple geometry $\mathbb{C}P^4_{[1,1,1,6,9]}$, and then extend our analysis to more general Swiss-cheese and fibred CY manifolds. We will show below that, unlike previous expectations in the literature, the moduli corresponding to small cycles that support chiral matter can reach thermal equilibrium with the matter fields.

5.1 Single-hole Swiss-cheese

As we have seen in Section 3.2, both $2 \leftrightarrow 2$ and $1 \leftrightarrow 2$ processes can establish and maintain thermal equilibrium. Let us now apply the general conditions of Sections 3.2.1 and 3.2.2 to our case.

As we have already pointed out, scattering and annihilation processes involving strong interactions will establish thermal equilibrium between MSSM particles for temperatures $T < \alpha_s^2 g_*^{-1/2} M_P \sim 10^{15}$ GeV. Let us now concentrate on the moduli.

Small modulus Φ

From Section 4.1, we know that the largest coupling of the small canonical modulus Φ is with the non-abelian gauge bosons denoted by X :

$$\mathcal{L}_{\Phi XX} = g_{\Phi XX} \Phi F_{\mu\nu} F^{\mu\nu}, \quad g_{\Phi XX} \sim \frac{\sqrt{\mathcal{V}}}{M_P} \sim \frac{1}{M_s}. \quad (5.1)$$

Therefore according to (3.20), scattering or annihilation and pair production processes with two gravitational vertices like $X + X \leftrightarrow \Phi + \Phi$, $X + \Phi \leftrightarrow X + \Phi$, or $X + X \leftrightarrow X + X$, can establish thermal equilibrium between Φ and X for temperatures:

$$T > T_f^{(1)} \equiv g_*^{1/6} \frac{M_P}{\mathcal{V}^{2/3}}, \quad (5.2)$$

where $T_f^{(1)}$ denotes the freeze-out temperature of the modulus. Taking the number of degrees of freedom g_* to be $\mathcal{O}(100)$, as in the MSSM, we find that (5.2) implies $T > 5 \times 10^8$ GeV for $\mathcal{V} \sim 10^{15}$, whereas $T > 10^{16}$ GeV for $\mathcal{V} \sim 10^4$.¹² In fact, for a typically large volume ($\mathcal{V} > 10^{10}$) a more efficient $2 \leftrightarrow 2$ process is $X + X \leftrightarrow X + \Phi$ with one gravitational and one renormalisable vertex with coupling constant g . Indeed, according to (3.21), such scattering processes maintain thermal equilibrium for temperatures:

$$T > T_f^{(2)} \equiv \frac{g_*^{1/2} M_P}{g^2 \mathcal{V}} \sim 10^3 \frac{M_P}{\mathcal{V}} \quad \text{for } g_* \sim 100 \text{ and } g \sim 0.1, \quad (5.3)$$

which for $\mathcal{V} \sim 10^{15}$ gives $T > 10^6$ GeV while for $\mathcal{V} \sim 10^4$ it gives $T > 10^{17}$ GeV.

Finally, let us investigate the rôle played by decay and inverse decay processes of the form $\Phi \leftrightarrow X + X$. We recall that such processes can, in principle, maintain thermal equilibrium only for temperatures:

$$T > m_\Phi \sim \frac{\ln \mathcal{V}}{\mathcal{V}} M_P, \quad (5.4)$$

because the energy of the gauge bosons is given by $E_X \sim T$ and hence for $T < m_\Phi$ it is insufficient for the inverse decay process to occur. However, for $T > m_\Phi$ the process $X + X \rightarrow \Phi$ does take place and so one only needs to know the rate of the decay $\Phi \rightarrow X + X$ in order to find out whether thermal equilibrium is achieved. According to (3.32) with

¹²Recall that M_P here is the reduced Planck mass, which equals $(8\pi G_N)^{-1/2} = 2.4 \times 10^{18}$ GeV.

$D \sim g_{\Phi XX}^2/4\pi \sim \mathcal{V}/4\pi$, where we have also used (5.1), the condition for equilibrium is that:

$$T < T_{eq} \equiv \left(\frac{\mathcal{V} m_{\Phi}}{4\pi g_*^{1/2} M_P} \right)^{1/3} \quad m_{\Phi} \sim \left(\frac{\ln \mathcal{V}}{4\pi g_*^{1/2}} \right)^{1/3} \quad m_{\Phi} \equiv \kappa m_{\Phi}. \quad (5.5)$$

Hence thermal equilibrium between Φ and X can be maintained by $1 \leftrightarrow 2$ processes only if $\kappa > 1$ ¹³. However, estimating the total number of degrees of freedom as $g_* \sim \mathcal{O}(100)$, and writing the volume as $\mathcal{V} \sim 10^x$, we obtain that $\kappa > 1 \Leftrightarrow x > 55$. Such a large value is unacceptable, as it makes the string scale too small to be compatible with observations. Therefore, we conclude that in LVS the small modulus Φ never thermalises via decay and inverse decay processes.

The final picture is the following:

- For \mathcal{V} of order 10^{15} (10^{10}), as in typical LVS, from (5.3) we deduce that the modulus Φ is in thermal equilibrium with MSSM particles for temperatures $T > T_f^{(2)} \simeq 10^6$ GeV ($T > T_f^{(2)} \simeq 10^{11}$ GeV) due to $X + X \leftrightarrow \Phi + X$ processes.
- On the other hand, for $\mathcal{V} < 10^{10}$, as for LVS that allow gauge coupling unification, the main processes that maintain thermal equilibrium of the modulus Φ with MSSM particles are purely gravitational: $X + X \leftrightarrow \Phi + \Phi$, $\Phi + X \leftrightarrow \Phi + X$ or $X + X \leftrightarrow X + X$ and the freeze-out temperature is given by (5.2). For example for $\mathcal{V} \sim 10^4$ ($\Leftrightarrow M_s \sim 10^{16}$ GeV), Φ is in thermal equilibrium for temperatures $T > T_f^{(1)} \simeq 5 \times 10^{15}$ GeV.

We stress that this is the first example in the literature of a modulus that reaches thermal equilibrium with ordinary particles for temperatures significantly less than M_P , and so completely within the validity of the low energy effective theory. Note that we did not focus on the interactions of Φ with other ordinary and supersymmetric particles, since the corresponding couplings, derived in Appendix A, are not large enough to establish thermal equilibrium.

Finally, let us also note that, once the modulus Φ drops out of thermal equilibrium, it will decay before its energy density can begin to dominate the energy density of the Universe, unlike traditional expectations in the literature. We will show this in more detail in Subsection 6.3.

Large modulus χ

As summarised in Section 4.1, the coupling of the large modulus χ with gauge bosons is given by

$$\mathcal{L}_{\chi XX} = g_{\chi XX} \chi F_{\mu\nu} F^{\mu\nu}, \quad g_{\chi XX} \sim \frac{1}{M_P \ln \mathcal{V}}. \quad (5.6)$$

¹³The exact value of κ can be worked out via a more detailed calculation, very similar to the one that we will carry out in Section 6.4. It turns out that this value differs from the ‘ \sim ’ estimate in (5.5) just by a multiplicative factor $c^{1/3}$ of $\mathcal{O}(1)$. More precisely, $c = 18(\pi \langle \tau_s \rangle)^{-3/2} e^{K_{cs}/2} W_0 \sqrt{10 g_s}$ and so, for natural values of all the parameters: $W_0 = 1$, $g_s = 0.1$, $\langle \tau_s \rangle = 5$, $K_{cs} = 3$, we obtain $c^{1/3} = 1.09$.

Consequently purely gravitational $2 \leftrightarrow 2$ processes like $X + X \leftrightarrow \chi + \chi$, $X + \chi \leftrightarrow X + \chi$, or $X + X \leftrightarrow X + X$, could establish thermal equilibrium between χ and X for temperatures:

$$T > T_f^{(1)} \equiv g_*^{1/6} M_P (\ln \mathcal{V})^{4/3}. \quad (5.7)$$

On the other hand, scattering processes like $X + X \leftrightarrow X + \chi$ with one gravitational and one renormalisable vertex with coupling constant g , could maintain thermal equilibrium for temperatures:

$$T > T_f^{(2)} \equiv \frac{g_*^{1/2} M_P}{g^2} (\ln \mathcal{V})^2 \sim 10^3 M_P (\ln \mathcal{V})^2, \quad \text{for } g_* \sim 100 \text{ and } g \sim 0.1. \quad (5.8)$$

Clearly, both $T_f^{(1)}$ and $T_f^{(2)}$ are greater than M_P and so we conclude that χ can never thermalise via $2 \leftrightarrow 2$ processes. It is also immediate to notice that thermal equilibrium cannot be maintained by $1 \leftrightarrow 2$ processes, like $\chi \leftrightarrow X + X$, either. The reason is that, as derived in [17], for typical LARGE values of the volume $\mathcal{V} \sim 10^{10} - 10^{15}$, the lifetime of the large modulus χ is greater than the age of the Universe. Hence this modulus could contribute to dark matter and its decay to photons or electrons could be one of the smoking-gun signal of LVS.

Furthermore, as can be seen from Section 4.1, the couplings of χ to other MSSM particles are even weaker than its coupling to gauge bosons. So χ cannot thermalise via any other kind of interaction. Finally, one can also verify that thermal equilibrium between χ and Φ can never be maintained via $1 \leftrightarrow 2$ and $2 \leftrightarrow 2$ processes involving only the moduli, which processes arise due to the moduli triple self-couplings computed in Appendix A.3. Therefore, χ behaves as a typical modulus studied in the literature.

5.2 Multiple-hole Swiss-cheese

We shall now extend the results of Section 5.1 to the more general case of CY three-folds with one large cycle and several small ones. We shall not focus on explicit models since this is beyond the scope of our paper, but we will try to discuss qualitatively the generic behaviour of small moduli in the case of ‘multiple-hole Swiss-cheese’ CY manifolds.

As we have seen in Section 4.1, the couplings with MSSM particles of all the small cycles wrapped by MSSM branes have the same volume scaling as the corresponding couplings of the single small modulus in the $\mathbb{C}P^4_{[1,1,1,6,9]}$ case. Moreover, in Section 5.1 we have learned that Φ can thermalise via its interaction with gauge bosons. Hence, we conclude that the same arguments as in Section 5.1 can be applied for $h_{1,1} > 2$ and so all small cycles, that support MSSM chiral matter, reach thermal equilibrium with the gauge bosons.

Note however that, as we already pointed out in Section 4.1, the situation may be more complicated in concrete phenomenological models due to the possibility that non-perturbative effects may be incompatible with MSSM branes, which are localized on the same 4-cycle [23]. Whether or not such an incompatibility arises depends on the particular features of the model one considers, including the presence or absence of charged matter fields with non-vanishing VEVs. As a consequence of these subtleties, the issue of moduli thermalisation is highly dependent on the possible underlying brane set-ups. To gain

familiarity with the outcome, let us explore in more detail several brane set-ups in the case of only two small moduli. At the end we will comment on the generalization of these results to the case of arbitrary $h_{1,1}$.

We will focus on the case $h_{1,1} = 3$ with two small moduli τ_1 and τ_2 , that give the volumes of the two rigid divisors Γ_1 and Γ_2 . The results of Subsection 5.1 imply the following for the different brane set-ups below:

1. If Γ_1 is wrapped by an ED3 instanton and Γ_2 is wrapped by MSSM branes:
 - τ_1 couples to MSSM gauge bosons with strength $g \sim 1/(\sqrt{\mathcal{V}}M_P) \Rightarrow \tau_1$ does not thermalise.¹⁴
 - τ_2 couples to MSSM gauge bosons with strength $g \sim \sqrt{\mathcal{V}}/M_P \Rightarrow \tau_2$ thermalises.
2. If Γ_1 is wrapped by an ED3 instanton and $\Gamma_1 + \Gamma_2$ is wrapped by MSSM branes with chiral intersections on Γ_2 ¹⁵:
 - τ_1 couples to MSSM gauge bosons with strength $g \sim \sqrt{\mathcal{V}}/M_P \Rightarrow \tau_1$ thermalises.
 - τ_2 couples to MSSM gauge bosons with strength $g \sim \sqrt{\mathcal{V}}/M_P \Rightarrow \tau_2$ thermalises.
3. If Γ_1 is supporting a pure $SU(N)$ theory, that undergoes gaugino condensation, and Γ_2 is wrapped by MSSM branes:
 - τ_1 couples to MSSM gauge bosons with strength $g \sim 1/(\sqrt{\mathcal{V}}M_P)$ and to hidden sector gauge bosons with strength $g \sim \sqrt{\mathcal{V}}/M_P \Rightarrow \tau_1$ thermalises via its interaction with hidden sector gauge bosons.
 - τ_2 couples to MSSM gauge bosons with strength $g \sim \sqrt{\mathcal{V}}/M_P$ and to hidden sector gauge bosons with strength $g \sim 1/(\sqrt{\mathcal{V}}M_P) \Rightarrow \tau_2$ thermalises via its interaction with MSSM gauge bosons.

Hence in this case there are two separate thermal baths: one contains τ_1 and the hidden sector gauge bosons at temperature T_1 , whereas the other one is formed by τ_2 and the MSSM particles at temperature T_2 . Generically, we would expect that $T_1 \neq T_2$ since the two thermal baths are not in contact with each other.

4. If Γ_1 is supporting a pure $SU(N)$ theory, that undergoes gaugino condensation, and $\Gamma_1 + \Gamma_2$ is wrapped by MSSM branes with chiral intersections on Γ_2 :
 - τ_1 couples both to MSSM and hidden sector gauge bosons with strength $g \sim \sqrt{\mathcal{V}}/M_P \Rightarrow \tau_1$ thermalises.

¹⁴The coupling $g \sim 1/(\sqrt{\mathcal{V}}M_P)$ can be worked out by substituting the expression (4.14) in (A.7). As pointed out in point 1 at the end of Subsection 4.2, the weakness of this coupling is due to the mixing term in (4.14) being highly suppressed by inverse powers of \mathcal{V} .

¹⁵We assume that a single D7 brane is wrapping Γ_2 in order to get chirality from the intersection with the MSSM branes. The same assumption applies throughout the paper everywhere we use the expression ‘chiral intersections on some divisor’.

- τ_2 couples to MSSM gauge bosons with strength $g \sim \sqrt{\mathcal{V}}/M_P$ and to hidden sector gauge bosons with strength $g \sim 1/(\sqrt{\mathcal{V}}M_P) \Rightarrow \tau_2$ thermalises via its interaction with MSSM gauge bosons.

Unlike the previous case, now there is only one thermal bath, which contains both τ_1 and τ_2 together with the MSSM particles and the hidden sector gauge bosons, since in the present case τ_1 interacts strongly enough with the MSSM gauge bosons.

We can now extend these results to the general case with $h_{1,1} > 3$ by noticing that a small 4-cycle wrapped by MSSM branes will always thermalise via its interaction with MSSM gauge bosons. On the other hand, for a 4-cycle that is not wrapped by MSSM branes there are the following two options. If it is wrapped by an ED3 instanton, it will not thermalise. If instead it is supporting gaugino condensation, it will reach thermal equilibrium with the hidden sector gauge bosons.

5.3 K3 Fibration

Let us now turn to the issue of moduli thermalisation for K3 fibrations. As we have seen in Subsection 4.3, there is an essential difference between the cases when the K3 fiber is stabilized at a large and at a small value. Let us consider separately each of these two situations.

Large K3 fiber

As we have already stressed in Subsection 4.3, in the case ‘LV’ where the K3 divisor is stabilised large, the small modulus Φ plays exactly the same role as the small modulus of the single-hole Swiss-cheese case, whereas both χ_1 and χ_2 behave as the single large modulus. Hence we can repeat the same analysis as in Subsection 5.1 and conclude that only Φ will reach thermal equilibrium with the MSSM particles via its interaction with the gauge bosons.

Small K3 fiber

The study of moduli thermalisation in the case of small K3 fiber is more complicated. We shall first focus on CY three-folds with just one blow-up mode and later on will infer the general features of the situation with several blow-ups.

K3 fibrations with $h_{1,1} = 3$ are characterised by two small moduli: τ_1 that gives the volume of the K3 divisor Γ_1 , and τ_s which is the volume of the rigid divisor Γ_s . The canonically normalised fields χ_1 and Φ are defined by (4.30) and (4.32). We recall that one has to be careful about the possible incompatibility of MSSM branes on Γ_s with the non-perturbative effects that this cycle supports. Hence, to avoid dealing with such subtleties, below we will assume that the MSSM branes are not wrapping Γ_s . Again, using the results of Subsection 5.1, we infer the following for the different brane set-ups below:

1. If Γ_s is wrapped by an ED3 instanton and Γ_1 is wrapped by MSSM branes:
 - χ_1 couples to MSSM gauge bosons with strength $g \sim 1/M_P \Rightarrow \chi_1$ does not thermalise.

- Φ couples to MSSM gauge bosons more weakly than $\chi_1 \Rightarrow \Phi$ does not thermalise.
2. If Γ_s is wrapped by an ED3 instanton and $\Gamma_s + \Gamma_1$ is wrapped by MSSM branes with chiral intersections on Γ_1 :
 - χ_1 couples to MSSM gauge bosons with strength $g \sim \sqrt{\mathcal{V}}/M_P \Rightarrow \chi_1$ thermalises.
 - Φ couples to MSSM gauge bosons with strength $g \sim \sqrt{\mathcal{V}}/M_P \Rightarrow \Phi$ thermalises.
 3. If Γ_s is supporting a pure $SU(N)$ theory, that undergoes gaugino condensation, and Γ_1 is wrapped by MSSM branes:
 - χ_1 couples to MSSM gauge bosons with strength $g \sim 1/M_P$ and to hidden sector gauge boson with strength $g \sim \sqrt{\mathcal{V}}/M_P \Rightarrow \chi_1$ thermalises via its interaction with hidden sector gauge bosons.
 - Φ couples to MSSM gauge bosons more weakly than χ_1 and to hidden sector gauge bosons with strength $g \sim \sqrt{\mathcal{V}}/M_P \Rightarrow \Phi$ thermalises via its interaction with hidden sector gauge bosons.

In this case, two separate thermal baths are established: one contains χ_1 , Φ and the hidden sector gauge bosons at temperature T_1 , whereas the other one is formed by the MSSM particles at temperature T_2 . Generically, we expect that $T_1 \neq T_2$ since the two thermal baths are not in contact with each other.

4. If Γ_s is supporting a pure $SU(N)$ theory, that undergoes gaugino condensation, and $\Gamma_s + \Gamma_1$ is wrapped by MSSM branes with chiral intersections on Γ_1 :
 - χ_1 couples both to MSSM and hidden sector gauge bosons with strength $g \sim \sqrt{\mathcal{V}}/M_P \Rightarrow \chi_1$ thermalises.
 - Φ couples both to MSSM and hidden sector gauge bosons with strength $g \sim \sqrt{\mathcal{V}}/M_P \Rightarrow \Phi$ thermalises.

Now only one thermal bath is established containing χ_1 , Φ , the hidden sector gauge bosons and the MSSM particles, since both moduli interact with equal strength with the gauge bosons of the MSSM and of the hidden sector.

It is interesting to notice that both moduli χ_1 and Φ thermalise in all situations, except when the blow-up mode is wrapped by an ED3 instanton only. In this particular case, no modulus thermalises. It is trivial to generalise these conclusions for more than one blow-up mode and the MSSM still localised on the K3 fiber.

On the other hand, if the MSSM is localised on one of the rigid divisors, then for the case of more than one blow-up mode one can repeat the same general conclusions as at the end of Subsection 5.2, with in addition the fact that χ_1 will always thermalise as soon as one of the blow-up modes thermalises. This is due to the leading order mixing between Φ and any other small modulus, as can be seen explicitly in (4.33) and (4.34).

5.4 Modulini thermalisation

The study of modulini thermalisation is straightforward since, as we have seen in Subsection 4.4, the canonical normalisation for the modulini takes exactly the same form as the canonical normalisation for the moduli. This implies that, after supersymmetrisation, the small modulino-gaugino-gauge boson coupling has the same strength as the small modulus-gauge boson-gauge boson coupling. Given that this is the relevant interaction for moduli thermalisation, we can repeat the same considerations as those in Subsections 5.1-5.3 and conclude that the modulini thermalise every time, when their supersymmetric partners reach thermal equilibrium with the MSSM thermal bath. Note however that, if for the moduli the relevant processes are $2 \leftrightarrow 2$ interactions with gauge bosons, the crucial $2 \leftrightarrow 2$ processes for the modulini are:

- $2 \leftrightarrow 2$ processes with two gravitational vertices dominant for $\mathcal{V} < 10^{10}$: $\tilde{X} + \tilde{X} \leftrightarrow \tilde{\Phi} + \tilde{\Phi}$, $X + X \leftrightarrow \tilde{\Phi} + \tilde{\Phi}$, $\tilde{X} + \tilde{\Phi} \leftrightarrow \tilde{X} + \tilde{\Phi}$, $X + \tilde{\Phi} \leftrightarrow X + \tilde{\Phi}$, $\tilde{X} + \tilde{X} \leftrightarrow X + X$, $\tilde{X} + X \leftrightarrow \tilde{X} + X$.
- $2 \leftrightarrow 2$ processes with one gravitational and one renormalisable vertex dominant for $\mathcal{V} > 10^{10}$: $X + \tilde{\Phi} \leftrightarrow \tilde{X} + \tilde{X}$, $\tilde{X} + \tilde{\Phi} \leftrightarrow X + X$.

6. Finite temperature corrections in LVS

In this Section we study the finite temperature effective potential in LVS. We show that it has runaway behaviour at high T and compute the decompactification temperature T_{max} . We also investigate the cosmological implications of the small modulus decay. By imposing that the temperature just after its decay (regardless of whether or not that decay leads to reheating) be less than T_{max} , in order to avoid decompactification of the internal space, we find important restrictions on the range of values of the CY volume.

6.1 Effective potential

We shall now derive the explicit form of the finite temperature effective potential for LVS, following the analysis of moduli thermalisation performed in Section 5. We will study in detail the behaviour of thermal corrections to the $T = 0$ potential of the simple $CP^4_{[1,1,1,6,9]}$ model, and then realise that the single-hole Swiss-cheese case already incorporates all the key properties of the general LVS.

Single-hole Swiss-cheese

As we have seen in Section 5.1, not only ordinary MSSM particles thermalise via Yang-Mills interactions but also the small modulus and modulino reach thermal equilibrium with matter via their interactions with the gauge bosons. Therefore, the general expression (3.6) for the 1-loop finite temperature effective potential, takes the following form:

$$V_T^{1-loop} = -\frac{\pi^2 T^4}{90} \left(g_B + \frac{7}{8} g_F \right) + \frac{T^2}{24} \left(m_{\tilde{\Phi}}^2 + m_{\tilde{\Phi}}^2 + \sum_i M_{\text{SOFT},i}^2 \right) + \dots \quad (6.1)$$

We recall that (6.1) is a high temperature expansion of the general 1-loop integral (3.4), and so it is valid only for $T \gg m_\Phi, m_{\tilde{\Phi}}, M_{\text{SOFT},i}$. The general moduli-dependent expression for the modulino mass-squared $m_{\tilde{\Phi}}^2$ is given by (4.40) without the vacuum expectation value. On the other hand, in the limit $\tau_b \gg \tau_s$, $m_{\tilde{\Phi}}^2$ can be estimated as follows:

$$m_{\tilde{\Phi}}^2 \simeq \text{Tr} M_b^2 = \frac{K^{ij}}{2} \frac{\partial^2 V_0}{\partial \tau_i \partial \tau_j} \simeq \frac{K^{ss}}{2} \frac{\partial^2 V_0}{\partial \tau_s^2}. \quad (6.2)$$

For $a_s \tau_s \gg 1$, the previous expression (6.2), at leading order, becomes:

$$m_{\tilde{\Phi}}^2 \simeq \frac{A_s a_s^3 g_s e^{K_{cs}} M_P^2}{\pi} \left(72 A_s a_s \tau_s e^{-2a_s \tau_s} - \frac{3 W_0 \tau_s^{3/2} e^{-a_s \tau_s}}{\sqrt{2\mathcal{V}}} \right). \quad (6.3)$$

It can be shown that the gaugino and scalar masses arising from gravity mediated SUSY breaking¹⁶ are always parametrically smaller than m_Φ and $m_{\tilde{\Phi}}$, and so we shall neglect them. Moreover we shall drop also the $\mathcal{O}(T^4)$ term in (6.1) since it has no moduli dependence. Therefore, the relevant 1-loop finite-temperature effective potential reads:

$$V_T^{1-loop} = \frac{T^2}{24} \left(m_{\tilde{\Phi}}^2 + m_{\tilde{\Phi}}^2 \right) + \dots, \quad (6.4)$$

which using (4.40) and (6.3), takes the form:

$$V_T^{1-loop} = \frac{T^2}{24} \left(\frac{g_s e^{K_{cs}} M_P^2}{\pi} \right) \left[\lambda_1 \tau_s e^{-2a_s \tau_s} - \lambda_2 (4 + a_s \tau_s) \frac{\sqrt{\tau_s} e^{-a_s \tau_s}}{\mathcal{V}} + \frac{W_0^2}{2\mathcal{V}^2} \right] + \dots, \quad (6.5)$$

with

$$\lambda_1 \equiv 108 A_s^2 a_s^4, \quad \lambda_2 \equiv 3 a_s^2 A_s W_0 / \sqrt{2}. \quad (6.6)$$

Given that the leading contribution in (6.1), namely the $\mathcal{O}(T^4)$ term, does not bring in any moduli dependence, we need to go beyond the ideal gas approximation and consider the effect of 2-loop thermal corrections, as the latter could in principle compete with the terms in (6.5). The high temperature expansion of the 2-loop contribution looks like:

$$V_T^{2-loops} = T^4 \left(\kappa_1 g_{MSSM}^2 + \kappa_2 g_{\tilde{\Phi}XX}^2 m_{\tilde{\Phi}}^2 + \kappa_3 g_{\tilde{\Phi}\tilde{X}X}^2 m_{\tilde{\Phi}}^2 + \dots \right) + \dots, \quad (6.7)$$

where the κ 's are $\mathcal{O}(1)$ coefficients and:

- the $\mathcal{O}(g_{MSSM}^2)$ contribution comes from two loops involving MSSM particles,
- the $\mathcal{O}(g_{\tilde{\Phi}XX}^2)$ contribution is due to two loop diagrams with $\tilde{\Phi}$ and two gauge bosons,
- the $\mathcal{O}(g_{\tilde{\Phi}\tilde{X}X}^2)$ contribution comes from two loops involving the modulino $\tilde{\Phi}$, the gaugino \tilde{X} and the gauge boson X ,

¹⁶The contribution from anomaly mediation is subleading with respect to gravity mediation as shown in [39].

- all the other two loop diagrams give rise to subdominant contributions, and so they have been neglected. Such diagrams are the ones with Φ or $\tilde{\Phi}$ plus other MSSM particles, the self-interactions of the moduli and of the modulini, and two loops involving both Φ and $\tilde{\Phi}$. For example, the subleading contribution originating from the two-loop vacuum diagram due to the Φ^3 self-interaction takes the form:
$$\delta V_T^{2-loops} = \kappa_4 T^4 \frac{g_{\Phi^3}^2}{m_{\tilde{\Phi}}^2} \sim T^4 \frac{const}{\mathcal{V}(\ln \mathcal{V})^2}.$$

Note that in (6.7) we have neglected the $\mathcal{O}(T^2)$ term since it is subleading compared to both the $\mathcal{O}(T^4)$ 2-loop term and the $\mathcal{O}(T^2)$ 1-loop one. Now, the relevant gauge couplings in (6.7), have the following moduli dependence:

- $g_{MSSM}^2 = 4\pi/\tau_s$ since we assume that the MSSM is built via magnetised D7 branes wrapping the small cycle. In the case of a supersymmetric $SU(N_c)$ gauge theory with N_f matter multiplets, the coefficient κ_1 reads [40]:

$$\kappa_1 = \frac{1}{64} (N_c^2 - 1) (N_c + 3N_f) > 0. \quad (6.8)$$

- $g_{\Phi XX}^2 \sim g_{\tilde{\Phi} \tilde{X} X}^2 \sim \frac{\sqrt{\mathcal{V}}}{M_P}$ as derived in (4.47) and (A.9).

Adding (6.4) and (6.7) to the $T = 0$ potential V_0 , we obtain the full finite temperature effective potential:

$$V_{TOT} = V_0 + T^4 \left(\kappa_1 g_{MSSM}^2 + \kappa_2 g_{\Phi XX}^2 m_{\tilde{\Phi}}^2 + \kappa_3 g_{\tilde{\Phi} \tilde{X} X}^2 m_{\tilde{\Phi}}^2 \right) + \frac{T^2}{24} \left(m_{\tilde{\Phi}}^2 + m_{\tilde{\Phi}}^2 \right) + \dots \quad (6.9)$$

Despite the thermalisation of Φ and $\tilde{\Phi}$, which in principle leads to a modification of V_{TOT} compared to previous expectations in the literature, we shall now show that the thermal corrections due to Φ and $\tilde{\Phi}$ are, in fact, negligible compared to the other contributions in (6.9), everywhere in the moduli space of these models. In particular, the 2-loop MSSM effects dominate the temperature-dependent term.¹⁷

Let us start by arguing that the $\mathcal{O}(T^4)$ corrections arising from the modulus Φ and the modulino $\tilde{\Phi}$ are subleading compared to the 1-loop $\mathcal{O}(T^2)$ term. Indeed, the relevant part of the effective scalar potential (6.9) may be rewritten as:

$$T^4 \left(\kappa_2 g_{\Phi XX}^2 m_{\tilde{\Phi}}^2 + \kappa_3 g_{\tilde{\Phi} \tilde{X} X}^2 m_{\tilde{\Phi}}^2 \right) \sim T^2 \left(m_{\tilde{\Phi}}^2 + m_{\tilde{\Phi}}^2 \right) \underbrace{T^2 \frac{\mathcal{V}}{M_P^2}}_{\left(\frac{T}{M_s}\right)^2 \ll 1}, \quad (6.10)$$

where the \ll inequality is due to the fact that our effective field theory treatment makes sense only at energies lower than the string scale M_s . Therefore, we can neglect the effect of 2-loop thermal corrections involving Φ and $\tilde{\Phi}$. So we see that, although the interactions of Φ and $\tilde{\Phi}$ with gauge bosons and gauginos are strong enough to make them thermalise,

¹⁷Note that this is consistent with the results of [41] in the context of the O'KKLT model, where it was also found that the T-dependent contribution of moduli, that were assumed to be in thermal equilibrium, is negligible compared to the dominant contribution of the rest of the effective potential.

they are not sufficient to produce thermal corrections large enough to affect the form of the total effective potential. Let us also stress that this result is valid everywhere in moduli space, i.e. for each value of m_Φ^2 and $m_{\tilde{\Phi}}^2$, not just in the region around the zero-temperature minimum.

We now turn to the study of the general behaviour of the 1-loop $\mathcal{O}(T^2)$ term arising from Φ and $\tilde{\Phi}$. We shall show that it is always subdominant compared to the zero-temperature potential (2.17), and so it can be safely neglected. In fact, the two relevant terms (2.17) and (6.5) can be written as (ignoring the subleading loop corrections in V_0):

$$V_0 + \frac{T^2}{24} (m_\Phi^2 + m_{\tilde{\Phi}}^2) = \frac{g_s e^{K_{cs}} M_P^4}{8\pi} \left[p_1 A_1 \sqrt{\tau_s} \frac{e^{-2a_s \tau_s}}{\mathcal{V}} - p_2 A_2 \frac{\tau_s e^{-a_s \tau_s}}{\mathcal{V}^2} + p_3 A_3 \frac{1}{\mathcal{V}^3} \right], \quad (6.11)$$

with

$$p_1 = 36 a_s^4 A_s^2, \quad p_2 = 4 a_s A_s W_0, \quad p_3 = W_0^2 / 6, \quad (6.12)$$

and

$$A_1 \equiv \frac{2\sqrt{2}}{3a_s^2} + \underbrace{\frac{T^2 \mathcal{V} \sqrt{\tau_s}}{M_P^2}}_{\left(\frac{T}{M_{KK}}\right)^2 \ll 1}, \quad A_2 \equiv 1 + \frac{a_s^2}{4\sqrt{2}} \underbrace{\frac{T^2 \mathcal{V} \sqrt{\tau_s}}{M_P^2}}_{\left(\frac{T}{M_{KK}}\right)^2 \ll 1} \left(1 + \frac{4}{a_s \tau_s}\right), \quad A_3 \equiv \frac{9\hat{\xi}}{2} + \underbrace{\frac{T^2 \mathcal{V}}{M_P^2}}_{\left(\frac{T}{M_s}\right)^2 \ll 1}.$$

where the appearance of the Kaluza-Klein scale comes from the assumption that the MSSM branes are wrapping the small cycle τ_s :

$$M_{KK} \sim \frac{M_s}{\tau_s^{1/4}} \simeq \frac{M_P}{\sqrt{\mathcal{V}} \tau_s^{1/4}}. \quad (6.13)$$

Therefore, we can see that the 1-loop $\mathcal{O}(T^2)$ thermal corrections can never compete with V_0 for temperatures below the compactification scale $M_{KK} < M_s$, where our low energy effective field theory is trustworthy. Once again, we stress that the previous considerations are valid in all the moduli space (within our large volume approximations) and not just in the vicinity of the $T = 0$ minimum. We have seen that the only finite-temperature contribution that can compete with V_0 is the 2-loop $T^4 g_{MSSM}^2$ term, and so we can only consider from now on the following potential:

$$V_{TOT} = V_0 + 4\pi\kappa_1 \frac{T^4}{\tau_s} = \left(\frac{g_s e^{K_{cs}}}{8\pi} \right) \left[\frac{\lambda \sqrt{\tau_s} e^{-2a_s \tau_s}}{\mathcal{V}} - \frac{\mu \tau_s e^{-a_s \tau_s}}{\mathcal{V}^2} + \frac{\nu}{\mathcal{V}^3} + \frac{4\pi\tilde{\kappa}_1}{\tau_s} \left(\frac{T}{M_P} \right)^4 \right] M_P^4, \quad (6.14)$$

valid for temperatures $T \gg M_{SOFT}$, and with the constants given in (2.18) and (6.8)¹⁸. We realize that the leading moduli-dependent finite temperature contribution to the effective potential comes from 2-loops instead of 1-loop. This, however, does not mean that perturbation theory breaks down, since 1-loop effects still dominate when one takes into account the moduli independent $\mathcal{O}(T^4)$ piece that we dropped.

Now, from (6.14) it is clear that the thermal correction cannot induce any new T -dependent extremum of the effective potential. Its presence only leads to destabilization

¹⁸For convenience, here we have redefined $\tilde{\kappa}_1 \equiv 8\pi\kappa_1 g_s^{-1} e^{-K_{cs}}$.

of the $T = 0$ minimum at a certain temperature, above which the potential has a runaway behaviour. Therefore, we are led to the following qualitative picture. Let us assume that at the end of inflation the system is sitting at the $T = 0$ minimum. Then, after reheating the MSSM particles thermalise and the thermal correction $T^4 g_{MSSM}^2 \sim T^4/\tau_s$ gets switched on. As a result, the system starts running away along the τ_s direction only, since V_T does not depend on \mathcal{V} . However, as soon as τ_s becomes significantly larger than its $T = 0$ VEV, the two exponential terms in (6.14) become very suppressed with respect to the $\mathcal{O}(\mathcal{V}^{-3})$ α' correction (the ν term). Hence, the potential develops a run-away behaviour also along the \mathcal{V} -direction, thus allowing the Kähler moduli to remain within the Kähler cone.

In Section 6.2, we shall compute the decompactification temperature, at which the $T = 0$ minimum gets destabilised. Hence we shall focus on the region in the vicinity of the zero-temperature minimum, where the regime of validity of the expression (6.14) takes the form:

$$M_{SOFT} \ll T \ll M_{KK} \quad \Leftrightarrow \quad \frac{1}{\mathcal{V} \ln \mathcal{V}} \ll \frac{T}{M_P} \ll \frac{1}{\sqrt{\mathcal{V}} \tau_s^{1/4}}. \quad (6.15)$$

In the typical LVS where $\mathcal{V} \sim 10^{14}$ allows low energy SUSY, we get $M_{SOFT} \sim 10^3$ GeV and $M_{KK} \sim 10^{11}$ GeV; thus, in that case, eq. (6.14) makes sense only for energies 10^3 GeV $\ll T \ll 10^{11}$ GeV. On the other hand, for LVS that allow GUT string scenarios, $\mathcal{V} \sim 10^4$, which implies $M_{SOFT} \sim 10^{13}$ GeV and $M_{KK} \sim 10^{16}$ GeV; thus, in that case, (6.15) becomes 10^{13} GeV $\ll T \ll 10^{16}$ GeV.

General LARGE Volume Scenario

As we have seen in Section 2.3, one of the conditions on an arbitrary Calabi-Yau to obtain LVS, is the presence of a blow-up mode resolving a point-like singularity (del Pezzo 4-cycle). The moduli scaling of the scalar potential, at leading order and in the presence of N_{small} blow-up modes τ_{s_i} , $i = 1, \dots, N_{small}$, is still of the form (2.17) (neglecting loop corrections):

$$V_0 = \left(\frac{g_s e^{K_{cs}} M_P^4}{8\pi} \right) \left[\sum_{i=1}^{N_{small}} \left(\frac{\lambda \sqrt{\tau_{s_i}} e^{-2a_{s_i} \tau_{s_i}}}{\mathcal{V}} - \frac{\mu \tau_{s_i} e^{-a_{s_i} \tau_{s_i}}}{\mathcal{V}^2} \right) + \frac{\nu}{\mathcal{V}^3} \right]. \quad (6.16)$$

All the other moduli which are neither the overall volume nor a blow-up mode will appear in the scalar potential at subleading order. Moreover, due to the topological nature of τ_{s_i} , $K_{s_i s_i}^{-1} \sim \mathcal{V} \sqrt{\tau_{s_i}} \forall i = 1, \dots, N_{small}$ [8].

As derived in Section 4.1, these blow-up modes correspond to the heaviest moduli and modulini, which play the same role as Φ and $\tilde{\Phi}$ in the single-hole Swiss-cheese case. Hence the leading order behaviour of the mass-squareds of the blow-up moduli τ_{s_i} and the corresponding modulini $\tilde{\tau}_{s_i}$ are still given by (6.3) and (4.40) $\forall i = 1, \dots, N_{small}$. Therefore we can repeat the same considerations made in the previous paragraph and conclude that, for a general LVS, the 1-loop $\mathcal{O}(T^2)$ thermal corrections are always subdominant with respect to V_0 for temperatures below the compactification scale¹⁹. The only finite-temperature

¹⁹As we have seen in Section 5.2, if all the τ_{s_i} are wrapped by ED3 instantons then they do not thermalise. Only the moduli corresponding to 4-cycles wrapped by MSSM branes would then thermalise but, since they are lighter than the ED3 moduli, our argument is still valid. The same is true for all the possible scenarios outlined for the K3 fibration case in Section 5.3.

contribution that can compete with V_0 is again the 2-loop $T^4 g_{MSSM}^2$ term.

6.2 Decompactification temperature

As we saw in the previous subsection, the finite temperature corrections destabilize the large volume minimum of a general LVS. In this subsection we will derive the decompactification temperature T_{max} , that is the temperature above which the full effective potential has no other minima than the one at infinity.

Before performing a more precise calculation of T_{max} , let us present a qualitative argument that gives a good intuition for its magnitude. Let us denote by V_b the height of the potential barrier that separates the supersymmetric minimum at infinity from the zero temperature SUSY breaking one. Now, in order for the moduli to overcome the potential barrier and run away to infinity, one needs to supply energy of at least the same order of magnitude as V_b . In our case, the source of energy is provided by the finite-temperature effects, which give a contribution to the scalar potential of the order $V_T \sim T^4$. Hence a very good estimate for the decompactification temperature is given by $T_{max} \sim V_b^{1/4}$.

It is instructive to compare the implications of this estimate for the KKLT and LVS cases. In the simplest KKLT models the potential reads:

$$V_{KKLT} = \lambda_1 \frac{e^{-2a\tau}}{\tau} - \lambda_2 W_0 \frac{e^{-a\tau}}{\tau^2}, \quad (6.17)$$

where λ_1 and λ_2 are constants of order unity. The minimum is achieved by fine tuning the flux parameter $W_0 \sim \tau e^{-a\tau}$ and so the height of the barrier is given by

$$V_b \sim \langle V_{KKLT} \rangle \sim \frac{W_0^2}{\mathcal{V}^2} M_P^4 \sim m_{3/2}^2 M_P^2, \quad (6.18)$$

where we have used the fact that $\mathcal{V} = \tau^{3/2}$ and $m_{3/2} = W_0 M_P / \mathcal{V}$. Therefore the decompactification temperature becomes $T_{max} \sim \sqrt{m_{3/2} M_P} \sim 10^{10}$ GeV, as estimated in [15].

In the case of LVS, the height of the barrier is lower and so we expect a lower decompactification temperature T_{max} . Indeed, to leading order the potential is given by

$$V_{LVS} = \lambda_1 \sqrt{\tau_s} \frac{e^{-2a_s \tau_s}}{\mathcal{V}} - \lambda_2 W_0 \tau_s \frac{e^{-a_s \tau_s}}{\mathcal{V}^2} + \lambda_3 \frac{W_0^2}{\mathcal{V}^3} \quad (6.19)$$

with λ_1 , λ_2 and λ_3 being constants of order one, as reviewed in Section 2. The minimum is achieved for natural values of the flux parameter $W_0 \sim \mathcal{O}(1)$ and at exponentially large values of the overall volume $\mathcal{V} \sim W_0 \sqrt{\tau_s} e^{a_s \tau_s}$. Hence the height of the barrier can be estimated as:

$$V_b \sim \langle V_{LVS} \rangle \sim \frac{W_0^2}{\mathcal{V}^3} M_P^4 \sim m_{3/2}^3 M_P, \quad (6.20)$$

which gives a decompactification temperature of the order:

$$T_{max} \sim \left(m_{3/2}^3 M_P \right)^{1/4} \sim \frac{M_P}{\mathcal{V}^{3/4}}. \quad (6.21)$$

Let us now turn to a more precise computation. Without loss of generality, we shall focus here on the effective potential (6.14), valid for the single-hole Swiss-cheese case, and

look for its extrema. Given that the thermal contribution does not depend on the volume, the derivative of the potential with respect to \mathcal{V} gives the same result as in the $T = 0$ case:

$$\frac{\partial V_{TOT}}{\partial \mathcal{V}} = 0 \quad \Longrightarrow \quad \mathcal{V}_* = \frac{\mu}{\lambda} A(\tau_s) \sqrt{\tau_s} e^{a_s \tau_s}, \quad (6.22)$$

where²⁰

$$A(\tau_s) \equiv 1 - \sqrt{1 - \frac{3}{4} \left(\frac{\langle \tau_s \rangle}{\tau_s} \right)^{3/2}}, \quad (6.23)$$

and $\langle \tau_s \rangle \simeq (4\lambda\nu/\mu^2)^{2/3}$ is the $T = 0$ VEV of τ_s . Substituting (6.22) in the derivative of V_{TOT} with respect to τ_s and working in the limit $a_s \tau_s \gg 1$, in which one can neglect higher order instanton corrections, we obtain:

$$\left. \frac{\partial V_{TOT}}{\partial \tau_s} \right|_{\mathcal{V}=\mathcal{V}_*} = 0 \quad \Longrightarrow \quad 4\pi\tilde{\kappa}_1 \frac{\mu e^{3a_s \tau_s}}{\lambda^2 a_s \tau_s^2} \left(\frac{T}{M_P} \right)^4 A(\tau_s)^2 + 2A(\tau_s) - 1 = 0. \quad (6.24)$$

Notice that at zero temperature (6.24) simplifies to $A(\tau_s) = 1/2$, which from (6.23) correctly implies $\tau_s = \langle \tau_s \rangle$. Now, since equation (6.24) is transcendental, one cannot write down an analytical solution, that gives the general relation between the location of the τ_s extrema and the temperature. Nevertheless, we will see shortly that it is actually possible to extract an analytic estimate for the decompactification temperature. To understand why, let us gain insight into the behaviour of the function on the LHS of (6.24) by plotting it and looking at its intersections with the τ_s -axis.

We plot the LHS of equation (6.24) on Figure 5 for several values of the temperature; T increases from right to left. From this figure it is easy to see that the temperature-dependent correction to V_{TOT} behaves effectively as an up-lifting term. Namely, the finite-temperature contribution lifts the potential, giving rise to a local maximum (the right intersection with the τ_s axis) in addition to the $T = 0$ minimum (the left intersection). As the temperature increases, the maximum increases as well and shifts towards smaller values of τ_s . On the other hand, the minimum remains very close to the zero-temperature one at all temperatures. Clearly, the decompactification temperature T_{max} is reached when the two extrema coincide. The key observation here is that this happens in a small neighborhood of the $T = 0$ minimum, located at $\langle \tau_s \rangle \simeq (4\lambda\nu/\mu^2)^{2/3}$.

In view of the considerations of the previous paragraph, to find an analytic estimate for T_{max} we shall utilize the following strategy. We will Taylor-expand the function $F(\tau_s)$, defined by the LHS of equation (6.24), to second order in a small neighborhood of the point $\tau_s = \langle \tau_s \rangle$. Then we will use the resulting quadratic function $f(\delta)$, where $\delta \equiv \tau_s - \langle \tau_s \rangle$, as an approximation of $F(\tau_s)$ in a larger neighborhood and will look for the zeros of $f(\delta)$. Requiring that the two roots of $f(\delta)$ coincide, will give us an estimate for the decompactification temperature. Clearly, this procedure is not exact. In particular, the

²⁰We discard the solution with the positive sign in front of the square root in (6.23) since, upon its substitution one finds that the other extremum condition, $\partial V_{TOT}/\partial \tau_s = 0$, does not have any solution.

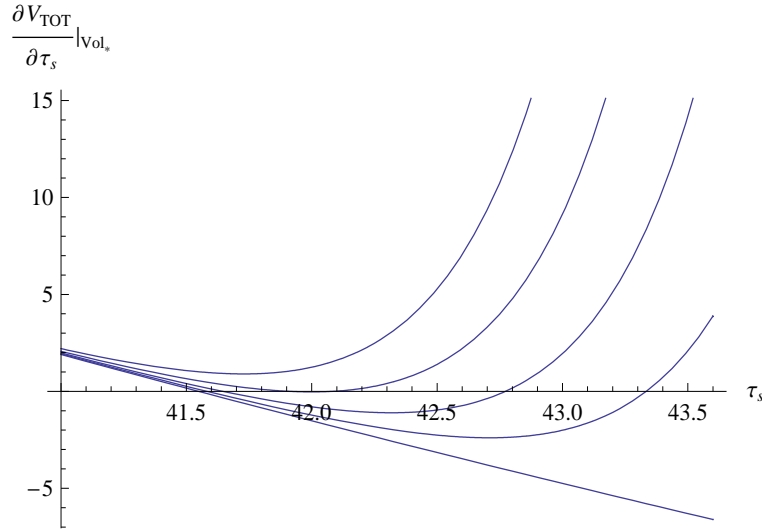


Figure 5: The LHS of eq. (6.24) is plotted versus τ_s . The temperature increases from right to left. The straight line represents the zero temperature case. The other values of the temperature are $T/M_P = 0.8 \cdot 10^{-10}, 1.0 \cdot 10^{-10}, 1.2 \cdot 10^{-10}, 1.4 \cdot 10^{-10}$. To obtain the plots we used the following numerical values: $\xi = 1.31, A_s = 1, W_0 = 1, a_s = \pi/4, e^{K_{cs}} = 8\pi/g_s, g_s = 0.1, N_c = 5, N_f = 7$. With these values one has that $\langle \tau_s \rangle = 41.55$ and $\langle \mathcal{V} \rangle = 7.02 \cdot 10^{13}$, which implies that $T_{max} = 1.58 \cdot 10^{-10} M_P \simeq 3.79 \cdot 10^8$ GeV according to (6.30). Note that the numerically found value of the decompactification temperature is $T_{max,num} = 1.20 \cdot 10^{-10} M_P$.

function $F(\tau_s)$ is better approximated by keeping higher orders in the Taylor expansion. In our case, we have checked numerically that a really good approximation is obtained by going to at least sixth order. However, in doing so one again ends up with an equation that cannot be solved analytically. So the key point is that the systematic error introduced by the quadratic approximation is rather small (we have checked that the analytical results obtained by following the above procedure are in very good agreement with the exact numerical values).

Now let us substitute $\tau_s = \langle \tau_s \rangle + \delta$ in (6.24) and read off the terms up to order δ^2 . The result is:

$$a \delta^2 + b \delta + c = 0, \quad (6.25)$$

where the corresponding coefficients, in the limit $a_s \langle \tau_s \rangle \gg 1$, take the form:

$$\begin{cases} a \simeq \frac{9}{2} \mathcal{T} a_s^2 + \frac{171}{8} \lambda^2 a_s, \\ b \simeq 3 \mathcal{T} a_s - 9 \lambda^2 a_s \langle \tau_s \rangle, \quad c \simeq \mathcal{T}, \end{cases} \quad (6.26)$$

and we have set

$$\mathcal{T} \equiv 4\pi \tilde{\kappa}_1 \left(\frac{T}{M_P} \right)^4 \mu e^{3a_s \langle \tau_s \rangle}. \quad (6.27)$$

Finally, to find the decompactification temperature, we require that the two solutions δ_1 and δ_2 coincide:

$$\delta_1 = \delta_2 \quad \Longleftrightarrow \quad b^2 - 4ac = 0, \quad (6.28)$$

which, for $a_s \langle \tau_s \rangle \gg 1$, gives:

$$T_{max} = 3(\sqrt{2} - 1)\lambda^2 \langle \tau_s \rangle \iff T_{max}^4 = \frac{3(\sqrt{2} - 1)\lambda^2 \langle \tau_s \rangle}{4\pi\tilde{\kappa}_1\mu} e^{-3a_s \langle \tau_s \rangle} M_P^4. \quad (6.29)$$

Notice that we can rewrite the decompactification temperature in terms of \mathcal{V} as:

$$T_{max}^4 = \frac{3(\sqrt{2} - 1)}{32\pi} \frac{\mu^2 \langle \tau_s \rangle^{5/2}}{\lambda\tilde{\kappa}_1 \mathcal{V}^3} M_P^4 \implies T_{max} \sim \left(m_{3/2}^3 M_P\right)^{1/4} \sim \frac{M_P}{\mathcal{V}^{3/4}}, \quad (6.30)$$

where we have used the relation between the $T = 0$ VEV of the volume and $\langle \tau_s \rangle$, which is given by (6.22) with $\tau_s = \langle \tau_s \rangle$ and $A = 1/2$. It is reassuring that (6.30) is of the same form as the result (6.21), obtained from the intuitive arguments based on the height of the potential barrier.

6.3 Small moduli cosmology

Clearly, the decompactification temperature (6.30) sets an upper bound on the temperature in the early Universe, in particular on the reheating temperature, T_{RH}^0 , at the end of inflation. We will investigate now how this constraint affects the moduli thermalisation picture studied in Subsection 5.1.²¹

Recall that there we derived the following:

- For small values of the volume ($\mathcal{V} < 10^{10}$), the freeze-out temperature for the small modulus Φ is given by (5.2): $T_f^{SV} \sim M_P \mathcal{V}^{-2/3}$.
- For large values of the volume ($\mathcal{V} > 10^{10}$), the freeze-out temperature for Φ is given by (5.3): $T_f^{LV} \sim 10^3 M_P \mathcal{V}^{-1}$.

Note also that, in both cases, the condition $T_f < T_{RH}^0 < T_{max}$ has to be satisfied in order for the modulus to reach equilibrium with the MSSM thermal bath. Now, for small values of \mathcal{V} we have that:

$$\frac{T_{max}}{T_f^{SV}} \sim \frac{\mathcal{V}^{2/3}}{\mathcal{V}^{3/4}} = \mathcal{V}^{-1/12} < 1, \quad (6.31)$$

which implies that Φ actually never thermalises. On the other hand, for large values of \mathcal{V} we have that (writing $\mathcal{V} \sim 10^x$):

$$\frac{T_{max}}{T_f^{LV}} \sim \frac{\mathcal{V}^{1/4}}{10^3} = 10^{x/4-3} > 1 \iff x > 12. \quad (6.32)$$

Hence, for $\mathcal{V} > 10^{12}$, Φ can reach thermal equilibrium with the MSSM plasma, as long as T_{RH}^0 is such that $T_f^{LV} < T_{RH}^0 < T_{max}$. Let us stress, however, that if $T_{RH}^0 < T_f^{LV}$ the modulus will never thermalise even though $T_f^{LV} < T_{max}$. Note that, since the temperature T_{RH}^0 depends on the concrete realization of inflation and the details of the initial reheating process, its determination is beyond the scope of the present paper. So we will treat it as a free parameter, satisfying only the constraint $T_{RH}^0 < T_{max}$.

We would like now to study the cosmological history of Φ which, in our case, presents two possibilities:

²¹Similar considerations apply for the more general multiple-hole Swiss-cheese and K3 fibration cases.

1. The modulus Φ decays at the end of inflation being the main responsible for initial reheating. We may envisage two physically different situations where this could happen: in one case, Φ is the inflaton and it decays at the end of inflation. In the other case, Φ is not the inflaton, but it starts oscillating around its VEV when the inflaton is still driving inflation by rolling down its flat potential. In this case, the decay of Φ occurs just after the slow-roll conditions stop being satisfied and the inflaton reaches its VEV.

After Φ decays, its energy density is converted into radiation. The decay products thermalise rapidly and re-heat the Universe to a temperature $T_{RH} = T_{RH}^0$. The latter can be computed by noticing that the Φ energy density $\rho_\Phi \sim \Gamma_{\Phi \rightarrow XX}^2 M_P^2$ will be converted into radiation energy density $\rho_R \sim g_* T^4$. Hence T_{RH}^0 can be obtained by comparing $\Gamma_{\Phi \rightarrow XX}$ with the value of H , given by the Friedmann equation for radiation dominance:

$$\begin{aligned} \Gamma_{\Phi \rightarrow XX} &\sim \frac{\ln \mathcal{V}}{16\pi} \frac{m_\Phi^2}{M_P} \simeq H \sim g_*^{1/2} \frac{(T_{RH}^0)^2}{M_P} \\ \Leftrightarrow T_{RH}^0 &\simeq \left(\frac{\ln \mathcal{V}}{16\pi \sqrt{g_*}} \right)^{1/2} m_\Phi = \frac{(\ln \mathcal{V})^{3/2} M_P}{4\sqrt{\pi} g_*^{1/4} \mathcal{V}}. \end{aligned} \quad (6.33)$$

In order for this picture to be compatible with the presence of a decompactification temperature (6.30), that sets the maximal temperature of the Universe, we need to require that $T_{RH}^0 < T_{max}$. As we shall see in Subsection 6.4, this requirement can be translated into a constraint on the values that the internal volume can take.

2. The modulus Φ is not the main source of initial reheating, which we suppose to be the inflaton. After the inflaton decays, the Universe is re-heated to a temperature T_{RH}^0 and an epoch of radiation dominance begins. The modulus Φ will only thermalise if $\mathcal{V} > 10^{12}$ and $T_f^{LV} < T_{RH}^0$. However, T_f^{LV} is rather close to T_{max} and so, even when Φ thermalises, it will drop out of equilibrium very quickly at T_f^{LV} . Then, for general values of \mathcal{V} , the modulus Φ will decay out of equilibrium at a temperature $T_D < T_{RH}^0$. As we shall show below, this decay will occur during radiation domination, since $T_D > T_{dom}$, with T_{dom} being the temperature at which the modulus energy density would dominate over the radiation energy density. So the temperature T_D at which Φ decays, is still given by (6.33) upon replacing T_{RH}^0 with T_D :

$$T_D \simeq \frac{(\ln \mathcal{V})^{3/2} M_P}{4\sqrt{\pi} g_*^{1/4} \mathcal{V}}. \quad (6.34)$$

Note that the above expression satisfies $T_D < T_f^{SV,LV}$, as should be the case for consistency. Another important observation is that (6.34) is also the usual expression for the temperature T_{RH} , to which the Universe is re-heated by the decay of a particle releasing its energy to the thermal bath. In other words, for us $T_{RH} = T_D$ since the modulus Φ decays during radiation domination. On the contrary, if a modulus decays when its energy density is dominating the energy density of the Universe, then

$T_D < T_{RH}$ and the decay produces an increase in the entropy density S , which is determined by:

$$\Delta \equiv \frac{S_{fin}}{S_{in}} \sim \left(\frac{T_{RH}}{T_D} \right)^3. \quad (6.35)$$

As already mentioned, since for us $T_{RH} = T_D$, the decay of Φ does not actually lead to reheating or, equivalently, to an increase in the entropy density, given that from (6.35) we have $\Delta = 1$. As a consequence, Φ cannot dilute any unwanted relics, like for example the large modulus χ which suffers from the cosmological moduli problem.²²

To recapitulate: in the present case 2, we have the following system of inequalities:

$$\text{for } \mathcal{V} < 10^{12}: \quad T_{dom} < T_D < T_{RH}^0 < T_{max}, \quad (6.36)$$

$$\text{for } \mathcal{V} > 10^{12}: \quad T_{dom} < T_D < T_f^{LV} < T_{RH}^0 < T_{max}. \quad (6.37)$$

As in case 1 above, the condition $T_D < T_{max}$ implies a constraint on \mathcal{V} , that we will derive in Subsection 6.4. We underline again that this condition is necessary but not sufficient, since for us T_{RH}^0 is an undetermined parameter. In concrete models, in which one could compute T_{RH}^0 , the condition $T_{RH}^0 < T_{max}$ might lead to further restrictions.

Let us now prove our claim above that, when the modulus Φ is not responsible for the initial reheating (case 2), it will decay before its energy density begins to dominate the energy density of the Universe. Φ will start oscillating around its VEV when $H \sim m_\Phi$ at a temperature T_{osc} given by:

$$T_{osc} \sim g_*^{-1/4} \sqrt{m_\Phi M_P}. \quad (6.38)$$

The energy density ρ_Φ , stored by Φ , and the ratio between ρ_Φ and the radiation energy density at T_{osc} read as follows:

$$\rho_\Phi|_{T_{osc}} \sim m_\Phi^2 \langle \tau_s \rangle^2 \quad \Rightarrow \quad \left(\frac{\rho_\Phi}{\rho_r} \right) \Big|_{T_{osc}} \sim \frac{m_\Phi^2 \langle \tau_s \rangle^2}{g_* T_{osc}^4} \sim \frac{\langle \tau_s \rangle^2}{M_P^2}. \quad (6.39)$$

By definition, the temperature T_{dom} , at which ρ_Φ becomes comparable to ρ_r and hence Φ begins to dominate the energy density of the Universe, is such that:

$$\left(\frac{\rho_\Phi}{\rho_r} \right) \Big|_{T_{dom}} \sim 1. \quad (6.40)$$

Now, given that ρ_Φ redshifts as T^3 whereas ρ_r scales as T^4 , we can relate T_{dom} with T_{osc} :

$$T_{dom} \left(\frac{\rho_\Phi}{\rho_r} \right) \Big|_{T_{dom}} \sim T_{osc} \left(\frac{\rho_\Phi}{\rho_r} \right) \Big|_{T_{osc}} \quad \Leftrightarrow \quad T_{dom} \sim g_*^{-1/4} \frac{\langle \tau_s \rangle^2}{M_P^2} \sqrt{m_\Phi M_P}. \quad (6.41)$$

We shall show now that $T_{dom} < T_D$ with T_D being the decay temperature during radiation dominance, which is obtained by comparing H with $\Gamma_{\Phi \rightarrow XX}$:

$$T_D \sim g_*^{-1/4} \sqrt{\Gamma_{\Phi \rightarrow XX} M_P}. \quad (6.42)$$

²²This kind of solution of the cosmological moduli problem, i.e. dilution via saxion or modulus decay, is used both in [43] and in [44].

The ratio of (6.42) and (6.41) gives:

$$\frac{T_D}{T_{dom}} \sim \frac{\sqrt{\Gamma_{\Phi \rightarrow XX}} M_P^2}{\sqrt{m_\Phi} \langle \tau_s \rangle^2}. \quad (6.43)$$

Using that $\Gamma_{\Phi \rightarrow XX} \sim \mathcal{V} m_\Phi^3 M_P^{-2}$ and $\langle \tau_s \rangle \sim 10 M_s \sim 10 M_P \mathcal{V}^{-1/2}$, the last relation becomes:

$$\frac{T_D}{T_{dom}} \sim \frac{(\ln \mathcal{V}) \sqrt{\mathcal{V}}}{100} > 1 \quad \text{for } \mathcal{V} > 10^{2.5}. \quad (6.44)$$

Hence, we conclude that $T_D > T_{dom}$ and, therefore, Φ decays before it can begin to dominate the energy density of the Universe. The main consequence of this is that Φ cannot dilute unwanted relics via its decay.

6.4 Lower bound on \mathcal{V}

As we saw in the previous Subsection, there are two possible scenarios for the cosmological evolution of the small modulus Φ . However, since the RHS of (6.33) and (6.34) coincide, in both cases the crucial quantity is the same, although with a different physical meaning. Let us denote this quantity by $T_* \sim (\Gamma_\Phi M_P)^{1/2}$. We shall impose that $T_* < T_{max}$ and shall show below that from this requirement one can derive a lower bound on the possible values of \mathcal{V} in a general LVS. Before we begin, let us first recall that:

1. If Φ is responsible for the initial reheating via its decay, then $T_* = T_{RH}^0$.
2. If Φ decays after the original reheating in a radiation dominated era, then $T_* = T_D < T_{RH}^0$.

Regardless of which of these two situations we consider, T_* is the temperature of the Universe after Φ decays. Then, in order to prevent decompactification of the internal space, we need to impose $T_* < T_{max}$. In general, this condition is necessary but not sufficient because in case 2 one must ensure also that $T_{RH}^0 < T_{max}$. This is a constraint that we cannot address given that in this case T_{RH}^0 is an undetermined parameter for us.

Let us now compute T_* precisely. We start by using the exact form of the decay rate $\Gamma_{\Phi \rightarrow XX}$:

$$\Gamma_{\Phi \rightarrow XX} = \frac{g_{\Phi XX}^2 m_\Phi^3}{64\pi M_P^2}, \quad (6.45)$$

where

$$g_{\Phi XX} = \frac{2^{5/4} \sqrt{3}}{\langle \tau_s \rangle^{3/4}} \sqrt{\mathcal{V}}. \quad (6.46)$$

The mass of Φ is given by:

$$m_\Phi = \sqrt{P} \frac{2a_s \langle \tau_s \rangle W_0}{\mathcal{V}} M_P, \quad (6.47)$$

where we are denoting with P the prefactor of the scalar potential: $P \equiv g_s e^{K_{cs}} / (8\pi)$. From the minimisation of the scalar potential we have that

$$a_s \langle \tau_s \rangle = \ln(p\mathcal{V}) = \ln p + \ln \mathcal{V}, \quad (6.48)$$

where

$$p \equiv \frac{12\sqrt{2}a_s A_s}{W_0\sqrt{\tau_s}} \sim \mathcal{O}(1) \quad \Rightarrow \quad a_s \langle \tau_s \rangle \simeq \ln \mathcal{V}, \quad (6.49)$$

and so

$$m_\Phi = \sqrt{P} \frac{2W_0 \ln \mathcal{V}}{\mathcal{V}} M_P. \quad (6.50)$$

Therefore, the decay rate $\Gamma_{\Phi \rightarrow XX}$ turns out to be:

$$\Gamma_{\Phi \rightarrow XX} = P^{3/2} \frac{3W_0^3 (\ln \mathcal{V})^3}{\sqrt{2\pi} \langle \tau_s \rangle^{3/2}} \frac{M_P}{\mathcal{V}^2}. \quad (6.51)$$

Finally, in order to obtain the total decay rate, we need to multiply $\Gamma_{\Phi \rightarrow XX}$ by the total number of gauge bosons for the MSSM $N_X = 12$:

$$\Gamma_{\Phi \rightarrow XX}^{TOT} = P^{3/2} \frac{36W_0^3 (\ln \mathcal{V})^3}{\sqrt{2\pi} \langle \tau_s \rangle^{3/2}} \frac{M_P}{\mathcal{V}^2}. \quad (6.52)$$

Now, we can find T_* by setting $4(\Gamma_{\Phi \rightarrow XX}^{TOT})^2/3$ equal to $3H^2$, with H read off from the Friedmann equation for radiation dominance:

$$T_* = \left(\frac{40}{\pi^2 g_*} \right)^{1/4} \sqrt{\Gamma_{\Phi}^{TOT} M_P} = P^{3/4} \frac{6}{\pi} \left(\frac{20}{g_*} \right)^{1/4} \frac{(W_0 \ln \mathcal{V})^{3/2}}{\langle \tau_s \rangle^{3/4}} \frac{M_P}{\mathcal{V}}. \quad (6.53)$$

We are finally ready to explore the constraint $T_* < T_{max}$. Recall that the maximal temperature is given by the decompactification temperature (6.30):

$$T_{max} = \left(\frac{P}{4\pi\kappa_1} \right)^{1/4} \left[\frac{(\sqrt{2}-1)}{4\sqrt{2}} \right]^{1/4} \frac{\sqrt{W_0} \langle \tau_s \rangle^{5/8}}{\mathcal{V}^{3/4}} M_P. \quad (6.54)$$

Let us now consider the ratio T_{max}/T_* and impose that it is larger than unity (using $g_*(MSSM) = 228.75$):

$$R \equiv \frac{T_{max}}{T_*} = c \frac{\mathcal{V}^{1/4}}{(\ln \mathcal{V})^{3/2}} \quad \text{with} \quad c \equiv J \left[\frac{(\sqrt{2}-1)g_*}{80\sqrt{2}} \right]^{1/4} \frac{\pi \langle \tau_s \rangle^{11/8}}{6W_0} \simeq \frac{\langle \tau_s \rangle^{11/8}}{2W_0}, \quad (6.55)$$

where we have defined:

$$J \equiv (4\pi\kappa_1 P^2)^{-1/4} = \frac{8.42}{\kappa_1^{1/4}} e^{-K_{cs}/2} \quad \text{for} \quad g_s = 0.1, \quad (6.56)$$

and in (6.55) we have set $J = 1$. In fact, from (6.8), we find that in the case of SQCD with $N_c = 3$ and $N_f = 6$, $\kappa_1 = 2.625$. However for the MSSM we expect a larger value of κ_1 which we assume to be of the order $\kappa_1 = 10$. Then for natural values of K_{cs} like $K_{cs} = 3^{23}$,

²³The dependence of the Kähler potential on the complex structure moduli can be worked out by computing the different periods of the CY three-fold under consideration. As derived in [42], for the simplest example of a CY manifold with just one complex structure modulus U (the mirror of the quintic), for natural values of U , $|U| \sim \mathcal{O}(1) \Rightarrow K_{cs} \sim \mathcal{O}(1)$.

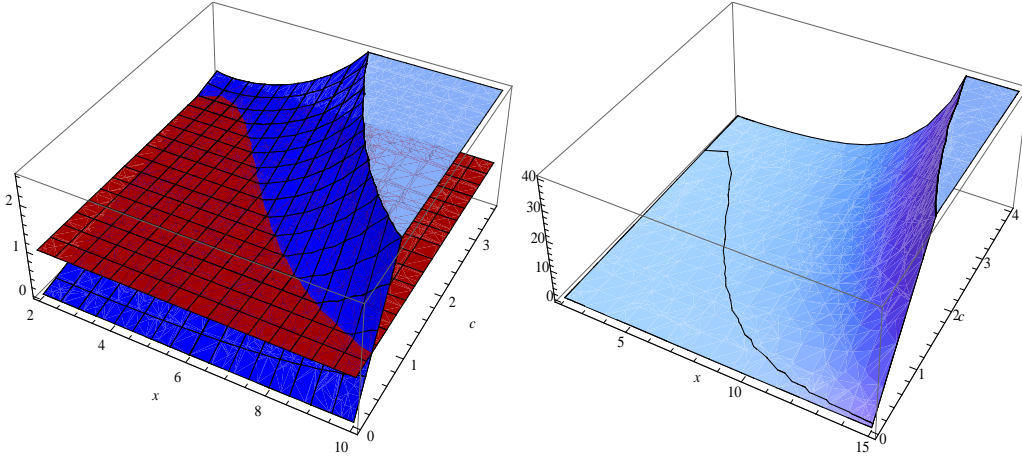


Figure 6: Plots of the ratio $R \equiv T_{max}/T_*$ as a function of $\mathcal{V} = 10^x$ and the parameter $c_{min} < c < c_{max}$ as defined in (6.55), (6.57) and (6.58). In the left plot, the red surface is the constant function $R = 1$, whereas in the right plot the black line denotes the curve in the (x,c) -plane for which $R = 1$.

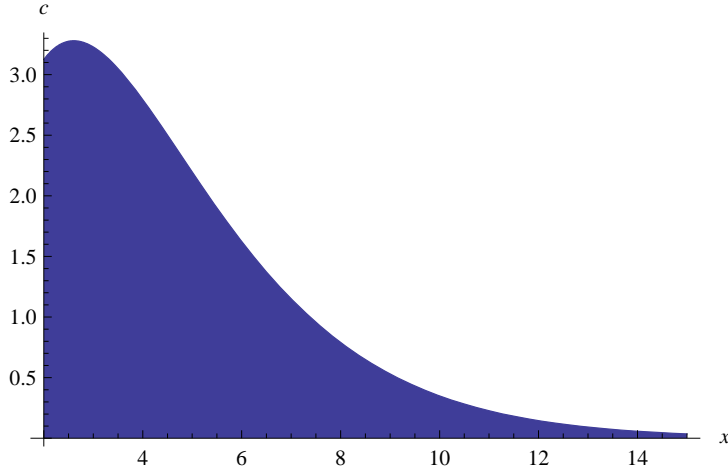


Figure 7: Plot of the $R = 1$ curve in the (x,c) -plane. The shaded region represents the phenomenologically forbidden area, in which the values of x and c are such that $R < 1 \Leftrightarrow T_{max} < T_*$.

from (6.56), we find $J = 1.05$. Let us consider now the maximum and minimum values that the parameter c can take for natural values of $\langle \tau_s \rangle$ and W_0 :

$$\begin{cases} \langle \tau_s \rangle_{max} = 100 \\ W_{0,min} = 0.01 \end{cases} \implies c_{max} \simeq 10^4, \quad (6.57)$$

$$\begin{cases} \langle \tau_s \rangle_{min} = 2 \\ W_{0,max} = 100 \end{cases} \implies c_{min} \simeq 10^{-2}. \quad (6.58)$$

Now writing $\mathcal{V} \simeq 10^x$, R becomes a function of x and c . Finally, we can make a 3D plot of R with $c_{min} < c < c_{max}$ and $2 < x < 15$, and see in which region $R > 1$. This is done in Figure 6. In order to understand better what values of \mathcal{V} are disfavoured, we

also plot in Figure 7, as the shaded region, the region in the (x,c) -plane below the curve $R = 1$, which represents the phenomenologically forbidden area for which $T_{max} < T_*$. We conclude that small values of the volume, which would allow the standard picture of gauge coupling unification and GUT theories, are disfavoured compared to larger values of \mathcal{V} , that naturally lead to TeV-scale SUSY and are thus desirable to solve the hierarchy problem. In Table 4, we show explicitly how the lower bound on the volume, for some benchmark scenarios, favours LVS with larger values of \mathcal{V} .

	$R > 1 \Leftrightarrow T_{max} > T_*$
$c = 4$	$\forall x$
$c = 3$	$x > 2.1$
$c = 2$	$x > 3.8$
$c = 1$	$x > 5.9$
$c = 0.5$	$x > 7.6$
$c = 0.1$	$x > 11.3$
$c = 0.05$	$x > 12.8$
$c = 0.01$	$x > 16.1$

Table 4: Lower bounds on the volume in the string frame $\mathcal{V}_s \sim 10^{x-3/2}$ for some benchmark scenarios.

From the definition (6.55) of the parameter c , it is interesting to notice that for values of $\langle \tau_s \rangle$ far from the edge of consistency of the supergravity approximation $\langle \tau_s \rangle \sim \mathcal{O}(10)$, c should be fairly large, and hence the bound very weak, for natural values of $W_0 \sim \mathcal{O}(1)$, while c should get smaller for larger values of W_0 that lead to a stronger bound. In addition, it is reassuring to notice that for typical values of $\mathcal{V} \sim 10^{15}$, $T_{max} > T_*$ except for a tiny portion of the (x,c) -space. It also important to recall that the physical value of the volume as seen by the string is the one expressed in the string frame \mathcal{V}_s , while we are working in the Einstein frame where $\mathcal{V}_s = g_s^{3/2} \mathcal{V}_E$. Hence if we write $\mathcal{V}_E \sim 10^x$, then we have that $\mathcal{V}_s = 10^{x-3/2}$, upon setting $g_s = 0.1$.

General LARGE Volume Scenario

Let us now generalise our lower bound on \mathcal{V} to the four cases studied in Subsections 5.2 and 5.3 for the multiple-hole Swiss-cheese and K3 fibration case (focusing on the small K3 fiber scenario) respectively.

First of all, we note that, since in all the cases the 4-cycle supporting the MSSM is stabilised by string loop corrections [8], we can estimate the actual height of the barrier seen by this modulus as (see (2.22)):

$$V_b \sim \frac{W_0^2}{\mathcal{V}^3 \sqrt{\tau}}, \quad (6.59)$$

where we are generically denoting any small cycle (either a blow-up or a K3 fiber divisor) as τ , given that the values of the VEV of all these 4-cycles will have the same order of magnitude. Then setting $V_b \sim T_{max}^4 / \tau$, we obtain:

$$T_{max}^4 \sim \frac{\sqrt{\tau} W_0^2}{\mathcal{V}^3}. \quad (6.60)$$

We notice that (6.60) is a bit lower than (6.30) but the two expressions for T_{max} share the same leading order \mathcal{V} -dependence.

Let us now examine the 4 cases of Subsection 5.2 in more detail, keeping the same notation as in that Subsection, and denoting as Φ the small modulus of the single-hole Swiss-cheese scenario studied above:

1. The relevant decay is the one of τ_2 to MSSM gauge bosons. The order of magnitude of the mass of τ_2 is:

$$m_{\tau_2}^2 \sim \frac{(\ln \mathcal{V})^2 W_0^2}{\mathcal{V}^2 \tau^2}, \quad (6.61)$$

and so τ_2 is lighter than Φ , and, in turn, T_* will be smaller. In fact, plugging (6.61) in (6.45), we end up with (ignoring numerical prefactors):

$$T_* \sim \frac{(\ln \mathcal{V})^{3/2} W_0^{3/2}}{\mathcal{V} \tau^{9/4}}. \quad (6.62)$$

Hence we obtain

$$R^{(1)} \equiv \frac{T_{max}}{T_*} = c^{(1)} \frac{\mathcal{V}^{1/4}}{(\ln \mathcal{V})^{3/2}} \quad \text{with} \quad c^{(1)} \sim \frac{\tau^{19/8}}{W_0}. \quad (6.63)$$

Comparing this result with (6.55), we realise that $R^{(1)} \sim R \tau$ and so the lower bound on \mathcal{V} turns out to be less stringent. The final results can still be read from Table 4 upon replacing c with $c^{(1)}$.

2. The relevant decay is the one of τ_1 to MSSM gauge bosons since $m_{\tau_1} \sim m_\Phi$, and so τ_1 is heavier than τ_2 . Therefore T_* will still be given by (6.53). Hence we obtain

$$R^{(2)} \equiv \frac{T_{max}}{T_*} = c^{(2)} \frac{\mathcal{V}^{1/4}}{(\ln \mathcal{V})^{3/2}} \quad \text{with} \quad c^{(2)} \sim \frac{\tau^{7/8}}{W_0}. \quad (6.64)$$

Comparing this result with (6.55), we realise that $R^{(2)} \sim R \tau^{-1/2}$ and so the lower bound on \mathcal{V} turns out to be more stringent. The final results can still be read from Table 4 upon replacing c with $c^{(2)}$.

3. The relevant decay is the one of τ_1 to hidden sector gauge bosons. Hence we point out that the considerations of case 2 apply also for this case.
4. The relevant decay is the one of τ_1 to MSSM gauge bosons, and so we can repeat the same considerations of case 2.

The final picture is that for all cases the \mathcal{V} -dependence of the ratio T_{max}/T_* is the same as in (6.55). The only difference is a rescaling of the parameter c . Thus we conclude that, as far as the lower bound on \mathcal{V} is concerned, the single-hole Swiss-cheese case shows all the qualitative features of a general LVS.

Finally, we mention that in the case of a K3 fibration with small K3 fiber, cases 2, 3, and 4 of Subsection 5.3 have the same behaviour as case 2 of the multiple-hole Swiss-cheese, so giving a more stringent lower bound on \mathcal{V} . We should note though that this lower bound does not apply to case 1 of Subsection 5.3, since both of the moduli have an M_P -suppressed, instead of M_s -suppressed, coupling to MSSM gauge bosons. However, these kinds of models tend to prefer larger values of \mathcal{V} (due to the fact that $a_s = 2\pi$ for an ED3 instanton) which are not affected by the lower bound that we derived.

7. Discussion

Let us now discuss some of the possible applications of these results, as well as directions for future work. As we have emphasized throughout the paper, there are two kinds of LVS, depending on the magnitude of the value of the internal volume \mathcal{V} . Their main cosmological characteristics are the following:

LV case

In this case the volume is stabilised at large values of the order $\mathcal{V} \sim 10^{15}$ which allows to solve the hierarchy problem yielding TeV scale SUSY naturally. Here are the main cosmological features of these scenarios:

- The moduli spectrum includes a light field χ related to the overall volume. This field is a source for the cosmological moduli problem (CMP) as long as $M_s < 10^{13}$ GeV, corresponding to $\mathcal{V} > 10^{10}$. In fact, in this case the modulus χ is lighter than 10 TeV and, coupling with gravitational strength interactions, it would overclose the Universe or decay so late to ruin Big-Bang nucleosynthesis. There are two main possible solutions to this CMP:
 1. The light modulus χ gets diluted due to an increase in the entropy that occurs when a short-lived modulus decays out of equilibrium and while dominating the energy density of the Universe [43, 44];
 2. The volume modulus gets diluted due to a late period of low energy inflation caused by thermal effects [45].

Assuming this problem is solved, the volume modulus becomes a dark matter candidate (with a mass $m \sim 1$ MeV, if $\mathcal{V} \sim 10^{15}$) and its decay to e^+e^- could be one of the sources that contribute to the observed 511 KeV line, coming from the centre of our galaxy.²⁴ The light modulus χ can also decay into photons, producing a clean monochromatic line that would represent a clear astrophysical smoking-gun signal for these scenarios [17]. We point out that in the case of K3 fibrations, where the K3 fiber is stabilised large [8], the spectrum of moduli fields includes an additional light field. This field is also a potential dark matter candidate with a mass $m \sim 10$ keV, that could produce another monochromatic line via its decay to photons.

- At present, there are no known models of inflation in LVS with intermediate scale M_s . However, the Fibre Inflation model of [16] can give rise to inflation for every value of \mathcal{V} . The only condition, which fixes $\mathcal{V} \sim 10^3$, and so $M_s \sim M_{GUT}$, is the matching with the COBE normalisation for the density fluctuations. Such a small value of \mathcal{V} is also necessary to have a very high inflationary scale (close to the GUT scale) which, in turn, implies detectable gravity waves. However, in principle it is

²⁴However, recently it has been discovered with the INTEGRAL spectrometer SPI [46] that the 511 KeV line emission appears to be asymmetric. This distribution of positron annihilation resembles that of low mass X-ray binaries, suggesting that these systems may be the dominant origin of the positrons and so reducing the need for more exotic explanations, such as the one presented in this paper.

possible that the density perturbations could be produced by another scalar field (not the inflaton), which is playing the role of a curvaton. In such a case, one could be able to get inflation also for $\mathcal{V} \sim 10^{15}$. In this way, both inflation and TeV scale SUSY would be achieved within the same model, even though gravity waves would not be observable. It would be interesting to investigate whether such scenarios are indeed realisable.

- As derived in Section 6.2, if the volume is stabilised such that $\mathcal{V} \sim 10^{15}$, the decompactification temperature is rather low: $T_{max} \sim 10^7$ GeV.

SV case

In this case the volume is stabilised at smaller values of the order $\mathcal{V} \sim 10^4$, which allows to reproduce the standard picture of gauge coupling unification with $M_s \sim M_{GUT}$. Here are the main cosmological features of these scenarios:

- Given that in this case $\mathcal{V} < 10^{13}$, all the moduli have a mass $m > 10$ TeV, and so they decay before Big-Bang nucleosynthesis. Hence these scenarios are not plagued by any CMP.
- As we have already pointed out in the LV case above, smaller values of \mathcal{V} more naturally give rise to inflationary models, as the one presented in [16]. Here we observe that the predictions for cosmological observables of Fiber Inflation were sensitive to the allowed reheating temperature. Since for $\mathcal{V} \sim 10^4$ GeV we have $T_{RH}^0 < T_{max} \sim 10^{15}$ GeV and since in [16] the authors considered already a more stringent upper bound $T_{RH}^0 < 10^{10}$ GeV (in order to avoid thermal gravitino overproduction), the presence of a maximal temperature does not alter the predictions of that inflationary scenario.
- Fixing the volume at small values of the order $\mathcal{V} \sim 10^3$, the decompactification temperature turns out to be extremely high: $T_{max} \sim 10^{15}$ GeV.

According to the discussion above, it would seem that cosmology tends to prefer smaller values of \mathcal{V} . The reason is that in the SV case there is no CMP and robust models of inflation are known, whereas for $\mathcal{V} \sim 10^{15}$ the light modulus suffers from the CMP and no model of inflation has been found yet. Interestingly enough, the lower bound on \mathcal{V} , derived in this paper, suggests exactly the opposite. Namely, larger values of \mathcal{V} are favoured since, writing the volume as $\mathcal{V} \sim 10^x$ and recalling the definition (6.55) of the parameter c , the constraint $T_* < T_{max}$ rules out a relevant portion of the (x, c) -parameter space, that corresponds to the SV case.

In view of this result, let us point out again that the LV case has its advantages. For example, the decay of the light modulus into e^+e^- could contribute to explain the origin of the 511 KeV line. In addition, its decay to photons could produce a clean smoking-gun signal of LVS. Furthermore, finding a realization of inflation, that is compatible with the LV case, is not necessarily an unsurmountable problem. In that regard, let us note that

the authors of [47] proposed a model, which relates the LV to the SV case. More precisely, the inflaton is the volume modulus and inflation takes place at a high scale for small values of \mathcal{V} . However, after inflation the modulus ends up at a VEV located at $\mathcal{V} \sim 10^{15}$, thus obtaining TeV scale SUSY. In fact, as we have already mentioned above, it could even be possible to realize inflation directly in the LV case. A way to achieve that would be to modify the the Fibre Inflation scenario of [16], so that the density fluctuations are generated by a field other than the inflaton. Such curvaton-like scenarios would be very promising for the generation of non-gaussianities in the CMB, as well as the realization of both low scale inflation and low-energy SUSY. However, due to the low inflationary scale, in these models gravity waves will be unobservable.

Now, even if inflation turns out not to be a problem for the LV case, there is still the CMP due to the presence of the light volume modulus. The results of this paper pose a challenge for the solution of this problem. Indeed, as we have shown in Subsection 6.3, the CMP cannot be solved by diluting the volume modulus via the entropy increase caused by the decay of the small moduli. The reason is that the latter moduli decay before they can begin to dominate the energy density of the Universe. So let us now discuss in more detail the prospects of the other main possible solution of the CMP in LVS, namely thermal inflation.

Thermal Inflation

Thermal inflation has been studied in the literature from the field theoretic point of view [45]. The basic idea is that a field ϕ , whose VEV is much larger than its mass (and so is called flaton) can be trapped by thermal corrections at a false vacuum in the origin. At a certain temperature, its vacuum energy density can start dominating over the radiation one, thus leading to a short period of inflation. This period ends when the temperature drops enough to destabilise the local minimum the flaton was trapped in.

Since the flaton ϕ has to have a VEV $\langle\phi\rangle \gg m_\phi$, it is assumed that the quartic piece in its potential is absent. However in this way, the 1-loop thermal corrections cannot trap the flaton in the origin because they go like

$$V_T \sim T^2 m_\phi^2 = T^2 \frac{d^2 V}{d\phi^2}, \quad (7.1)$$

and there is no quartic term in V that would give rise to a term like $T^2 \phi^2$. Hence, it is usually assumed that there is an interaction of the flaton with a very massive field, say a scalar ψ , of the form $g\psi^2\phi^2$, where $g \sim 1$ so that ψ thermalises at a relatively low temperature. At this point, a 1-loop thermal correction due to ψ would give the required term

$$V_T \sim T^2 m_\psi^2 = gT^2 \phi^2. \quad (7.2)$$

When ϕ gets a nonzero VEV, the interaction term $g\psi^2\phi^2$ generates a mass term for ψ of the order $m_\psi \sim \langle\phi\rangle$. Hence, when ϕ is trapped in the origin at high T , ψ becomes very light. Close to the origin, the potential looks like:

$$V = V_0 + (gT^2 - m_\phi^2)\phi^2 + \dots, \quad (7.3)$$

where V_0 is the height of the potential in the origin. A period of thermal inflation takes place in the temperature window $T_c < T < T_{in}$, where $T_{in} \sim V_0^{1/4}$ is the temperature at which the flaton starts to dominate the energy density of the Universe (beating the radiation energy density $\rho_r \sim T^4$) and $T_c \sim m_\phi/g$ is the critical temperature at which the flaton undergoes a phase transition rolling towards the $T = 0$ minimum. The number of e-foldings of thermal inflation is given by:

$$N_e \sim \ln \left(\frac{T_{in}}{T_c} \right) \sim \ln \sqrt{\frac{\langle \phi \rangle}{m_\phi}}. \quad (7.4)$$

Let us see how the above picture relates to the LVS. In the case of $\mathcal{V} \sim 10^{15}$, the modulus τ_s has the right mass scale and VEV to produce $N_e \sim 10$ e-foldings of inflation, which would solve the CMP without affecting the density perturbations generated during ordinary high-energy inflation. However, in Subsection 6.1 we derived the relevant 1-loop temperature corrections to the scalar potential and showed that they are always subleading with respect to the $T = 0$ potential, for temperatures below the Kaluza-Klein scale. Hence, since thermal inflation requires the presence of new minima at finite-temperature, we would be tempted to conclude that it does not take place in the LVS. In fact, this was to be expected also for the following reason. According to the field theoretic arguments above, in order for thermal inflation to occur, it is crucial that the flaton be coupled to a very massive field ψ . However, in our model there is no particle, which is heavier than the flaton candidate τ_s . It is not so surprising, then, that we are not finding thermal inflation.

Let us now discuss possible extensions of our model that could, perhaps, allow for thermal inflation to occur, as well as the various questions that they raise.

1. Since in our case τ_s is the candidate flaton field, the necessary ψ field would have a mass of the order $m_\psi \sim \langle \tau_s \rangle M_s$, and so it is likely to be a stringy mode. In such a case, it is not a priori clear how to compute thermal corrections to V_T due to the presence of ψ in the thermal bath.
2. Even if we can compute V_T , it is not clear why these corrections should trap τ_s at the origin. Note, however, that this is not implausible, as the origin is a special point in moduli space, where new states may become massless or the local symmetry may get enhanced. Any such effect might turn out to play an important role.
3. Even assuming that V_T does trap τ_s in the origin, one runs into another problem. Namely, the corresponding small cycle shrinks below M_s and so we cannot trust our low-energy EFT. For a full description, we should go to the EFT that applies close to the origin. The best known examples of these are EFTs for blow-up fields at the actual orbifold point. In addition, one should verify that \mathcal{V} stays constant when the τ_s cycle shrinks to zero size.
4. When τ_s goes to zero, the field ψ should become massless, according to the comparison with the field theoretic argument (if this comparison is valid). So possible candidates for the role of the ψ field could be winding strings or D1-branes wrapping a 1-cycle of the collapsing 4-cycle.

5. If ψ corresponds to a winding string, the interaction of the flaton τ_s with ψ cannot be seen in the EFT and it would be very difficult to have a detailed treatment of this issue.
6. The field ψ could also be a right handed neutrino, or sneutrino, heavier than τ_s . The crucial question would still be if it would be possible to see ψ in our EFT description. In addition, one would need to write down m_ψ as a function of τ_s and \mathcal{V} . It goes without saying that this issue is highly dependent on the particular mechanism for the generation of neutrino masses.
7. Besides the small modulus τ_s , another possible flaton candidate could be a localised matter field such as an open string mode. However we notice that the main contribution to the scalar potential of this field should come from D-terms, and that a D-term potential usually gives rise to a mass of the same order of the VEV. Hence it may be difficult to find an open string mode with the typical behaviour of a flaton field.

In general, all of the above open questions are rather difficult to address. This poses a significant challenge for the derivation of thermal inflation in LVS and the corresponding solution of the CMP. However, let us note that the CMP could also be solved by finding different models of low-energy inflation, which do not rely on thermal effects.

8. Conclusions

In this paper, we studied how finite-temperature corrections affect the $T = 0$ effective potential of type IIB LVS and what are the subsequent cosmological implications in this context.

We showed that the small moduli and modulini can reach thermal equilibrium with the MSSM particles. Despite that, we were able to prove that their thermal contribution to the effective potential is always subleading compared to the $T = 0$ potential, for temperatures below the Kaluza-Klein scale. As a result, the leading temperature-dependent part of the effective potential is due only to the MSSM thermal bath and it turns out to have runaway behaviour at high T . We derived the decompactification temperature T_{max} , above which the $T = 0$ minimum is completely erased and the volume of the internal space starts running towards infinity. Clearly, in this class of IIB compactifications the temperature T_{max} represents the maximal allowed temperature in the early Universe. Hence, in particular, it gives an upper bound on the initial reheating temperature after inflation: $T_{RH}^0 < T_{max}$.²⁵ The temperature T_{RH}^0 is highly dependent on the details of the concrete inflationary model and re-heating process, and so in principle its determination is beyond the scope of our paper. Nevertheless, we can compute the temperature of the Universe after the small moduli decay. They are rather short-lived and their decay can either be the main source of

²⁵Note, however, that it may be possible to relax this constraint to a certain degree by studying the dynamical evolution of the moduli in presence of finite temperature corrections, in the vein of the considerations of [35] for the KKLT set-up.

initial reheating (in which case the temperature after their decay is exactly T_{RH}^0) or it can occur during a radiation dominated epoch, after initial reheating has already taken place. In both cases, the resulting temperature of the Universe T_* has to satisfy $T_* < T_{max}$, which implies a lower bound on the allowed values of \mathcal{V} . We were able to derive this bound and show that it rules out a large range of smaller \mathcal{V} values (which lead to standard GUT theories), while favouring greater values of \mathcal{V} (that lead to TeV scale SUSY). Note though, that the condition $T_* < T_{max}$ is both necessary and sufficient in the case the decay of the small moduli is the origin of initial reheating, whereas it is just necessary but not sufficient in the case the small moduli decay below T_{RH}^0 .

Finally, we discussed possible cosmological applications of our work. In particular, we argued that, to realize thermal inflation in this type of compactifications, one needs to go beyond the current effective field theory description of the closed string moduli sector.

Acknowledgements

We would like to thank Joe Conlon, Anshuman Maharana, Nelson Nunes and Michael Ratz for useful conversations. We are especially grateful to Fernando Quevedo for fruitful discussions and valuable comments on the paper. L.A. is supported by DOE grant FG02-84-ER40153. V.C. is supported by a Queen Mary Westfield Trust Scholarship. M.C. is partially funded by St John's College, EPSRC and CET.

A. Moduli couplings

We shall now assume that the MSSM is built via magnetised $D7$ branes wrapping an internal 4-cycle within the framework of 4D $\mathcal{N} = 1$ supergravity. The full Lagrangian of the system can be obtained by expanding the superpotential W , the Kähler potential K and the gauge kinetic functions f_i as a power series in the matter fields:

$$W = W_{mod}(\varphi) + \mu(\varphi)H_u H_d + \frac{Y_{ijk}(\varphi)}{6} C^i C^j C^k + \dots, \quad (\text{A.1})$$

$$K = K_{mod}(\varphi, \bar{\varphi}) + \tilde{K}_{i\bar{j}}(\varphi, \bar{\varphi}) C^i C^{\bar{j}} + [Z(\varphi, \bar{\varphi})H_u H_d + h.c.] + \dots, \quad (\text{A.2})$$

$$f_i = \frac{T_{MSSM}}{4\pi} + h_i(F)S. \quad (\text{A.3})$$

In the previous expressions, φ denotes globally all the moduli fields, and W_{mod} and K_{mod} are the superpotential and the Kähler potential for the moduli, which we have discussed in depth in Section 2. H_u and H_d are the two Higgs doublets of the MSSM, and the C 's denote collectively all the matter fields. In the expression for the gauge kinetic function (A.3), T_{MSSM} is the modulus related to the 4-cycle wrapped by the MSSM $D7$ branes, and $h_i(F)$ are 1-loop topological functions of the world-volume fluxes F on different branes (the index i runs over the three MSSM gauge group factors). Finally the moduli scaling of the Kähler potential for matter fields $\tilde{K}_{i\bar{j}}(\varphi, \bar{\varphi})$ and $Z(\varphi, \bar{\varphi})$, for LVS with the small cycle

τ_s supporting the MSSM, has been derived in [38] and looks like:²⁶

$$\tilde{K}_{i\bar{j}}(\varphi, \bar{\varphi}) \sim \frac{\tau_s^{1/3}}{\tau_b} k_{i\bar{j}}(U) \quad \text{and} \quad Z(\varphi, \bar{\varphi}) \sim \frac{\tau_s^{1/3}}{\tau_b} z(U). \quad (\text{A.4})$$

A.1 Moduli couplings to ordinary particles

We now review the derivation of the moduli couplings to gauge bosons, matter particles and Higgs fields for high temperatures $T > M_{EW}$. In this case all the gauge bosons and matter fermions are massless.

• Couplings to Gauge Bosons

The coupling of the gauge bosons X to the moduli arise from the moduli dependence of the gauge kinetic function (A.3). We shall assume that the MSSM $D7$ branes are wrapping the small cycle²⁷, and so we identify $T_{MSSM} \equiv T_s$. We also recall that the gauge couplings of the different MSSM gauge groups are given by the real part of the gauge kinetic function, and that one obtains different values by turning on different fluxes. Thus the coupling of τ_s with the gauge bosons is the same for $U(1)$, $SU(2)$ and $SU(3)$. We now focus on the $U(1)$ factor without loss of generality. The kinetic terms read (neglecting the τ_s -independent 1-loop contribution)

$$\mathcal{L}_{gauge} = -\frac{\tau_s}{M_P} F_{\mu\nu} F^{\mu\nu}. \quad (\text{A.5})$$

We then expand τ_s around its minimum and go to the canonically normalised field strength $G_{\mu\nu}$ defined as

$$G_{\mu\nu} = \sqrt{\langle \tau_s \rangle} F_{\mu\nu}, \quad (\text{A.6})$$

and obtain

$$\mathcal{L}_{gauge} = -G_{\mu\nu} G^{\mu\nu} - \frac{\delta\tau_s}{M_P \langle \tau_s \rangle} G_{\mu\nu} G^{\mu\nu}. \quad (\text{A.7})$$

Now by means of (4.8) we end up with the following *dimensionful* couplings

$$\mathcal{L}_{\chi XX} \sim \left(\frac{1}{M_P \ln \mathcal{V}} \right) \chi G_{\mu\nu} G^{\mu\nu}, \quad (\text{A.8})$$

$$\mathcal{L}_{\Phi XX} \sim \left(\frac{\sqrt{\mathcal{V}}}{M_P} \right) \Phi G_{\mu\nu} G^{\mu\nu}. \quad (\text{A.9})$$

• Couplings to matter fermions

The terms of the supergravity Lagrangian which are relevant to compute the order of magnitude of the moduli couplings to an ordinary matter fermion ψ are its kinetic and mass terms²⁸:

$$\mathcal{L} = \tilde{K}_{\bar{\psi}\psi} \bar{\psi} i \gamma^\mu \partial_\mu \psi + e^{K/2} \lambda H \bar{\psi} \psi, \quad (\text{A.10})$$

²⁶Note that, in the case of more than one small cycle supporting the MSSM, these expressions would be more complicated.

²⁷The large cycle would yield an unrealistically small gauge coupling: $g^2 \sim \langle \tau_b \rangle^{-1} \sim 10^{-10}$.

²⁸Instead of the usual 2-component spinorial notation, we are using here the more convenient 4-component spinorial notation.

where H is the corresponding Higgs field (either H_u or H_d). The moduli scaling of $\tilde{K}_{\bar{\psi}\psi}$ is given in (A.4), whereas $e^{K/2} = \mathcal{V}^{-1}$. Expanding the moduli and the Higgs around their VEVs, we obtain

$$\mathcal{L} = \frac{\langle \tau_s \rangle^{1/3}}{\langle \tau_b \rangle} \left(1 + \frac{1}{3} \frac{\delta \tau_s}{\langle \tau_s \rangle} - \frac{\delta \tau_b}{\langle \tau_b \rangle} + \dots \right) \bar{\psi} i \gamma^\mu \partial_\mu \psi + \frac{1}{\langle \tau_b \rangle^{3/2}} \left(1 - \frac{3}{2} \frac{\delta \tau_b}{\langle \tau_b \rangle} + \dots \right) \lambda (\langle H \rangle + \delta H) \bar{\psi} \psi. \quad (\text{A.11})$$

We now canonically normalise the ψ kinetic terms ($\psi \rightarrow \psi_c$) and rearrange the previous expression as

$$\begin{aligned} \mathcal{L} = & \bar{\psi}_c (i \gamma^\mu \partial_\mu + m_\psi) \psi_c + \left(\frac{1}{3} \frac{\delta \tau_s}{\langle \tau_s \rangle} - \frac{\delta \tau_b}{\langle \tau_b \rangle} \right) \bar{\psi}_c (i \gamma^\mu \partial_\mu + m_\psi) \psi_c \\ & - \left(\frac{1}{3} \frac{\delta \tau_s}{\langle \tau_s \rangle} + \frac{1}{2} \frac{\delta \tau_b}{\langle \tau_b \rangle} \right) m_\psi \bar{\psi}_c \psi_c + \mathcal{L}_{\delta H}, \end{aligned} \quad (\text{A.12})$$

where

$$m_\psi \equiv \frac{\lambda \langle H \rangle}{\langle \tau_s \rangle^{1/3} \langle \tau_b \rangle^{1/2}}, \quad \text{and} \quad \mathcal{L}_{\delta H} = \left(\frac{\lambda}{\langle \tau_b \rangle^{1/2} \langle \tau_s \rangle^{1/3}} \right) \delta H \bar{\psi}_c \psi_c - \left(\frac{3\lambda}{2 \langle \tau_b \rangle^{3/2} \langle \tau_s \rangle^{1/3}} \right) \delta \tau_b \delta H \bar{\psi}_c \psi_c. \quad (\text{A.13})$$

The second term of (A.12) does not contribute to the moduli interactions since Feynman amplitudes vanish for on-shell final states satisfying the equations of motion. Writing everything in terms of Φ and χ , we end up with the following *dimensionless* couplings

$$\mathcal{L}_{\chi \bar{\psi}_c \psi_c} \sim \left(\frac{m_\psi}{M_P} \right) \chi \bar{\psi}_c \psi_c, \quad (\text{A.14})$$

$$\mathcal{L}_{\Phi \bar{\psi}_c \psi_c} \sim \left(\frac{m_\psi \sqrt{\mathcal{V}}}{M_P} \right) \Phi \bar{\psi}_c \psi_c. \quad (\text{A.15})$$

Moreover the first term in the Higgs Lagrangian (A.13) gives rise to the usual Higgs-fermion-fermion coupling, whereas the second term yields a modulus-Higgs-fermion-fermion vertex:

$$\mathcal{L}_{\delta H \bar{\psi}_c \psi_c} \sim \left(\frac{1}{\mathcal{V}^{1/3}} \right) \delta H \bar{\psi}_c \psi_c, \quad (\text{A.16})$$

$$\mathcal{L}_{\chi \delta H \bar{\psi}_c \psi_c} \sim \left(\frac{1}{M_P \mathcal{V}^{1/3}} \right) \chi \delta H \bar{\psi}_c \psi_c, \quad (\text{A.17})$$

$$\mathcal{L}_{\Phi \delta H \bar{\psi}_c \psi_c} \sim \left(\frac{1}{M_P \mathcal{V}^{5/6}} \right) \Phi \delta H \bar{\psi}_c \psi_c. \quad (\text{A.18})$$

We notice that for $T > M_{EW}$ the fermions are massless since $\langle H \rangle = 0$, and so the two direct moduli couplings to ordinary matter particles (A.14) and (A.15) are absent.

• Couplings to Higgs Fields

The form of the un-normalised kinetic and mass terms for the Higgs from the supergravity Lagrangian, reads:

$$\mathcal{L}_{Higgs} = \tilde{K}_{\bar{H}H} \partial_\mu H \partial^\mu \bar{H} - \tilde{K}_{\bar{H}H} (\hat{\mu}^2 + m_0^2) H \bar{H}, \quad (\text{A.19})$$

where H denotes a Higgs field (either H_u or H_d), and $\hat{\mu}$ and m_0 are the canonically normalised supersymmetric μ -term and SUSY breaking scalar mass respectively. Their volume dependence, in the dilute flux limit, is [39]:

$$|\hat{\mu}| \sim m_0 \sim \frac{M_P}{\mathcal{V} \ln \mathcal{V}}. \quad (\text{A.20})$$

In addition to (A.19), there is also a mixing term of the form

$$\mathcal{L}_{Higgs \text{ mix}} = Z \left(\partial_\mu H_d \partial^\mu H_u + \partial_\mu \bar{H}_d \partial^\mu \bar{H}_u \right) - \tilde{K}_{\bar{H}H} B \hat{\mu} \left(H_d H_u + \bar{H}_d \bar{H}_u \right), \quad (\text{A.21})$$

with

$$B \hat{\mu} \sim m_0^2. \quad (\text{A.22})$$

However given that we are interested only in the leading order volume scaling of the Higgs coupling to the moduli, we can neglect the $\mathcal{O}(1)$ mixing of the *up* and *down* components, and focus on the simple Lagrangian:

$$\begin{aligned} \mathcal{L}_{Higgs} &= \tilde{K}_{\bar{H}H} \left(\partial_\mu H \partial^\mu \bar{H} - \frac{M_P^2}{(\mathcal{V} \ln \mathcal{V})^2} H \bar{H} \right) \\ &= -\frac{1}{2} \tilde{K}_{\bar{H}H} \left[\bar{H} \left(\square + \frac{M_P^2}{(\mathcal{V} \ln \mathcal{V})^2} \right) H + H \left(\square + \frac{M_P^2}{(\mathcal{V} \ln \mathcal{V})^2} \right) \bar{H} \right], \end{aligned} \quad (\text{A.23})$$

where we have integrated by parts. We now expand $\tilde{K}_{\bar{H}H}$ and $(\mathcal{V} \ln \mathcal{V})^{-2}$ and get:

$$\begin{aligned} \mathcal{L}_{Higgs} &\simeq -\frac{1}{2} K_0 \left(1 + \frac{1}{3} \frac{\delta \tau_s}{\langle \tau_s \rangle} - \frac{\delta \tau_b}{\langle \tau_b \rangle} \right) \left[\bar{H} \left(\square + m_H^2 \left(1 - 3 \frac{\delta \tau_b}{\langle \tau_b \rangle} \right) \right) H + \right. \\ &\quad \left. H \left(\square + m_H^2 \left(1 - 3 \frac{\delta \tau_b}{\langle \tau_b \rangle} \right) \right) \bar{H} \right], \end{aligned} \quad (\text{A.24})$$

where $K_0 = \langle \tau_s \rangle^{1/3} \langle \mathcal{V} \rangle^{-2/3}$ and the Higgs mass is given by

$$m_H \simeq \frac{M_P}{\langle \mathcal{V} \rangle \ln \langle \mathcal{V} \rangle}. \quad (\text{A.25})$$

Now canonically normalising the scalar kinetic terms $H \rightarrow H_c = \sqrt{K_0} H$, we obtain

$$\begin{aligned} \mathcal{L}_{Higgs} &= -\frac{1}{2} \left[\bar{H}_c \left(\square + m_H^2 \right) H_c + H_c \left(\square + m_H^2 \right) \bar{H}_c \right] \\ &\quad -\frac{1}{2} \left(\frac{1}{3} \frac{\delta \tau_s}{\langle \tau_s \rangle} - \frac{\delta \tau_b}{\langle \tau_b \rangle} \right) \left[\bar{H}_c \left(\square + m_H^2 \right) H_c + H_c \left(\square + m_H^2 \right) \bar{H}_c \right] + 3 \frac{\delta \tau_b}{\langle \tau_b \rangle} m_H^2 \bar{H}_c H_c. \end{aligned} \quad (\text{A.26})$$

The second term in the previous expression does not contribute to scattering amplitudes since Feynman amplitudes vanish for final states satisfying the equations of motion. Thus the *dimensionful* moduli couplings to Higgs fields arise only from the third term once we express $\delta \tau_b$ in terms of Φ and χ using (4.7). The final result is

$$\mathcal{L}_{\Phi \bar{H}_c H_c} \sim \left(\frac{m_H^2}{M_P \sqrt{\mathcal{V}}} \right) \Phi \bar{H}_c H_c \sim \left(\frac{M_P}{\mathcal{V}^{5/2} (\ln \mathcal{V})^2} \right) \Phi \bar{H}_c H_c, \quad (\text{A.27})$$

$$\mathcal{L}_{\chi \bar{H}_c H_c} \sim \left(\frac{m_H^2}{M_P} \right) \chi \bar{H}_c H_c \sim \left(\frac{M_P}{\mathcal{V}^2 (\ln \mathcal{V})^2} \right) \chi \bar{H}_c H_c. \quad (\text{A.28})$$

A.2 Moduli couplings to supersymmetric particles

We shall now work out the moduli couplings to gauginos, SUSY scalars and Higgsinos. Given that we are interested in thermal corrections at high temperatures, we shall focus on $T > M_{EW}$. Thus we can neglect the mixing of Higgsinos with gauginos into charginos and neutralinos, which takes place at lower energies due to EW symmetry breaking.

• Couplings to Gauginos

The relevant part of the supergravity Lagrangian involving the gaugino kinetic terms and their soft masses looks like

$$\mathcal{L}_{gaugino} \simeq \frac{\tau_s}{M_P} \bar{\lambda}' i \bar{\sigma}^\mu \partial_\mu \lambda' + \frac{F^s}{2} (\lambda' \lambda' + h.c.), \quad (\text{A.29})$$

where in the limit of dilute world-volume fluxes on the D7-brane, the gaugino mass is given by $M_{1/2} = \frac{F^s}{2\tau_s}$ [39]. Now if the small modulus supporting the MSSM is stabilised via non-perturbative corrections, then the corresponding F-term scales as

$$F^s \simeq \frac{\tau_s}{\mathcal{V} \ln \mathcal{V}}. \quad (\text{A.30})$$

Notice that the suppression factor $\ln \mathcal{V} \sim \ln(M_P/m_{3/2})$ in (A.30) would be absent in the case of perturbative stabilisation of the MSSM cycle [8]. Let us expand τ_s around its VEV and get:

$$\mathcal{L}_{gaugino} \simeq \langle \tau_s \rangle \left[\bar{\lambda}' i \bar{\sigma}^\mu \partial_\mu \lambda' + \frac{1}{2} \frac{M_P}{\mathcal{V} \ln \mathcal{V}} (\lambda' \lambda' + h.c.) \right] + \frac{\delta \tau_s}{M_P} \left[\bar{\lambda}' i \bar{\sigma}^\mu \partial_\mu \lambda' + \frac{M_P}{\langle \mathcal{V} \rangle \ln \langle \mathcal{V} \rangle} \frac{(\lambda' \lambda' + h.c.)}{2} \right]. \quad (\text{A.31})$$

We need now to expand also τ_b around its VEV in the first term of (A.31):

$$\frac{1}{\mathcal{V} \ln \mathcal{V}} \simeq \frac{1}{\tau_b^{3/2} \ln \mathcal{V}} \simeq \frac{1}{\langle \mathcal{V} \rangle \ln \langle \mathcal{V} \rangle} \left(1 - \frac{3}{2} \frac{\delta \tau_b}{\langle \tau_b \rangle} + \dots \right), \quad (\text{A.32})$$

and canonically normalise the gaugino kinetic terms $\lambda' \rightarrow \lambda = \sqrt{\langle \tau_s \rangle} \lambda'$. At the end we obtain:

$$\mathcal{L}_{gaugino} \simeq \bar{\lambda} i \bar{\sigma}^\mu \partial_\mu \lambda + \frac{M_P}{\langle \mathcal{V} \rangle \ln \langle \mathcal{V} \rangle} \frac{(\lambda \lambda + h.c.)}{2} + \frac{(\lambda \lambda + h.c.)}{2 \langle \mathcal{V} \rangle \ln \langle \mathcal{V} \rangle} \left(\frac{\delta \tau_s}{\langle \tau_s \rangle} - \frac{3}{2} \frac{\delta \tau_b}{\langle \tau_b \rangle} \right) + \frac{\delta \tau_s}{\langle \tau_s \rangle M_P} \bar{\lambda} i \bar{\sigma}^\mu \partial_\mu \lambda. \quad (\text{A.33})$$

From (A.33) we can immediately read off the gaugino mass:

$$M_{1/2} \simeq \frac{M_P}{\langle \mathcal{V} \rangle \ln \langle \mathcal{V} \rangle} \simeq \frac{F^s}{\tau_s} \sim \frac{m_{3/2}}{\ln(M_P/m_{3/2})}. \quad (\text{A.34})$$

Let us now rewrite (A.33) as:

$$\mathcal{L}_{gaugino} \simeq \left(1 + \frac{\delta \tau_s}{\langle \tau_s \rangle M_P} \right) \left[\bar{\lambda} i \bar{\sigma}^\mu \partial_\mu \lambda + \frac{M_{1/2}}{2} (\lambda \lambda + h.c.) \right] - \frac{3}{4} \frac{\delta \tau_b}{\langle \tau_b \rangle} \frac{M_{1/2}}{M_P} (\lambda \lambda + h.c.). \quad (\text{A.35})$$

We shall now focus only on the last term in (A.35) since it is the only one that contributes to decay rates. In fact, Feynman amplitudes with on-shell final states that satisfy the equations of motion, are vanishing. Using (4.7), we finally obtain the following *dimensionless* couplings:

$$\mathcal{L}_{\Phi\lambda\lambda} \sim \left(\frac{M_{1/2}}{M_P \sqrt{\mathcal{V}}} \right) \Phi\lambda\lambda \sim \left(\frac{1}{\mathcal{V}^{3/2} \ln \mathcal{V}} \right) \Phi\lambda\lambda, \quad (\text{A.36})$$

$$\mathcal{L}_{\chi\lambda\lambda} \sim \left(\frac{M_{1/2}}{M_P} \right) \chi\lambda\lambda \sim \left(\frac{1}{\mathcal{V} \ln \mathcal{V}} \right) \chi\lambda\lambda. \quad (\text{A.37})$$

• Couplings to SUSY Scalars

The form of the un-normalised kinetic and soft mass terms for SUSY scalars from the supergravity Lagrangian, reads:

$$\mathcal{L}_{scalars} = \tilde{K}_{\alpha\bar{\beta}} \partial_\mu C^\alpha \partial^\mu \bar{C}^{\bar{\beta}} - \frac{\tilde{K}_{\alpha\bar{\beta}}}{(\mathcal{V} \ln \mathcal{V})^2} C^\alpha \bar{C}^{\bar{\beta}}. \quad (\text{A.38})$$

Assuming diagonal Kähler metric for matter fields

$$\tilde{K}_{\alpha\bar{\beta}} = \tilde{K}_\alpha \delta_{\alpha\bar{\beta}}, \quad (\text{A.39})$$

the initial Lagrangian (A.38) simplifies to

$$\begin{aligned} \mathcal{L}_{scalars} &= \tilde{K}_\alpha \left(\partial_\mu C^\alpha \partial^\mu \bar{C}^{\bar{\alpha}} - \frac{1}{(\mathcal{V} \ln \mathcal{V})^2} C^\alpha \bar{C}^{\bar{\alpha}} \right) \\ &= -\frac{1}{2} \tilde{K}_\alpha \left[\bar{C}^{\bar{\alpha}} \left(\square + \frac{1}{(\mathcal{V} \ln \mathcal{V})^2} \right) C^\alpha + C^\alpha \left(\square + \frac{1}{(\mathcal{V} \ln \mathcal{V})^2} \right) \bar{C}^{\bar{\alpha}} \right]. \end{aligned} \quad (\text{A.40})$$

We note that (A.40) is of exactly the same form as the Higgs Lagrangian (A.23). This is not surprising since for temperatures $T > M_{EW}$, the Higgs behaves effectively as a SUSY scalar with mass of the order the scalar soft mass: $m_H \sim m_0$. Thus we can read off immediately the *dimensionful* moduli couplings to the canonically normalised SUSY scalars φ from (A.27) and (A.28):

$$\mathcal{L}_{\Phi\bar{\varphi}\varphi} \sim \left(\frac{m_0^2}{M_P \sqrt{\mathcal{V}}} \right) \Phi\bar{\varphi}\varphi \sim \left(\frac{M_P}{\mathcal{V}^{5/2} (\ln \mathcal{V})^2} \right) \Phi\bar{\varphi}\varphi, \quad (\text{A.41})$$

$$\mathcal{L}_{\chi\bar{\varphi}\varphi} \sim \left(\frac{m_0^2}{M_P} \right) \chi\bar{\varphi}\varphi \sim \left(\frac{M_P}{\mathcal{V}^2 (\ln \mathcal{V})^2} \right) \chi\bar{\varphi}\varphi. \quad (\text{A.42})$$

• Couplings to Higgsinos

The relevant part of the supergravity Lagrangian involving the Higgsino kinetic terms and their supersymmetric masses looks like:

$$\mathcal{L}_{Higgsino} \simeq \tilde{K}_{\bar{H}\bar{H}} \left[\bar{\tilde{H}}_u i \bar{\sigma}^\mu \partial_\mu \tilde{H}_u + \bar{\tilde{H}}_d i \bar{\sigma}^\mu \partial_\mu \tilde{H}_d + \hat{\mu} \left(\tilde{H}_u \tilde{H}_d + h.c. \right) \right]. \quad (\text{A.43})$$

After diagonalising the supersymmetric Higgsino mass term, we end up with a usual Lagrangian of the form:

$$\mathcal{L}_{Higgsino} \simeq \tilde{K}_{\tilde{H}\tilde{H}} \left[\tilde{H} i \bar{\sigma}^\mu \partial_\mu \tilde{H} + \hat{\mu} \left(\tilde{H} \tilde{H} + h.c. \right) \right], \quad (\text{A.44})$$

where \tilde{H} denotes collectively both the Higgsino mass eigenstates, which are the result of a mixing between the *up* and *down* gauge eigenstates. We recall also that since we are focusing on temperatures above the EWSB scale, we do not have to deal with any mixing between Higgsinos and gauginos to give neutralinos and charginos. Expanding the Kähler metric (A.4) and the μ -term (A.20), we obtain:

$$\mathcal{L}_{Higgsino} \simeq K_0 \left(1 + \frac{1}{3} \frac{\delta\tau_s}{\langle\tau_s\rangle} - \frac{\delta\tau_b}{\langle\tau_b\rangle} \right) \left[\tilde{H} i \bar{\sigma}^\mu \partial_\mu \tilde{H} + \frac{m_{\tilde{H}}}{2} \left(1 - \frac{3}{2} \frac{\delta\tau_b}{\langle\tau_b\rangle} \right) \left(\tilde{H} \tilde{H} + h.c. \right) \right], \quad (\text{A.45})$$

where $K_0 = \langle\tau_s\rangle^{1/3} \langle\mathcal{V}\rangle^{-2/3}$ and the physical Higgsino mass is of the same order of magnitude of the soft SUSY masses:

$$m_{\tilde{H}} \simeq \frac{M_P}{\langle\mathcal{V}\rangle \ln\langle\mathcal{V}\rangle} \simeq M_{1/2}. \quad (\text{A.46})$$

Now canonically normalising the scalar kinetic terms $\tilde{H} \rightarrow \tilde{H}_c = \sqrt{K_0} \tilde{H}$, we end up with:

$$\begin{aligned} \mathcal{L}_{Higgsino} = & \left(1 + \frac{1}{3} \frac{\delta\tau_s}{\langle\tau_s\rangle} - \frac{\delta\tau_b}{\langle\tau_b\rangle} \right) \left[\tilde{H}_c i \bar{\sigma}^\mu \partial_\mu \tilde{H}_c + \frac{m_{\tilde{H}}}{2} \left(\tilde{H}_c \tilde{H}_c + h.c. \right) \right] \\ & - \frac{3}{4} \frac{\delta\tau_b}{\langle\tau_b\rangle} m_{\tilde{H}} \left(\tilde{H}_c \tilde{H}_c + h.c. \right). \end{aligned} \quad (\text{A.47})$$

Writing everything in terms of Φ and χ , from the last term of (A.47), we obtain the following *dimensionless* couplings:

$$\mathcal{L}_{\chi\tilde{H}_c\tilde{H}_c} \sim \left(\frac{m_{\tilde{H}}}{M_P} \right) \chi \tilde{H}_c \tilde{H}_c \sim \left(\frac{1}{\mathcal{V} \ln \mathcal{V}} \right) \chi \tilde{H}_c \tilde{H}_c, \quad (\text{A.48})$$

$$\mathcal{L}_{\Phi\tilde{H}_c\tilde{H}_c} \sim \left(\frac{m_{\tilde{H}}}{M_P \sqrt{\mathcal{V}}} \right) \Phi \tilde{H}_c \tilde{H}_c \sim \left(\frac{1}{\mathcal{V}^{3/2} \ln \mathcal{V}} \right) \Phi \tilde{H}_c \tilde{H}_c. \quad (\text{A.49})$$

A.3 Moduli self couplings

In this Section we shall investigate if moduli reach thermal equilibrium among themselves. In order to understand this issue, we need to compute the moduli self interactions, which can be obtained by first expanding the moduli fields around their VEV

$$\tau_i = \langle\tau_i\rangle + \delta\tau_i, \quad (\text{A.50})$$

and then by expanding the potential around the LARGE Volume vacuum as follows:

$$V = V(\langle\tau_s\rangle, \langle\tau_b\rangle) + \frac{1}{2} \frac{\partial^2 V}{\partial\tau_i \partial\tau_j} \Big|_{\min} \delta\tau_i \delta\tau_j + \frac{1}{3!} \frac{\partial^3 V}{\partial\tau_i \partial\tau_j \partial\tau_k} \Big|_{\min} \delta\tau_i \delta\tau_j \delta\tau_k + \dots \quad (\text{A.51})$$

We then concentrate on the trilinear terms which can be read off from the third term of (A.51). We neglect the $\mathcal{O}(\delta\tau_i^4)$ terms since the strength of their couplings will be subleading

with respect to the $\mathcal{O}(\delta\tau_i^3)$ terms since one has to take a further derivative which produces a suppression factor. Taking the third derivatives and then expressing these self-interactions in terms of the canonically normalised fields

$$\begin{aligned}\delta\tau_b &\sim \mathcal{O}\left(\mathcal{V}^{1/6}\right)\Phi + \mathcal{O}\left(\mathcal{V}^{2/3}\right)\chi, \\ \delta\tau_s &\sim \mathcal{O}\left(\mathcal{V}^{1/2}\right)\Phi + \mathcal{O}(1)\chi,\end{aligned}$$

we end up with the following Lagrangian terms at leading order in a large volume expansion:

$$\mathcal{L}_{\Phi^3} \simeq \frac{M_P}{\mathcal{V}^{3/2}}\Phi^3, \quad \mathcal{L}_{\Phi^2\chi} \simeq \frac{M_P}{\mathcal{V}^2}\chi\Phi^2, \quad (\text{A.52})$$

$$\mathcal{L}_{\chi^2\Phi} \simeq \frac{M_P}{\mathcal{V}^{5/2}}\Phi\chi^2, \quad \mathcal{L}_{\chi^3} \simeq \frac{M_P}{\mathcal{V}^3}\chi^3. \quad (\text{A.53})$$

References

- [1] S. Gukov, C. Vafa and E. Witten, ‘‘CFT’s from Calabi-Yau four-folds,’’ Nucl. Phys. B **584** (2000) 69 [Erratum-ibid. B **608** (2001) 477] [arXiv:hep-th/9906070].
- [2] K. Dasgupta, G. Rajesh and S. Sethi, ‘‘M Theory, Orientifolds and G-Flux,’’ JHEP **9908** (1999) 023 [hep-th/9908088].
- [3] S. B. Giddings, S. Kachru and J. Polchinski, ‘‘Hierarchies from fluxes in string compactifications,’’ Phys. Rev. D **66** (2002) 106006 [hep-th/0105097].
- [4] J.-P. Derendinger, C. Kounnas, P. M. Petropoulos and F. Zwirner, ‘‘Superpotentials in IIA Compactifications with General Fluxes,’’ Nucl. Phys. **B715**, (2005) 211 [hep-th/0411276]; G. Villadoro and F. Zwirner, ‘‘ $N = 1$ Effective Potential from Dual Type-IIA D6/O6 Orientifolds with General Fluxes,’’ JHEP **0506** (2005) 047 [hep-th/0503169]; O. DeWolfe, A. Giriyavets, S. Kachru and W. Taylor, ‘‘Type IIA Moduli Stabilization,’’ JHEP **0507** (2005) 066 [hep-th/0505160].
- [5] S. Kachru, R. Kallosh, A. Linde and S. P. Trivedi, ‘‘De Sitter vacua in string theory,’’ Phys. Rev. D **68** (2003) 046005 [hep-th/0301240].
- [6] V. Balasubramanian, P. Berglund, J. P. Conlon and F. Quevedo, ‘‘Systematics of moduli stabilisation in Calabi-Yau flux compactifications,’’ JHEP **0503** (2005) 007 [hep-th/0502058].
- [7] M. Graña, ‘‘Flux Compactifications in String Theory: A Comprehensive Review,’’ Phys. Rept. **423** (2006) 91, hep-th/0509003.
- [8] M. Cicoli, J. P. Conlon and F. Quevedo, ‘‘General Analysis of LARGE Volume Scenarios with String Loop Moduli Stabilisation,’’ JHEP **0810** (2008) 105 [arXiv:0805.1029 [hep-th]].
- [9] R. Kallosh and A. Linde, ‘‘Landscape, the scale of SUSY breaking, and inflation,’’ JHEP **0412** (2004) 004 [arXiv:hep-th/0411011].
- [10] N. J. Craig, P. J. Fox, and J. G. Wacker, ‘‘Reheating metastable O’Raifeartaigh models,’’ Phys. Rev. **D75** (2007) 085006 [arXiv:hep-th/0611006].
- [11] S. A. Abel, C.-S. Chu, J. Jaeckel, and V. V. Khoze, ‘‘SUSY breaking by a metastable ground state: Why the early universe preferred the non-supersymmetric vacuum,’’ JHEP **01** (2007) 089 [arXiv:hep-th/0610334].

- [12] W. Fischler, V. Kaplunovsky, C. Krishnan, L. Mannelli, and M. A. C. Torres, “Meta-Stable Supersymmetry Breaking in a Cooling Universe,” *JHEP* **03** (2007) 107 [arXiv:hep-th/0611018].
- [13] L. Anguelova, R. Ricci, and S. Thomas, “Metastable SUSY breaking and supergravity at finite temperature,” *Phys. Rev.* **D77** (2008) 025036 [arXiv:hep-th/0702168].
- [14] C. Papineau, “Finite temperature behaviour of the ISS-uplifted KKLT model,” arXiv:0802.1861 [hep-th].
- [15] W. Buchmuller, K. Hamaguchi, O. Lebedev and M. Ratz, “Maximal Temperature in Flux Compactifications,” *JCAP* **0501** (2005) 004, hep-th/0411109; W. Buchmuller, K. Hamaguchi, O. Lebedev and M. Ratz, “Dilaton Destabilization at High Temperature,” *Nucl. Phys.* **B699** (2004) 292, hep-th/0404168.
- [16] M. Cicoli, C. P. Burgess and F. Quevedo, “Fibre Inflation: Observable Gravity Waves from IIB String Compactifications,” arXiv:0808.0691 [hep-th].
- [17] J. P. Conlon and F. Quevedo, “Astrophysical and Cosmological Implications of Large Volume String Compactifications,” *JCAP* **0708** (2007) 019 [arXiv:0705.3460 [hep-ph]].
- [18] M. R. Douglas and S. Kachru, “Flux compactification,” *Rev. Mod. Phys.* **79** (2007) 733 [hep-th/0610102];
F. Denef, M. R. Douglas and S. Kachru, “Physics of string flux compactifications,” arXiv:hep-th/0701050.
- [19] E. Witten, “Dimensional Reduction Of Superstring Models,” *Phys. Lett. B* **155**, 151 (1985);
C. P. Burgess, A. Font and F. Quevedo, “Low-Energy Effective Action For The Superstring,” *Nucl. Phys. B* **272**, 661 (1986); S. P. de Alwis, “On integrating out heavy fields in SUSY theories,” *Phys. Lett. B* **628** (2005) 183 [hep-th/0506267].
- [20] M. Berg, M. Haack and E. Pajer, “Jumping Through Loops: On Soft Terms from Large Volume Compactifications,” arXiv:0704.0737 [hep-th].
- [21] M. Berg, M. Haack and B. Kors, “On volume stabilization by quantum corrections,” *Phys. Rev. Lett.* **96** (2006) 021601 [arXiv:hep-th/0508171].
- [22] M. Cicoli, J. P. Conlon and F. Quevedo, “Systematics of String Loop Corrections in Type IIB Calabi-Yau Flux Compactifications,” *JHEP* **0801** (2008) 052 [arXiv:0708.1873 [hep-th]].
- [23] R. Blumenhagen, S. Moster and E. Plauschinn, “Moduli Stabilisation versus Chirality for MSSM like Type IIB Orientifolds,” *JHEP* **0801** (2008) 058 [arXiv:0711.3389 [hep-th]].
- [24] A. Collinucci, M. Kreuzer, C. Mayrhofer and N. O. Walliser, “Four-modulus ‘Swiss Cheese’ chiral models,” arXiv:0811.4599 [hep-th].
- [25] R. Blumenhagen, V. Braun, T. W. Grimm and T. Weigand, “GUTs in Type IIB Orientifold Compactifications,” arXiv:0811.2936 [hep-th].
- [26] R. Blumenhagen, B. Kors, D. Lust and S. Stieberger, “Four-dimensional String Compactifications with D-Branes, Orientifolds and Fluxes,” *Phys. Rept.* **445** (2007) 1 [hep-th/0610327].
- [27] C. P. Burgess, R. Kallosh and F. Quevedo, “de Sitter string vacua from supersymmetric D-terms,” *JHEP* **0310** (2003) 056 [hep-th/0309187].
- [28] A. Saltman and E. Silverstein, “The scaling of the no-scale potential and de Sitter model building,” *JHEP* **0411** (2004) 066 [hep-th/0402135].

- [29] J. P. Conlon, F. Quevedo and K. Suruliz, “Large-volume flux compactifications: Moduli spectrum and D3/D7 soft supersymmetry breaking,” *JHEP* **0508** (2005) 007 [hep-th/0505076].
- [30] K. Becker, M. Becker, M. Haack and J. Louis, “Supersymmetry breaking and alpha'-corrections to flux induced potentials,” *JHEP* **0206** (2002) 060 [hep-th/0204254].
- [31] P. Binetruy and M. Gaillard, “Temperature Corrections, Supersymmetric Effective Potentials and Inflation,” *Nucl. Phys.* **B254** (1985) 388.
- [32] P. Binetruy and M. Gaillard, “Temperature Corrections in the Case of Derivative Interactions,” *Phys. Rev.* **D32** (1985) 931.
- [33] L. Dolan and R. Jackiw, “Symmetry Behavior at Finite Temperature,” *Phys. Rev.* **D9** (1974) 3320.
- [34] R. Jackiw, “Functional Evaluation of the Effective Potential,” *Phys. Rev.* **D9** (1974) 1686.
- [35] T. Barreiro, B. de Carlos, E. J. Copeland and N. J. Nunes, “Moduli evolution in the presence of thermal corrections,” arXiv:0712.2394 [hep-ph].
- [36] K. Enqvist and J. Sirkka, “Chemical equilibrium in QCD gas in the early universe,” *Phys. Lett. B* **314** (1993) 298 [hep-ph/9304273].
- [37] Z. Lalak, G. G. Ross, and S. Sarkar, “Racetrack inflation and assisted moduli stabilisation,” *Nucl. Phys.* **B766** (2007) 1–20 [arXiv:hep-th/0503178].
- [38] J. P. Conlon, D. Cremades and F. Quevedo, “Kähler potentials of chiral matter fields for Calabi-Yau string compactifications,” *JHEP* **0701** (2007) 022 [arXiv:hep-th/0609180].
- [39] J. P. Conlon, S. S. Abdussalam, F. Quevedo and K. Suruliz, “Soft SUSY breaking terms for chiral matter in IIB string compactifications,” *JHEP* **0701** (2007) 032 [arXiv:hep-th/0610129].
- [40] J. I. Kapusta, “Finite Temperature Field Theory,” Cambridge, 1989.
- [41] L. Anguelova and V. Calo, “O'KKLT at Finite Temperature,” *Nucl. Phys.* **B801** (2008) 45, arXiv:0708.4159 [hep-th]; “Finite Temperature Behaviour of O'KKLT Model,” *Fortsch. Phys.* **56** (2008) 901, arXiv:0804.0770 [hep-th].
- [42] P. Berglund, P. Candelas, X. De La Ossa, A. Font, T. Hubsch, D. Jancic and F. Quevedo, “Periods for Calabi-Yau and Landau-Ginzburg vacua,” *Nucl. Phys. B* **419** (1994) 352 [arXiv:hep-th/9308005].
- [43] J. J. Heckman, A. Tavanfar and C. Vafa, “Cosmology of F-theory GUTs,” arXiv:0812.3155 [hep-th].
- [44] B. S. Acharya, P. Kumar, K. Bobkov, G. Kane, J. Shao and S. Watson, “Non-thermal Dark Matter and the Moduli Problem in String Frameworks,” *JHEP* **0806** (2008) 064 [arXiv:0804.0863 [hep-ph]].
- [45] D. H. Lyth and E. D. Stewart, “Cosmology With A Tev Mass GUT Higgs,” *Phys. Rev. Lett.* **75** (1995) 201 [arXiv:hep-ph/9502417]; D. H. Lyth and E. D. Stewart, “Thermal Inflation And The Moduli Problem,” *Phys. Rev. D* **53** (1996) 1784 [arXiv:hep-ph/9510204].
- [46] G. Weidenspointner *et al.* “An asymmetric distribution of positrons in the Galactic disk revealed by gamma-rays,” *Nature* **451**, 159-162 (10 January 2008).
- [47] J. P. Conlon, R. Kallosh, A. Linde and F. Quevedo, “Volume Modulus Inflation and the Gravitino Mass Problem,” *JCAP* **0809** (2008) 011 [arXiv:0806.0809 [hep-th]].